EXPLORING THE CELL CYCLE-REGULATED DEGRADATION OF THE *SACCHAROMYCES CEREVISIAE* TELOMERASE RECRUITMENT SUBUNIT EST1

By

Jenifer Lynn Ferguson

Dissertation

Submitted to the Faculty of the

Graduate School of Vanderbilt University

in partial fulfillment of the requirements

for the degree of

DOCTOR OF PHILOSOPHY

in

Biological Sciences

May, 2013

Nashville, Tennessee

Approved:

Katherine Friedman

Todd Graham

James Patton

Kathleen Gould

Laura Lee

This dissertation is dedicated to my parents, Vickie and Jerry Ferguson, whose continuous support, encouragement, and love have sustained me throughout my life.

I love you!

ACKNOWLEDGEMENTS

I would like to thank my advisor, Dr. Katherine Friedman, for all of her support and advice throughout these years. Though this project has been frustrating at times, her confidence in my abilities to see it come to fruition kept me pressing onward. I will be taking with me valuable lessons, both professionally and personally.

I would also like to thank my committee members, Drs. Todd Graham, Jim Patton, Kathy Gould, and Laurie Lee. Their suggestions, helpful discussions, and support were invaluable.

I could not have completed the *in vitro* studies in this project without the expertise, guidance, and support of Drs. Laurie and Ethan Lee. Thank you for allowing me to collaborate with your labs and generously supplying the reagents necessary for these experiments. This work was substantially aided by a great partner-in-science, Sarah Hainline, who made my time in the Lee Lab extra-enjoyable. I also wish to acknowledge the help of Tony Chen, who trained me to handle *Xenopus* frogs. Working with these critters (i.e. squeezing out eggs) was a highlight of my graduate years.

This project relied heavily upon the VMC Flow Cytometry Shared Resource. A heartfelt thanks goes to Brittany Matlock and Dave Flaherty for making the many hours spent in the basement of MCN feel like a vacation visiting friends. I enjoyed our vast and varied conversations.

I also thank the members of the Friedman lab for their friendship and discussions about this project. I would specifically like to thank Dr. Robin Bairley for her special friendship and uncanny ability to make me laugh. I have thoroughly enjoyed our

conversations and time together. Dr. Jennell Talley has also become one of my greatest friends. I thank her for the wonderful friendship, varied conversations, helpful discussions during the dark days, and sympathetic ears. I will always think fondly of the times we shared 'the look' across the lab or during lab meeting. I look forward to continuing friendships with these two terrific women, even as we matriculate to different corners of the country. Though we only spent two years together, I thank Dr. Laura Bechard for being a great office-mate and engaging me in both scientific and random conversations. I also thank Margaret Platts for her ability to juggle fifteen tasks at once to keep the lab going.

I could not have survived graduate school intact without the support of my friends. These ladies have been helpful both professionally and personally. I met Dr. Elizabeth Thatcher during my rotation in Dr. Jim Patton's lab, where we became fast friends. I thank her for being my best friend and for the continuous support and encouragement. I also thank Elizabeth for always being there when I needed to vent and standing in my corner. I look forward to many more adventures and fun times! Seema Sinha's friendship has become invaluable. I appreciate her wicked sense of humor, outgoing personality, and unwavering encouragement these last few years. I have thoroughly relished all of the fun things we have ventured out and done together. I also thank Dr. Tiffany Farmer for being a great friend to me these last years. I have appreciated all of our lunch conversations and I thank you for being a great listener.

Last but definitely not least, I would like to thank my family. I will always be appreciative of their support and encouragement as I pursue my dreams. I thank my parents for nurturing my thirst for knowledge from a young age and teaching me the

value of hard work, without which none of this would have been possible. I thank my Mom for being a staunch advocate but also a stern 'just do it' motivator. I appreciate her trying to understand what I do and listening when I just need to talk. I love that my Dad has probably forgotten more than I will ever know. I cherish our Daddy-Daughter time at the Nashville Predators games and chats on the phone. I also thank him for being a voice of reason and encouragement. I would also like to thank my sister, Michelle, for her support and putting up with me all these years.

The work in this dissertation was supported by Vanderbilt University and a National Institutes of Health (NIH) grant GM080393 to Katherine Friedman. Flow Cytometry experiments were performed in the VMC Flow Cytometry Shared Resource and supported by the Vanderbilt Ingram Cancer Center (P30 CA68485) and the Vanderbilt Digestive Disease Research Center (DK058404).

TABLE OF CONTENTS

Page

LIST OF TABLES

Table Page

LIST OF FIGURES

LIST OF ABBREVIATIONS

3'-OH	3'-Hydroxyl
5-FOA	5-Floroorotic Acid
A or Ala	Alanine
aa	Amino acid
αF or AF	α-factor
ALT	Alternative lengthening of telomeres
APC	Anaphase Promoting Complex
APC^{Cdc20p}	Cdc20p-activated Anaphase Promoting Complex
APC^{Cdh1p}	Cdh1p-activated Anaphase Promoting Complex
ATM	Ataxia Telangiectasia Mutated
ATP	Adenosine tri-phosphate
bp	Base pair
C	Celcius
C2	D-box from Clb2p of sequence RLALNNVTN
Cdc13	Cell division cycle 13
Cdh1	Cdc20 homolog 1
CDK	Cyclin-dependent kinase
CEN	Centromere
ChIP	Chromatin immunoprecipitation
CP	Core particle
CST	Cdc13-Stn1-Ten1

CTE	C-terminal extension
DAC	Division of animal care
dATP	Deoxyadenosine tri-phosphate
DB or D-box	Destruction box
DBD	DNA-binding domain
dCTP	Deoxycytosine tri-phosphate
DDK	Dbf4-dependent kinase
dGTP	Deoxyguanosine tri-phosphate
DMSO	Dimethyl sulfoxide
DNA	Deoxyribonucleic acid
ds	Double stranded
DTT	Dithiothreitol
dTTP	Deoxythymidine tri-phosphate
Dub	De-ubiquitinating enzyme
E1	Enzyme 1: ubiquitin activating enzyme
E2 or Ubc	Enzyme 2: ubiquitin conjugating enzyme
E3	Enzyme 3: ubiquitin ligase
EM	Electron Microscopy
EST	Ever shorter telomere
ev	Empty vector
FEAR	Cdc14 early anaphase release
G	Guanosine
G1	Gap phase 1

G2	Gap phase 2
GAL	Galactose
GFP	Green fluorescent protein
h	Hour
HA	Hemagglutinin
HCG	Human chorionic gonadotropin
hph	Hygromycin B phosphotransferase
hTERT	Human telomerase reverse transcriptase
hTR	Human telomerase RNA
HU	Hydroxyurea
Hyg or Hygro	Hygromycin
IACUC	Institutional animal care and use committee
IFD	Insertion in finger domain
IVT	*In vitro* transcription/translation
K or Lys	Lysine
KAN	Kanamycin
kb	Kilobase
kDa	Kilo-dalton
KEN-box	Lysine-Glutamate-Asparagine box
L or Leu	Leucine
LLnL	N-acetyl-leu-leu-norleu-aldehyde
M	Molecular weight marker
M phase	Mitosis phase

MEN	Mitotic exit network
µg	Microgram
mg	Milligram
min	Minute
mini-T	Miniature telomerase RNA
µL	Microliter
ml	Milliliter
µM	Micromolar
mM	Millimolar
MMR	Marc's modified ringer
mRNA	Messenger ribonucleic acid
MRX	Mre11-Rad50-Xrs2 complex
mutC2	D-box from Clb2p mutated to ALAANNVTA
MYC	Myelocytomatosis
N or Asn	Aparagine
NAP	Nucleotide addition processivity
ng	Nanogram
NHEJ	Nonhomologous end-joining
NLS	Nuclear localization signal
NOC	Nocodazole
nt	Nucleotide
OB	Oligonucleotide/oligosaccharide binding
OD	Optical density

ORF	Open Reading Frame
PBS-T	Phosphate buffered saline with Tween
PCR	Polymerase chain reaction
PMSG	Pregnant mare serum gonadotropin
R or Arg	Arginine
Raff	Raffinose
RAP	Repeat addition processivity
RING	Really interesting new gene
RNase A	Ribonuclease A
RP	Regulatory particle
RRL	Rabbit reticulocyte lysate
RT	Reverse transcriptase
S	Synthesis phase
SDS-PAGE	Sodium dodecyl sulfate polyacrylamide gel electrophoresis
SILAC	Stable isotope labeling by amino acids in cell culture
SOEing	Splicing by overlap extension
ss	Single stranded
STEX	Single telomere extension
T	Thymidine
$T_{1/2}$	Protein half-life
TCA	Trichloroacetic acid
TEN	Telomerase essential N-terminus
TERC	Telomerase RNA component

TERT	Telomerase reverse transcriptase
TLC1	Telomerase component 1
TMG	Trimethylguanosine
TPE	Telomere position effect
TPR	Tetratricopeptide repeat
TR	Telomerase RNA
ts	Temperature sensitive
TSA-T	Triple-stiff-arm TLC1
Ub	Ubiquitin
UPP	Ubiquitin-proteasome pathway
Ura	Uracil
WT	Wild type
w/v	Weight per volume
XB	*Xenopus* extract buffer

CHAPTER I

INTRODUCTION

Telomeres are the protein-DNA complexes found at the termini of linear chromosomes in eukaryotic organisms. These regions maintain chromosome integrity by distinguishing normal chromosome ends from double-strand breaks and preventing end-to-end fusions. Without a means to combat the progressive shortening of telomeres following each replication cycle, cells undergo senescence and cease to divide. While telomere shortening serves to limit cell proliferation and acts as a tumor-suppressor in somatic cells, germ-line and stem cell populations require continuous renewal. Therefore, a mechanism is required to maintain telomere lengths. In eukaryotes, except *Dipterans*, this task is accomplished by the enzyme telomerase. Telomerase is a multi-subunit ribonucleoprotein and adds TG-rich telomere repeats by reverse transcribing a short template region contained in its intrinsic RNA component. Telomerase activity is highly regulated, being controlled temporally, post-translationally, and physically. Because telomere structure is evolutionarily conserved, general insight into telomere maintenance can be gleaned from organisms that are genetically malleable, such as the yeast *S. cerevisiae* used in this study.

For this dissertation, I focus on the temporal regulation of telomerase assembly by protein degradation of a core subunit during G1 phase of the cell cycle (Chapters II and III). In Chapter V, I discuss the conclusions and future directions of this project and offer a critique of the standard assays used for addressing fundamental questions about cell

cycle-regulated protein degradation. In this section (Chapter I), I detail the history of telomere biology and our current understanding of telomerase regulation in yeast. I then present an introduction of protein degradation, and specifically, the Anaphase Promoting Complex (APC).

A History of Telomeres and Telomerase

Discovery of telomeres

During the 1920's and 30's, Hermann Müller irradiated fruit flies to generate mutants with chromosome abnormalities such as translocations, inversions, and deletions. Interestingly, he was unable to identify any mutants in which the natural end of a chromosome was involved in such an event. He concluded that the end of the chromosome must serve a special function critical for organismal survival and coined the term "telomere" for this region, derived from the Greek word "telos" meaning end and "meros" meaning part [1]. During this same time, Barbara McClintock was also studying the chromosome in a different system, maize. Like Hermann Müller, she used irradiation as a means to introduce chromosome abnormalities and found that while broken chromosomes fused to each other, the natural chromosome termini were never involved in these fusion events [2]. Therefore, these two pioneers independently postulated that the natural end of a chromosome exhibits special qualities important for chromosome stability and organism survival, namely that of preventing chromosome fusions.

The end-replication problem

The next 30 years after the initial observations by Drs. Müller and McClintock saw little telomere research progression. However, the discovery of the chemical composition and structure of DNA by Drs. James Dr. and Francis Crick in 1953 [3], the identification of DNA polymerase I by Dr. Arthur Kornberg in 1956 [4-6], and the understanding of lagging strand replication by Reiji Okazaki in 1967 [7] pushed research forward toward investigating the molecular mechanisms of DNA replication. In the early 1970's, two independent researchers, Drs. James Watson and Alexey Olovnikov each proposed that the chromosome termini would pose a particular problem during replication. During DNA replication, the two parental strands separate and are used as a template for the production of two complete DNA molecules. DNA polymerases synthesize in a 5'– to – 3' direction, requiring a free 3'-hydroxyl (3'-OH) for successive base incorporation. Therefore, while leading strand synthesis proceeds continuously, lagging strand replication occurs in sections, called Okazaki fragments, which are initiated by the synthesis of an RNA primer. In his 1971 paper, Dr. Olovnikov suggested that the end of the chromosome cannot be completely replicated because the DNA polymerase is unable to fill in the 5'-gap or 3'-overhang that remains following the removal of the RNA primer from the terminus of the lagging strand. He concluded that this incremental loss of sequence from the end of chromosomes could result in loss of critical genomic information [8]. Dr. Watson developed a very similar model and published his conclusions in 1972. Here he termed this phenomenon of incomplete copying of the DNA template "the end-replication problem" [9]. However, Dr. Olovnikov took his model one step further; he proposed that the incremental shortening

of the chromosome termini each replication cycle acts as a counting mechanism for cellular aging and explains the limited potential for divisions (senescence) that Dr. Leonard Hayflick and others described in the 1960's [10-12].

Dr. Olovnikov's work went largely unrecognized because his manuscript was originally published in a Russian journal with few US readers. Furthermore, when finally able to present his work at an international meeting held in Kiev, Ukraine, the sudden disappearance and suspected kidnapping of Dr. Zhores Medvedev, a friend of Dr. Hayflick and prominent biochemist, distracted the audience and his presentation was largely ignored. It turned out that Dr. Medvedev was followed to the conference, forcibly detained, and escorted back to Moscow by the Soviets. In 1973, Dr. Olovnikov was allowed to re-publish his 1971 manuscript in English in the *Journal of Theoretical Biology*. However, Dr. Watson, a more prominent figure in the field, was still viewed as publishing first (1972) and therefore continued getting full credit for realizing and modeling the end-replication problem. Between 1972 and 1990, Dr. Watson's paper was cited 225 times, while Dr. Olovnikov's received only four citations. Dr. Olovnikov was later quoted, "I was glad that I, a young researcher, was ahead of the Nobel Laureate in several central positions" [13]. Drs. Calvin Harley, Bruce Futcher, and Carol Greider thrust Dr. Olovnikov's work into the spotlight with the number one reference in their groundbreaking 1990 *Nature* article documenting that, as predicted, telomeres shorten as human fibroblasts age [14].

The model proposed by Drs. Olovnikov and Watson for the end-replication problem was revised following the discovery that the telomere constitutively exists with a 3'-overhang [15-17]. Therefore, telomere attrition is a consequence of leading-strand

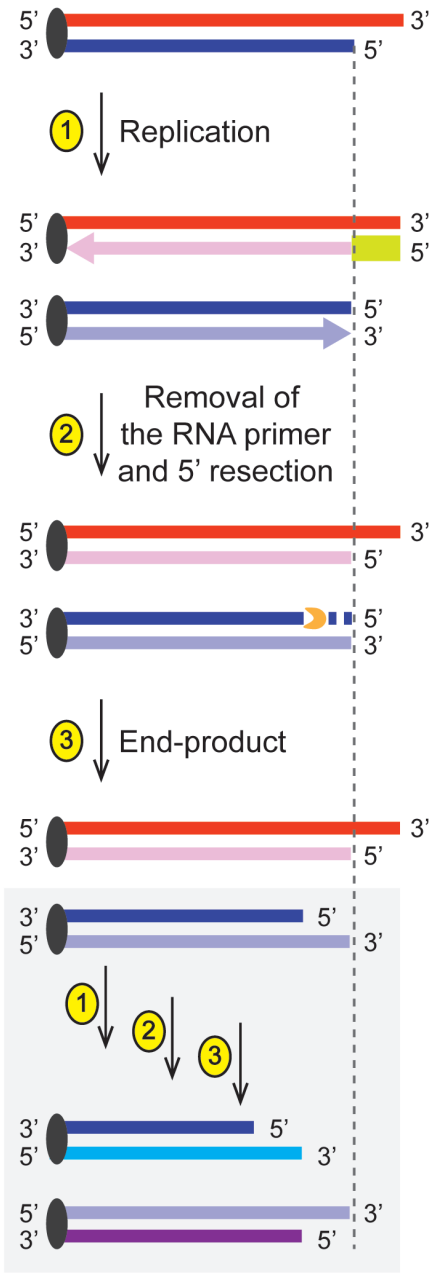

Figure 1. Model of the end-replication problem.
(1) During replication, each strand acts as a template for the synthesis of a complementary strand. (2) Lagging strand replication (pink) recreates a 3' overhang following removal of the terminal RNA primer (lime). Leading strand replication (light blue) results in a blunt-ended molecule that undergoes exonucleolytic resection (orange "pac-man") of the 5' end to re-establish the normal 3' overhang. (3) The end product has a 3' overhang on each new dsDNA molecule. Additionally, there is shortening of the parental strand involved in leading strand replication, as compared to the starting length (dashed vertical line). Additional rounds of replication further shorten the leading parental strand length (gray box). Black circles represent centromeres.

replication that results in a blunt-ended molecule, and the 5'-strand resection that occurs to recreate the 3'-overhang (Figure 1; also see section "Telomere Structure").

Sequencing the telomere

Following the theoretical modeling of the end-replication problem, research interest in telomere biology was reignited and turned toward determining the sequence of telomeres. Dr. Elizabeth Blackburn, working with the ciliate *Tetrahymena thermophila* in the lab of Dr. Joseph Gall, realized that this organism would be ideal for these types of experiments. *Tetrahymena* is a pond-dwelling, unicellular organism with two functionally distinct nuclei: a germ-line micronucleus that is transcriptionally silent, and a somatic macronucleus that is transcriptionally active. The micronucleus is diploid and contains 5 chromosomes; the macronucleus is highly polyploid resulting from the breakup of the five chromosomes into mini-chromosomes. Since these mini-chromosomes are then amplified multiple times and a telomere is added to each end, the maturation of the macronucleus results in ~40,000 telomeres in a single *Tetrahymena* cell [18], a great enrichment over other species such as diploid *S. cerevisiae* (64 telomeres) or *H. sapiens* (92 telomeres).

In 1978, Dr. Blackburn purified and sequenced telomeres from the macronucleus in *Tetrahymena* and discovered that they consist of tandem repeats of a hexanucleotide unit TTGGGG/CCCCAA, with the G-rich strand present at the 3' terminus. These telomeres were also found to be heterogeneous in the number of repeats they contained, varying from 20 to 70, and averaging 300 base pairs (bp) in length [19]. In 1995, Drs. Karen Kirk and Elizabeth Blackburn reported that the micronucleus consists of telomeres

containing the same terminal tandem repeats, but these telomeres are seven times longer (2-3.4 kilo-base pairs (kbp)) than those found in the macronucleus [20]. Over the next few years, the telomeres from other ciliates were sequenced and found to be comprised of similar tandem repeats [18].

Since the telomeres of ciliates were found to contain very similar tandem repeats despite being distantly related, researchers started examining the conservation of this aspect of telomere biology. In 1982, Drs. Elizabeth Blackburn and Jack Szostak found that telomeres of one species could be recognized by a different species. In this work, a plasmid was linearized to expose *Tetrahymena* telomeres on each end and introduced into *S. cerevisiae*. Surprisingly, this linear piece of DNA was maintained through multiple generations. In each case, the telomeres were elongated by the addition of yeast-specific repeats 100-300 bp in length, suggesting the yeast telomere maintenance mechanism was able to recognize and act upon the foreign *Tetrahymena* sequence. This plasmid was then used as a tool to clone yeast telomeres. One *Tetrahymena* telomere was removed and replaced with a library of yeast chromosomal restriction fragments; those that resulted in retention of the linearized plasmid mapped to the yeast telomere [21]. In 1984, *S. cerevisiae* telomeres were cloned and found to be ~300 bp in length and composed of tandem repeats with an irregular pattern, denoted $T_{(1\text{-}3)}G$ [22]. The finding that telomeres could be recognized and elongated by other species suggested that a recombination or fold-back method of replication was improbable and rather that telomere replication was likely to be mediated through some type of enzymatic activity.

Discovery of telomerase

After sequencing telomeres from multiple organisms and demonstrating that their maintenance is evolutionarily conserved, research interest shifted toward identifying the molecular players and mechanism of telomere replication. As described above, since telomeres in the macronucleus of *Tetrahymena* are heterogeneous in length [19], and *S. cerevisiae* telomere sequences can be added to *Tetrahymena* telomeres being maintained in yeast [21], Dr. Blackburn hypothesized that telomeres are maintained by a terminal transferase. In 1985, Drs. Carol Greider and Elizabeth Blackburn found that a single stranded (ss) primer containing *Tetrahymena* or *S. cerevisiae* telomeric DNA could be extended in a 6-base repetitive pattern in the presence of *Tetrahymena* protein extract, dGTP, and dTTP, consistent with the known telomere sequence (TTGGGG). They were unable to detect this activity using a non-telomeric primer. Furthermore, the reaction was unaffected by pre-treatment with micrococcal nuclease to remove the endogenous *Tetrahymena* double stranded (ds) DNA but was inhibited by proteinase K treatment and heat denaturation [23]. Drs. Greider and Blackburn also reported that telomere addition is inhibited in the presence of RNase [24]. Collectively, this work demonstrated that enzymatic activity from a ribonucleoprotein (RNP), which they named telomere terminal transferase (telomerase), was responsible for telomere additions.

Armed with the knowledge that telomerase was an RNP, Drs. Greider and Blackburn hypothesized that the telomere repeat sequence may be specified in the RNA component. Following a multi-step purification process of *Tetrahymena* telomerase, a 159 base RNA repeatedly co-purified with telomerase activity. This RNA was then sequenced and found to contain a region (5'-CAACCCCAA-3') that was complementary

to the *Tetrahymena* telomere repeat (5'-TTGGGG-3'). The authors hypothesized that this region acted as the template for DNA synthesis by the telomerase enzyme. In support of this idea, *in vitro* telomerase activity was inhibited by an anti-sense oligonucleotide that hybridized across this region. Likewise, a G-rich oligonucleotide, whose 3' end was complementary to the region immediately adjacent to the template, was elongated by telomerase. From this work, a mechanism of telomerase action (Figure 2) was proposed: 1) the 3' end of the telomere hybridizes to the RNA template region, 2) telomerase adds sequence one nucleotide at a time by reverse transcription, 3) the enzyme translocates and the new 3' end hybridizes to the RNA template, and 4) elongation of the sequence occurs again [25]. Remarkably, this model is still essentially correct today.

In 1990, the proposed template portion of the *Tetrahymena* RNA (5'-CAACCCCAA-3') was mutated. These mutations were incorporated into newly synthesized native telomeres *in vivo*, demonstrating that telomerase is a reverse transcriptase that uses the template region provided by its own internal RNA component. Importantly, one template mutant failed to incorporate any of the sequence onto telomere ends. This mutant instead underwent progressive telomere shortening and eventual senescence, suggesting that telomerase activity is necessary for cellular lifespan [26], as predicted by Dr. Olovnikov nearly 20 years earlier [10]. Telomerase activities were found in other ciliates (*Oxytricha* and *Euplotes*) [27,28] and in humans in the late 1980's [29]. Each telomerase synthesized its own species-specific G-rich telomere repeat using a template provided from an RNA molecule essential to telomerase activity [30,31].

In 1997, the catalytic subunit of telomerase from the ciliate *Euplotes* was purified and the gene encoding this protein was cloned [32]. After a BLAST search of protein

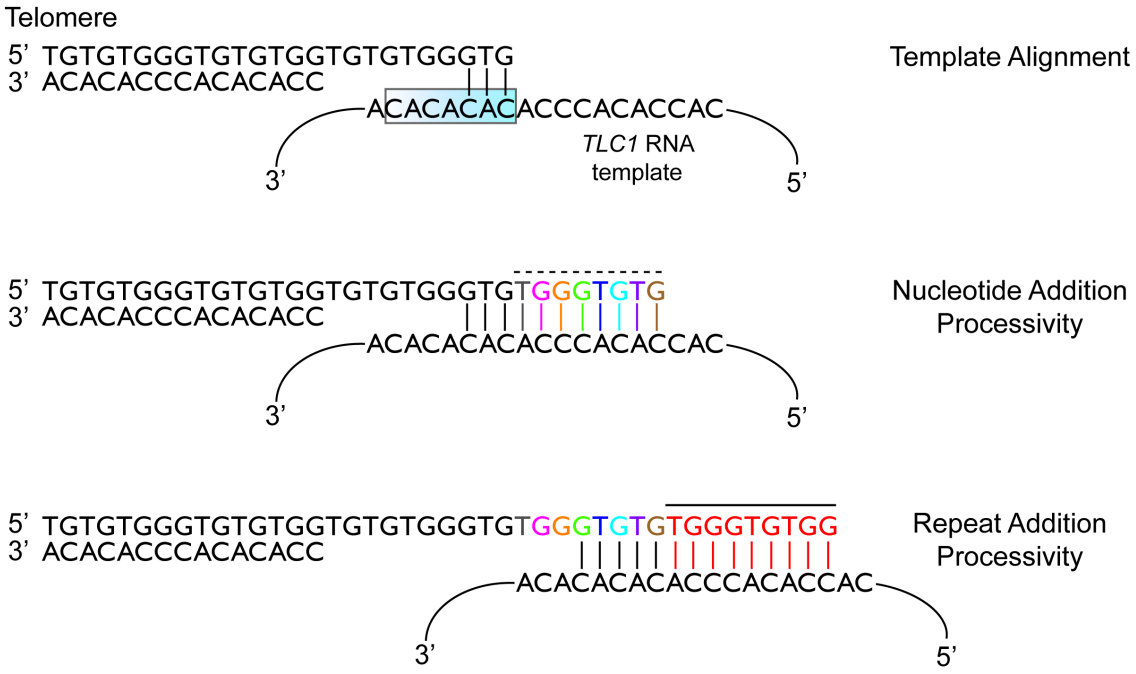

Figure 2. *S. cerevisiae* telomere elongation.
The telomeric 3' overhang is complementary to the template region of the *TLC1* RNA molecule, but can base-pair in a variety of alignment orientations (blue gradient). Upon alignment, telomerase reverse-transcribes the template region one base at a time, called nucleotide addition processivity (various colors). The enzyme then translocates and synthesizes an additional telomere repeat, called repeat addition processivity (red). The multiple template alignment registers and incomplete copying (abortive synthesis) of the template contributes to the degenerate sequence of yeast telomeres.

databases, this protein (p123) was found to be similar to the recently identified *S. cerevisiae* telomerase component, Est2p [33]. A detailed discussion of the screen that identified Est2p is below. The sequence identity between Est2p and p123 was only 20%, but similarity could be identified across the length. Closer inspection of this sequence revealed reverse-transcriptase motifs within both p123 and Est2p. Mutation of these conserved motifs in Est2p caused short telomeres and eventual senescence, indicating importance of these regions to telomere maintenance *in vivo*. Likewise, *in vitro* activity depended upon the expression of *EST2* and the RNA component, *TLC1* [32]. Soon after, catalytic subunits from other organisms were identified, including mouse [34], *S. pombe* [35], and humans [35,36], demonstrating the conservation of the telomerase enzymatic core across taxa. In 1998, the catalytic subunits began being referred to as the Telomerase Reverse Transcriptase (TERT) family of proteins [37].

The budding yeast, *S. cerevisiae,* has been an enlightening model system for examining telomerase action at a molecular level. Benefits of using this organism include the ease and variety of genetic manipulation since the genome has been sequenced, the rapid growth rate, detectible telomerase activity each cell cycle, and functional conservation of general mechanisms to other organisms.

The *Saccharomyces cerevisiae* telomerase complex

Identification of complex components

In 1989, Drs. Victoria Lundblad and Jack Szostak designed a yeast genetic screen to identify genes compromised for telomere maintenance in *S. cerevisiae*. Since a

telomere length defect is a difficult phenotype for which to screen, their study exploited the plasmid linearization assay previously used by Drs. Blackburn and Szostak [21]. They theorized that any mutant defective in telomerase activity would be unable to extend the *Tetrahymena* telomere repeats when introduced into *S. cerevisiae* and would result in loss of the linear DNA molecule. After randomly mutagenizing the yeast background, a gene was isolated that failed to maintain the linearized DNA, exhibited shortened chromosomal telomeres, and displayed a senescence phenotype associated with telomere shortening over time. This newly identified and cloned gene was named *EST1*, for Ever Shorter Telomeres [38]. A second, larger screen from Dr. Lundblad's lab identified three additional genes: *EST2*, *EST3*, and *EST4* (later determined to be a separation-of-function allele of *CDC13*) [33,39].

Since telomerase is a ribonucleoprotein [24] and the RNA component had previously been identified in *Tetrahymena* [25], researchers worked on identifying the RNA component in *S. cerevisiae*. It had been discovered that genes lying in close proximity to telomeres were transcriptionally repressed, a phenomenon called the telomere position effect (TPE) [40]. Screening for overexpression suppressors of TPE using a genetic library, Drs. Miriam Singer and Daniel Gottschling identified one gene that specifically repressed telomere silencing but did not affect silencing at other loci. They called this gene *TLC1*, for Telomerase Component 1. Intriguingly, they noticed that *TCL1* did not contain a long open reading frame (ORF) and hypothesized that the functional product was the RNA itself. Additionally, examination of the gene sequence revealed a 16-nucleotide (nt) segment that matched the *S. cerevisiae* telomere [22], suggesting this may be the templateing RNA. They confirmed their theory by

demonstrating that mutations within this region were incorporated into newly synthesized native telomeres [41], as had been previously demonstrated with the *Tetrahymena* RNA component [25,26].

Functional characterization of each subunit

With the identification of genes that affected telomere maintenance and hypothesized to be components of the telomerase enzyme complex [33,38,41], *S. cerevisiae* as a model system for telomerase was fully established. Work then shifted toward determining the functional role of each subunit and the conservation of these functions across a diverse range of taxa.

Telomerase RNA (*TLC1*)

Telomerase reverse-transcribes a TERC (telomerase RNA component) to synthesize telomere repeats (Figure 2). In *S. cerevisiae*, this RNA molecule is called *TLC1* but homologs in other organisms are referred to simply as TR, for telomerase RNA. The TR has been identified in 28 ciliates, 14 yeasts, and 43 vertebrates [42]. While TERCs across taxa share similarity in their template region, the size and sequence of the molecules vary substantially. In ciliates, the RNA is ~150 nt long, ~500 nt in vertebrates and ~1,300 nt in yeasts [25,30,41-45]. Even with this challenge, secondary structure similarities can be identified. For accurate telomere synthesis, the RNA must base-pair correctly with the telomere primer and have a defined template boundary. All TRs create this boundary with a 5' long-range base pairing element and a 3' pseudoknot

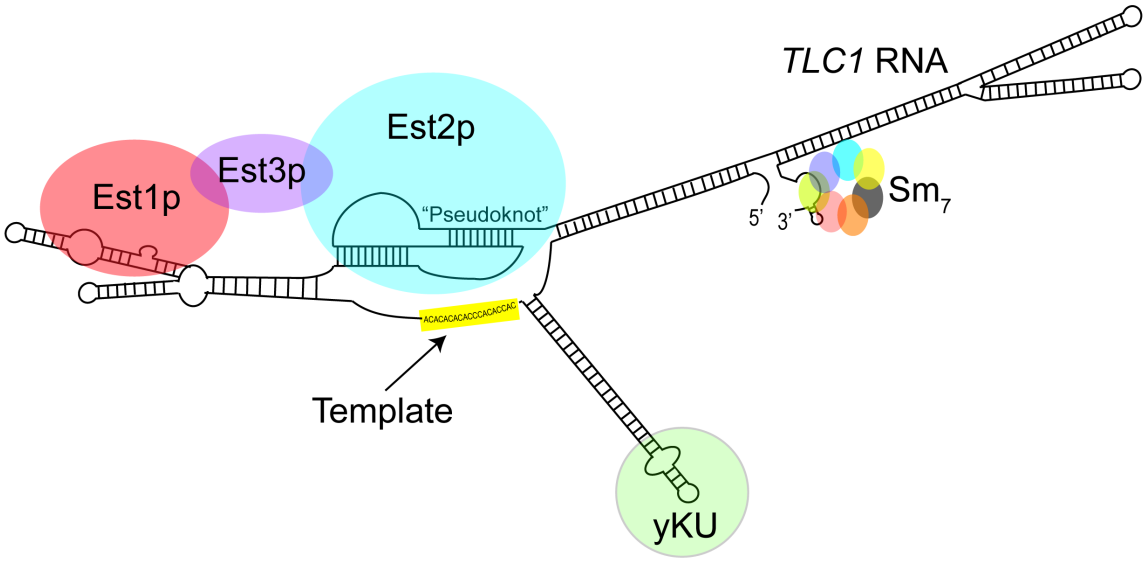

Figure 3. Multiple proteins bind the *S. cerevisiae* telomerase RNA molecule, *TLC1*. *TLC1* RNA folds into secondary structures that create separate binding sites for multiple proteins. The catalytic subunit, Est2p, associates with the pseudoknot structure located near the template (in yellow). Est1p and the yKu heterodimer associate with stem-loops on separate arms. Est3p does not bind directly to the RNA, but interacts with both Est1p and Est2p through protein-protein interactions. The 7-member Sm-complex associates with the sequence –AAUUUUG—located near the 3' terminus. The template boundaries are defined by the 3' pseudoknot structure and the 5' duplex at the base of the yKu arm. These structures help with alignment of the template-RNA and prevent run-through reverse transcription.

structure (Figure 3). These elements ensure proper alignment with the DNA and efficient polymerization and translocation of the catalytic core (reviewed in [45]). Following transcription by RNA Polymerase II, *TLC1* RNA is polyadenylated and gets a 5'-trimethylguanosine (TMG) cap to produce the mature form of the molecule. The 7-member Sm protein complex binds in a heptameric ring-shape around a site located near the 3' end of the RNA and is required for RNA stability and complete maturation (Figure 3). A strain lacking the Sm-binding site demonstrates a growth defect, short telomeres, and near background levels of the mature *TLC1* RNA. Finally, immunoprecipitation of an Sm protein can co-immunoprecipitate functional telomerase as measured by an *in vitro* primer extension assay, arguing that the Sm-protein bound form of *TCL1* RNA is enzymatically active [46].

TLC1 RNA acts as a flexible scaffold, providing multiple protein binding sites (Figure 3) [47]. Est2p, the reverse transcriptase, binds to the central core containing the template region [48-50]. Est1p, an accessory protein described in more detail below, binds a sub-helix [51,52]. The yKu heterodimer binds the *TLC1* RNA through a 48 nt stem-loop; this interaction is necessary for proper intracellular location and efficient recruitment of telomerase to telomeres [53-55].

The full length *TLC1* RNA is not functional when *in vitro* transcribed in rabbit reticulocyte lysate (RRL) most likely because it is unable to fold correctly. This characteristic has created obstacles for scientists interested in using biochemical assays to investigate telomerase complex assembly and reconstitute telomerase activity *in vitro*. Largely due to this technical limitation, studies of telomerase in *S. cerevisiae* have relied heavily upon genetic strategies as compared to studies in ciliates, which have used almost

exclusively biochemical approaches [25,33,38,41,56-58]. To combat this folding issue, miniature telomere RNA (Mini-T) versions have been produced. In these cases, the "extraneous" sequences between protein binding sites have been removed, reducing the molecule's size to 384 or 500 nt. Both of these Mini-T versions support some telomere maintenance *in vivo* and reconstitute telomerase activity *in vitro* when produced in RRL. However, these versions do not maintain wild-type telomere length nor robust cell growth, indicating that the yeast *TLC1* RNA has evolved to be a larger size for maximum efficiency [50]. An even smaller variant, called the Micro-T, contains only the template and pseudoknot in a 170 nt RNA. Micro-T is active *in vitro* when combined with Est2p [59]. Recently, a 956 nt variant called the triple-stiff-arm TLC1 (TSA-T) was introduced. TSA-T removes the secondary structures (bulges and loops) from the long arms separating the binding sites for yKu, Est2p, Est1p and Sm proteins, replacing them with "stiffened" duplex RNA sequences. Since this approach maintains the relative spacing between the binding sites, the authors were interested in whether the *TLC1* RNA requires flexibility to support telomerase function. They found that the TSA-T variant was functional both *in vitro* and *in vivo*, maintaining telomeres even better than the wild-type *TLC1*. The authors then stiffened one arm at a time and found that the stiffened Est1p and yKu arms contribute to telomere lengthening while the stiffened Sm arm reduced telomere length (but not as severely as the Mini-T) and RNA abundance. The remarkable malleability of the RNA is consistent with the idea that the RNA serves only as a tether and is not required to position the proteins in a specific way relative to each other [60].

Telomerase Catalytic Subunit (*EST2*)

The *S. cerevisiae* TERT subunit is encoded by *EST2*. Est2p, a 102 kDa protein discovered in the 1996 screen described above [33], shows conservation of both sequence and function across taxa. These conserved regions are grouped into the N-terminal domain, reverse transcriptase (RT) domain, and the C-terminal extension (CTE) domain (Figure 4). Within the RT domain, several motifs (1, 2, A, B', C, D, E) are universally conserved among RTs; the N and C-terminal domains are specific to telomerase (reviewed in [45]).

The N-terminal domain is comprised of four regions [61]. Region I, also called the telomerase essential N-terminal (TEN) domain, is important for telomerase complex assembly (Figure 4). Temperature sensitive (ts) mutations in this region can be suppressed by the overexpression of Est3p and a lethal mutant in the region loses the ability to co-immunoprecipitate Est3p, suggesting that the TEN domain may function to recruit Est3p to the complex [62]. Indeed, Dr. Jennell Talley, a recent graduate of our lab, showed that the Est2p TEN domain and Est3p interact directly and that this interaction stimulates telomerase activity *in vitro* [63]. Likewise, in *Candida parapsilosis* and *Lodderomyces elongisporus*, Est3p directly interacts with the TEN domain of TERT *in vitro*. This interaction also facilitates Est3p binding to telomeric DNA, suggesting that the TEN-Est3p interaction unmasks a DNA binding activity in Est3p [64]. The N-terminal domain is important for *TLC1* RNA binding [65] and telomere DNA binding [66-68]. Dr. Robin Bairley, a recent graduate of our lab, confirmed that the anchor site lies in the TEN domain of Est2p and that a mutation in this

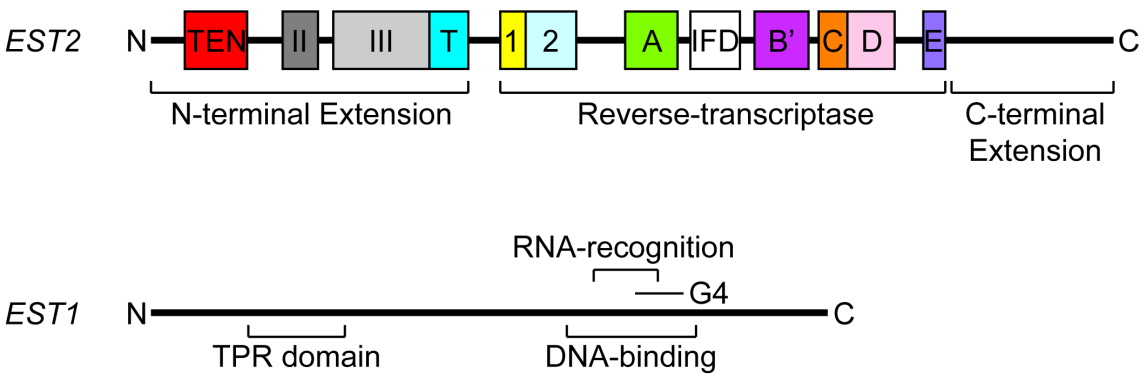

Figure 4. Functional domains of *EST2* and *EST1*.
The *S. cerevisiae EST2* gene encodes the reverse-transcriptase (RT) subunit of telomerase. The domain motifs (1, 2, A, B', C, D, E) are universally conserved amongst RTs. The IFD (insertion in finger domain) and the N and C-terminal extensions are specific to telomerase. The *EST1* gene encodes the telomerase recruitment protein, Est1p. The region of highest homology across species includes the TPR-consensus sequences. Est1p binds nucleotides (RNA and DNA) in an overlapping region near the C-terminus. Also within this region are the residues important for G-quadruplex formation activity.

domain (E76K) enhances the binding affinity of the TEN domain for telomeric DNA and alters the telomere-RNA alignment [69].

The RT domain is the catalytic center of telomerase (Figure 4) (reviewed in [45]). Three conserved aspartic acid residues in motifs A and C are essential for RT activity. These residues lie in the active site of the enzyme and coordinate two magnesium ions, defining the nucleotide-binding pocket that orients correct nucleotides for incorporation [70]. In *S. cerevisiae*, specific residues in motif C and E of the RT influence nucleotide addition processivity (NAP; Figure 2), the ability to incorporate each successive base onto the telomere end [71]. Repeat addition processivity (RAP; Figure 2), the ability to synthesize multiple repeats on the same telomere without dissociating, is compromised when mutations are made in the telomerase specific insertion in finger domain (IFD) which lies in the RT domain between motifs A and B' (Figure 4) [72].

The CTE domain exhibits weak conservation but mutations in this domain affect telomerase processivity [73,74]. While the domain is essential in TERTs of some species, such as humans and *Tetrahymena*, the region is dispensable for telomerase activity in *S. cerevisiae* [61,75]. In mammalian telomerase, the CTE domain may also influence telomerase multimerization and provide binding sites for the 14-3-3 and CRM1 proteins that regulate the localization of the TERT protein [76-79].

Telomerase Accessory Protein (*EST3*)

The *S. cerevisiae* accessory protein, Est3p, is the smallest (19 kDa) integral component of telomerase. This subunit is essential for telomerase function *in vivo* but is dispensable for activity *in vitro*, suggesting it is a regulatory or accessory protein. It was

first identified in the genetic screen that identified Est2p-Est4p [33] but has remained an enigma until recently. *S. cerevisiae EST3* encodes two ORFs that must undergo a programmed +1 translational shift to produce full length Est3p. At steady state, the frameshifted peptide is estimated to represent 75-90% of the total Est3 protein pool [80]. *S. cerevisiae* Est3p is recruited to the telomerase complex through a direct interaction with the catalytic subunit, Est2p, and recruitment subunit, Est1p (Figure 3) [63,81]. There have been no Est3 proteins identified outside of budding yeast. However, using structure prediction programs, Est3p is predicted to exhibit an oligonucleotide/oligosaccharide-binding (OB) fold with similarity to the mammalian shelterin component TPP1 [82,83]. TPP1 binds to the C-terminus of POT1, a ssDNA binding protein, and facilitates its recruitment to the telomere where it functions to protect the end of the chromosome from degradation or fusion events [84-86]. TPP1 is also a telomerase processivity factor, stimulating telomere repeat addition *in vitro* [87,88] and stimulating recruitment of telomerase *in vivo* [89-91]. Est3p was reported to increase the repeat addition processivity of telomerase in *Saccharomyces castelli*, a close relative to *S. cerevisiae* [92], consistent with the suggestion that Est3p may be a homolog of TPP1. *S. cerevisiae* Est3p also stimulates telomerase activity *in vitro,* although these experiments were done under conditions that did not measure processivity [63]. These results continue to support the prevailing notion that Est3p is structurally and functionally related to TPP1. These studies are beginning to tease apart the function of Est3p in the telomerase complex.

Telomerase Recruitment Protein (*EST1*)

S. cerevisiae EST1 encodes a highly basic 81 kDa protein that was the first telomerase component cloned in yeast [38]. Like Est3p, Est1p is not required for *in vitro* telomerase activity but is necessary for *in vivo* activity. Sequence alignment of Est1p homologs across species revealed a conserved tetratricopeptide repeat (TPR) in the N-terminus of the molecule (Figure 4). TPR domains are often involved in protein-protein interactions and several *EST1* mutants that map to this region are defective for assembly with the complex [93]. Est1p recruits telomerase to the telomere through its direct interaction with the ssDNA binding protein Cdc13p. Est1p exhibits three biochemical activities: interaction with single-stranded telomeric DNA, association with *TLC1* RNA, and interaction with the ssDNA binding protein Cdc13p (Figure 4).

Titrating purified Est1 protein into an *in vitro* telomerase extension assay stimulates telomerase activity, in a manner similar to that observed with Est3p [94]. Est1p binds directly to the *TLC1* RNA through three secondary structural elements within the sub-helix IVc: a pentanucleotide bulge, an adjacent internal loop, and a single-stranded region at the base of the sub-helix (Figure 3) [51,52]. Interestingly, when the stimulation assay was performed in the presence of *TLC1* molecules lacking this structural element, the stimulation of telomerase activity was unchanged. This result suggests that telomerase activity is only partially dependent upon Est1p binding to *TLC1* RNA and that other, possibly protein-protein, interactions are important for stimulating activity [94]. It was reported that Est1p exhibits weak but specific affinity for single-stranded telomeric DNA. This DNA binding activity maps to a 130 amino-acid (aa) region in the C-terminus of the protein (Figure 4) and requires a free 3' terminus,

suggesting that it specifically mediates the recognition of chromosome ends [95]. However, stimulation of *in vitro* activity was not affected when DNA molecules lacking a sufficient 3' overhang for Est1p interaction were used. Est1p stimulated the DNA extension irrespective of when telomerase was assembled with the DNA, suggesting that Est1p does not bind to telomeres during DNA extension, but instead tethers the DNA bound telomerase and modulates overall enzymatic activity independent of direct DNA binding [94].

The primary regulatory role for Est1p is to recruit telomerase to the site of action. This recruitment function is accomplished through the direct protein-protein interaction between Est1p and the ssDNA binding protein Cdc13p [96-100]. As a test of this model, telomerase was recruited to non-telomeric sites using a Cdc13p-Est1p fusion construct. This construct was able to relocalize the catalytic subunit, Est2p, leading to the conclusion that Est1p exhibits a recruitment function and does not merely activate the complex by binding [98]. Est1p's recruitment function can be bypassed by tethering the enzyme to the telomere through expression of a Cdc13p-Est2p fusion construct. In this context, cells can survive without *EST1* but die if *EST3* is deleted, providing additional evidence for this recruitment model and further suggesting that Est3p has function(s) other than recruitment. When the Cdc13p-Est2p fusion is expressed in a wild-type background, telomeres get substantially longer due to excessive recruitment of the telomerase complex to telomeres. Although deletion of Est1p is tolerated in cells expressing the fusion protein, telomere overelongation is not observed. This result suggests that Est1p has a function independent from recruitment. One possibility is that Est1p stimulates the recruitment of Est3p into the complex. Consistent with this idea,

Est1p and Est3p directly interact *in vitro* [81]. Additionally, this hypothesis is consistent with work from a previous student in the Friedman laboratory, Dr. Jennifer Osterhage. She found that overexpression of Est1p resulted in an increased association of Est3p in the telomerase complex. She went on to demonstrate that Est1p is both necessary and sufficient for Est3p recruitment to the telomerase complex [101].

G-quadruplexes are known to form at telomeres because the telomeric sequence is highly guanine-rich. These structures are formed from G-quartets, four guanines arranged into a cyclic orientation. These G-quartets can then stack on top of each other to result in a G-quadruplex structure that is stabilized with a potassium or sodium ion in the central core (reviewed in [102]). Est1p has been implicated in the induction of G-quadruplex formation *in vitro*. This activity maps to a region near the C-terminus of the protein and overlaps with the region involved in DNA binding (Figure 4). Mutations that disrupt this function exhibit cellular senescence *in vivo*, suggesting that G-quadruplex formation is a positive regulator of telomerase activity. Consistent with the hypothesis that Est1p activates telomere-associated telomerase [103], Est1p can unwind DNA-RNA heteroduplexes and concomitantly produce G-quadruplexes [104]. Furthermore, fusion of Est1p, but not Est2p, to Cdc13p can rescue the ts phenotype of *yku80*Δ, important for chromosome capping, suggesting a role for Est1p in the protection of telomeres [105]. In support of this role, the Est1p homolog in humans, hEST1A, has been implicated in the protection of chromosome ends [106]. Both unwinding and telomere protection are compromised by mutations that affect G-quadruplex formation [104,105]. These studies suggest a model for the function of Est1p-dependent G-quadruplex formation: Est2p is telomere-associated through an interaction with the *TLC1* RNA and yKu heterodimer

(see "Cell Cycle Regulated Assembly and Recruitment of Yeast Telomerase") [54], Est1p binds to the telomere end and unwinds the *TLC1* RNA-DNA heteroduplex, causing dissociation of the Est2p-*TLC1* complex. Est1p then forms G-quadruplex from the G-rich ssDNA, simultaneously protecting the telomere end from recombination events and facilitating telomerase recruitment/activation at the terminal 3' end [104,105].

Regulation of Yeast Telomeres

Telomere structure

Unlike human telomeres that are composed of perfect repeats, *S. cerevisiae* telomeres are made up of degenerate repeats with a consensus sequence $G_{2\text{-}3}(TG)_{1\text{-}6}$, but simply referred to as $G_{1\text{-}3}T$. The sequence heterogeneity arises from use of the template sequence 3'-^{484}ACACACACCCACACCAC^{468}-5'. Since a DNA substrate that ends in a TG has multiple possibilities for alignment, the number and sequence of nucleotides that telomerase synthesizes each round can, and most likely will, vary. Additionally, the probability of incorporation decreases as synthesis reaches the 5' boundary of the template. For example, there is only a 53% chance of copying the ^{471}CC^{470} di-nucleotide located near the end of the template [107,108]. Nucleolytic degradation and the continual ebb and flow resulting from the end-replication problem in combination with telomerase activity may also influence the heterogeneity of the telomere sequence and keep the distal portion of the telomere highly dynamic.

S. cerevisiae telomeres contain sub-telomeric repeats located immediately centromeric to the G-rich tract. This region is composed of repetitive sequences called X

and Y' elements. All chromosomes have an X element, while ~50-65% of chromosomes have one or more Y' elements separated by $G_{1-3}T$ sequence. While these elements are not conserved even within closely related species, they are a useful readout for telomerase-independent telomere maintenance because the Y' elements are amplified during such time. This phenomenon will be discussed in the following section.

To date, all telomeres examined end with a single-stranded 3'-overhang of the G-rich strand, called the G-tail. However, the mechanism through which the overhang is generated is incompletely understood (reviewed in [109]). This structure is critical for cell survival and is thus under strict regulation to ensure its fidelity. In *S. cerevisiae*, this G-tail is short (12-14 nt) throughout the cell cycle. During DNA replication, the lagging strand contains an overhang upon removal of the terminal RNA primer but the leading strand is blunt ended. Following passage of the replication fork in late S phase, the 3'-overhangs on both leading and lagging telomeres are transiently increased in length [110,111]. This transient elongation is due to exonucleolytic digestion of the 5'-strand [17,110,112]. This resection is dependent upon the MRX (Mre11p-Rad50p-Xrs2p) complex in yeast [111,113]. However, this 5' resection of the C-strand utilizes a redundant mechanism, as G-tails are shorter but not eliminated in the absence of *MRE11*, the exonuclease of the MRX complex [111]. Telomeric C-strand resection is also dependent upon Sgs1p, a member of the RecQ DNA helicase family; Sae2p, an endonuclease that undergoes cyclin-dependent kinase (CDK) phosphorylation critical for activity; the exonuclease Exo1p; and the nuclease/helicase Dna2p that is involved in long flap processing during removal of the RNA/DNA primers in Okazaki fragments [114-117]. Consistent with these findings, passage of the replication fork, the completion of S

phase, and CDK activity were previously implicated as being necessary for 3' overhang formation at both native and *de novo* telomeres [111,112,118,119]. In the absence of both *SAE2* and *SGS1*, C-strand resection was nearly undetectable, suggesting that these two proteins work in separate but redundant pathways involved in overhang formation. Exo1p and Dna2p acquire access to the telomere after the initiation by Sae2p or Sgs1p [117]. Therefore, the resection of telomeric 5' strands involves several redundant pathways to ensure proper formation.

Protection of chromosome ends

As discussed above, the telomere end exists as a single stranded 3'-overhang throughout the cell cycle. There are several proteins that are necessary for capping the telomere and ensuring the fidelity of the chromosome end. Loss of these factors can result in telomere uncapping and expose the termini to unregulated resection and/or catastrophic chromosome end-to-end fusions. As discussed above, the Est1 protein has been implicated in the protection of chromosome ends. Here is a discussion of two additional pathways of telomere protection.

In yeast, the 3'-overhang is bound by the ssDNA binding protein Cdc13p in a sequence-specific manner. Cdc13p contributes to both telomere capping and telomerase recruitment through its interaction with Est1p. It is essential for protecting the chromosome termini from degradation; loss of *CDC13* function results in excessive resection of the 5' strand, resulting in a Rad9p-mediated cell cycle arrest. Cdc13p is a component of the CST protein complex along with Stn1p and Ten1p. The Stn1 protein was found as a suppressor of the *cdc13-1* temperature sensitive (ts) allele and Ten1p was

identified by its ability to rescue the ts phenotype of *stn1-13* [120,121]. Like with Cdc13p, a defect in either *TEN1* or *STN1* results in a Rad9p-dependent arrest. Stn1p and Ten1p may also act independently from Cdc13p since overexpression of these two components can suppress the lethality of a *CDC13* deletion [122-124]. Cdc13p interacts with the telomeric 3' overhang through a single OB fold, called the DNA-binding domain (DBD), located between residues 497 and 694 of the 924 aa protein [125,126]. This domain is structurally similar to another ssDNA binding protein found in *S. pombe* and many other higher eukaryotes, POT1 [84,125]. As introduced above, POT1 is a binding partner with TPP1, a potential homolog to Est3p. Stn1p's N-terminal domain interacts with Ten1p while the C-terminal domain interacts with Cdc13p [127]. The CST complex plays the primary telomere capping function in *S. cerevisiae*.

Although one of the main functions of telomeres is to prevent non-homologous end-joining (NHEJ) of chromosomal ends, the main effector of this pathway, Ku, also surprisingly binds to telomeres. The yKu heterodimer, consisting of a 70 kDa and 80 kDa subunits, binds with high affinity to dsDNA ends in a sequence-independent manner [128]. yKu binds the telomere end to serve as a protective cap and also binds directly to the telomerase RNA molecule. It binds to the extreme terminus, near the double-single stranded junction. The heterodimer is constitutively associated with telomeres and binds in a ring-like shape, threading the DNA through the channel. In the absence of yKu function, the ssDNA 3'-overhang is much longer than normal, suggesting that yKu is important for telomere end protection, even in the presence of a wild type CST complex. This elongation of the ssDNA is due to increased nucleolytic digestion of the 5' strand since deletion of the exonuclease Exo1p results in a partial rescue. Increased temperature

exacerbates this resection phenotype. These results clearly suggest that yKu is important for preventing nuclease attack of the telomeric end. Additionally, separation-of-function alleles of yKu that impart compromised end-structure but are unaffected for *TLC1* binding have been identified. Therefore, yKu exhibits three functional roles: *TLC1* interaction, telomere protection, and repair of double-strand breaks.

Telomere length homeostasis

Stable telomere length is governed by the balance of activities that generate telomeric DNA, such as telomerase, and events that result in telomere loss, such as nuclease digestion and semi-conservative replication. Telomere length is regulated in part by several proteins that interact with the telomere and influence telomerase activity. *S. cerevisiae* Rap1p binds to double-stranded telomeric DNA via two tandem myb-like DNA-binding domains. While bound to telomeres, Rap1p enhances telomeric silencing and negatively regulates telomere length through its C-terminus. Regulation by Rap1p is essentially a counting mechanism to determine if the telomere is in need of elongation. The laboratory of Dr. David Shore illustrated this function by inserting an 80 bp telomeric tract upstream of a native telomere. Even though a 40 bp linker separated this inserted sequence from the normal telomere, the native telomere shortened, suggesting that the newly inserted sequence was being "counted" as part of the whole telomere. Inversion of this inserted DNA resulted in the native terminal telomere being elongated, consistent with a requirement for correct orientation. Since it was known that Rap1p binds to telomere duplexes, the authors asked whether this protein was playing a role in telomere length regulation. Either Rap1p or its C-terminus alone was artificially tethered

(via the Gal4 DNA binding domain) to an area adjacent to the telomere tract. Once again, the native telomere shortened to an extent proportional to the number of Rap1p molecules present. This work demonstrated that Rap1p molecules are "counted" to determine the length of the telomere. When the telomere is long, many Rap1p binding sites are bound and telomerase does not extend this chromosome end [129]. Two proteins, Rif1p and Rif2p, interact with the Rap1p C-terminus. In fact, tethering these two proteins to telomeres (as done with Rap1p) also shortens telomeres. Therefore, while Rap1p is bound to the telomere itself, the effectors of this negative feedback loop are its C-terminal binding partners Rif1p and Rif2p.

While the negative feedback loop involving Rap1p was established, it remained unresolved if the regulation was achieved by modulating the probability with which telomerase initiates synthesis or by regulating the extent to which telomerase acts once elongation begins. To investigate this question, a new method was developed that allows the monitoring of telomeres within a single cell cycle. This single telomere extension (STEX) assay method provided insight into both the frequency and extent of telomere addition. After monitoring the number of individual telomeres that are extended and the number of nucleotides that are added, the Lingner lab established that only ~10% of telomeres get elongated in a single cell cycle. The amount of addition occurring at different telomeres was quite varied and was, for the most part, independent of telomere length. However, the probability of telomere elongation was inversely proportional to the beginning length of the telomere. Deletion of either *RIF1* or *RIF2*, important for the negative feedback loop described above, resulted in a larger percentage of telomeres being elongated in a single cell cycle [130]. This observation suggests that telomerase is

regulated at the initiation point, with telomeres existing in an extendable or non-extendable state.

The shortest telomeres are preferentially and more extensively elongated by telomerase. To elucidate the reason for this extensive elongation, a modified STEX assay was developed to allow monitoring of telomerase repeat addition processivity *in vivo*. This assay used cells expressing two different *TLC1* template molecules. Incorporation of a string of one type of template sequence demonstrated processivity, while an interspersion of the two templates would indicate synthesis by non-processive enzymes. Using this assay, it was determined that telomerase is non-processive at most wild-type telomeres, but switches to a processive mode of synthesis on critically short telomeres, resulting in extensive telomere elongation. Tel1p kinase, the *S. cerevisiae* ATM ortholog involved in the DNA damage response, is required for this enhancement of processivity at critically short telomeres [131]. It remains unclear how Tel1p exerts this affect on processivity.

In the absence of Rif1p or Rif2p, telomeres over-elongate in a Tel1p-dependent manner, suggesting Tel1p plays a positive role in telomere length regulation [132]. In support of this role, Tel1p specifically associates with short telomeres in a manner dependent upon the C-terminus of Xrs2, a component of the MRX complex involved in DNA damage repair. In the absence of Rif2p, Tel1p no longer shows a preference for short telomeres [133], suggesting low Rif2p levels mark short telomeres for elongation. Additionally, preferential association of the telomerase subunits Est2p and Est1p with short telomeres is Tel1p-dependent [134]. Together, these data are consistent with the following model for preferential elongation of short telomeres (Figure 5): 1) as telomeres

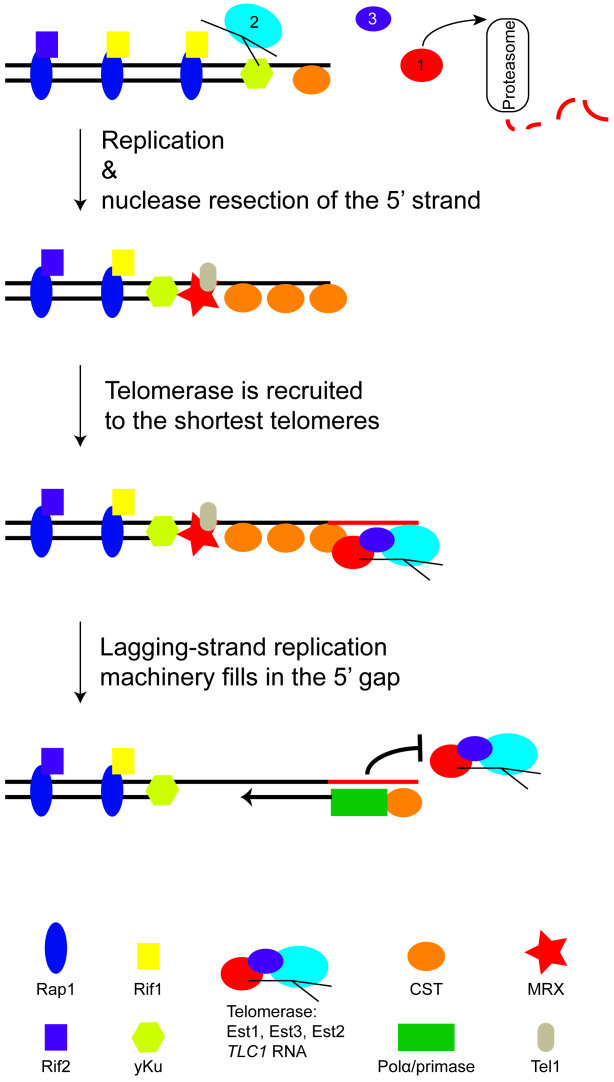

Figure 5. Cell cycle regulated recruitment of telomerase.
In G1 phase, the catalytic subunit Est2p associates with the telomere in a manner that requires the *TLC1*-yKu interaction. While the exact mechanism remains unclear, it is hypothesized to involve a handing off of yKu from *TLC1* to the telomere, since yKu is unable to bind the RNA and DNA simultaneously. During this time, Est1p undergoes proteasome-dependent degradation, preventing Est3p assembly with the complex. Following replication in S phase, the 3' overhang is elongated by resection of the 5' strand by MRX, Sgs1p, Sae2p, Exo1p, and Dna2p (not shown for simplicity). The shortest telomeres have a decreased amount of Rif2p, which is sensed by Tel1p, marking these ends for elongation. This elongation of the 3' overhang allows additional CST (Cdc13p-Stn1p-Ten1p)-complex association, which recruits the telomerase complex through the direct interaction between Cdc13p and Est1p. Following telomere elongation by telomerase, the lagging-strand replication machinery inhibits telomerase and fills in the gap.

shorten, the Rap1p/Rif2p concentration decreases and allows the MRX complex to associate with telomeres, 2) Tel1p is recruited to these short telomeres and phosphorylates some telomere protein (possibly Cdc13p [135]), and 3) telomerase is recruited and actively elongates the telomere.

Cell cycle regulated assembly and recruitment of yeast telomerase

Telomerase is able to synthesize telomeric repeats at a double-strand break that is induced adjacent to a telomeric seed when the cells are arrested in G2/M phase but not when arrested in G1 phase [136]. Additionally, a telomere that has been artificially shortened through an induced recombination event is not elongated when cells are arrested in G1 phase but is elongated during late S/G2 phase [137]. These two studies showed that telomerase activity is restricted to a window of time from late S phase through G2/M phase, suggesting there are mechanism(s) in place to prevent it from elongating telomeres at other times. Consistent with this, CDK activity (which is very low in G1 phase) and passage of the replication fork are associated with telomerase addition [118,119,136]. As described above, the telomere end structure changes through the cell cycle (Figure 5). After passage of the replication fork, the short single-stranded 3'-overhang (G-tail) gets longer due to exonuclease activity on the complementing 5'-strand (Figure 5) [17,112,118,119]. This lengthening of the ssDNA portion of the telomere exposes additional binding sites for Cdc13p, as it requires as little as 11 nt to bind efficiently [39,138,139]. Since Est1p binds directly to Cdc13p and Est2p, this increased association to the telomere recruits the telomerase complex [81,96-100]. The

mechanism(s) of temporal regulation on yeast telomerase intrigued researchers and much effort has been expended toward understanding it.

Utilizing chromatin immunoprecipitation (ChIP) experiments to examine the temporal association of telomerase components with the telomere, it became apparent that these telomere proteins exhibit cell-phase specific binding patterns. Cdc13p is associates with the telomere throughout the cell cycle but its binding increases dramatically during late S phase, which is expected as the G-tails are longer (Figure 5) [103]. The telomerase subunit Est1p and Est3p associate solely in late S/G2 phases [81,103]. However, it was the catalytic subunit that was the most intriguing. Est2p exhibits biphasic binding to the telomere during late S/G2 as well as in G1 phase, when telomerase is inactive *in vivo* [103]. The two peaks of binding are a result of two modes of Est2p recruitment to the telomeres.

During G1 phase, Est2p and *TLC1* RNA are located at the telomere through an interaction with the yKu heterodimer [54]. However, because yKu is unable to simultaneously bind DNA and RNA *in vitro*, the dependence upon yKu for this positioning is hypothesized to be due to yKu associating with *TLC1* RNA and then handing it off to bind to the telomere, for which it has a higher affinity [55]. Est1 protein levels are very low during G1 phase, preventing its association with the telomere (Figure 5) [101,103]. However, Est1p levels stabilize as cells proceed into late S phase, when telomeres are replicated, and can now associate with the telomere due to its direct interaction with Cdc13p, also peaking at this time [100,101,103,137]. The concomitant association of Est1 and Est3 proteins with the telomere supports the finding that Est1p is necessary and sufficient for Est3p recruitment into the complex (Figure 5) [81,103].

Since the stabilization of Est1 protein levels with the proteasome inhibitor MG132 did not result in telomere addition during G1 phase [101], regulated degradation is not the entire reason telomerase is inactive at this time. There must be an additional mechanism that restricts telomerase activity to late S/G2 phase. The work in this thesis will be focused on the mechanism that targets Est1p for degradation during G1 phase.

Telomerase-independent telomere maintenance

In a last ditch effort to maintain telomere lengths that have become critically short due to some deficiency in telomerase activity, a small percentage of an *S. cerevisiae* population will switch to an alternative lengthening of telomeres (ALT) mechanism. The ALT pathway utilizes homologous recombination to extend telomeres, and can therefore be inhibited by deletion of the central recombination gene *RAD52*. Cells that have switched to an ALT pathway are termed "survivors", for they survived the senescence fate of their brethren. There are two types of *RAD52*-dependent pathways that yield survivors: Type I and Type II events. Type I survivors have amplified their Y' elements (both the long and short forms) or spread them to chromosomes where Y' elements were previously lacking. Intriguingly, a very short terminal telomere tract remains present, but the mechanism of its maintenance remains unresolved. It is possible that a strand invasion from a shorter telomere into a longer telomere could be followed by DNA synthesis, using the telomere tracts as a template. Type II survivors have undergone rolling-circle replication, which leads to substantial lengthening of their telomeres. Type II survivors arise much more slowly in the population, but grow faster than Type I once established. Therefore, in liquid culture, Type II survivors tend to out-compete Type I

survivors. It is also common for survivor clones to exhibit a mixture of Type I and II survivor traits (reviewed in [140]).

Protein Degradation

Within a cell, protein levels are determined by the rates of synthesis and turnover. Selective proteolysis is important for sustaining normal cellular processes. In yeast, the lysosome/vacuole and the proteasome are the two major pathways involved in protein degradation. Lysosomes contain a variety of enzymes that degrade proteins and other molecules delivered by endocytosis, phagocytosis, or autophagy. Nevertheless, the majority of short-lived proteins are degraded by the proteasome after being post-translationally modified with ubiquitin. In eukaryotes, the ubiquitin-proteasome pathway (UPP) is essential for many fundamental cellular processes, such as cell cycle progression, protein quality control, DNA repair, and signal transduction.

The ubiquitin-proteasome pathway

In 1975, an 8.5 kDa polypeptide was isolated from bovine thymus and found to be expressed in many other tissues and organisms, including guinea pig, mouse, chicken, fish, plants, and fungi. The widespread expression profile and the original finding that this peptide stimulated differentiation of thymocytes and the activity of adenyl cyclase (though these functions were later debunked) led this protein to be called UBIP, for ubiquitous immunopoietic polypeptide [141], or ubiquitin.

In 1953, Dr. Melvin Simpson showed that proteolysis requires energy but the reason remained unclear [142]. In the late 1970's, research from Dr. Avram Hershko, his

graduate student Dr. Aaron Ciechanover, and collaborator Dr. Irwin Rose showed that proteolysis in rabbit reticulocyte lysate (RRL) required a heat-stable polypeptide they named APF-1 (ATP-dependent proteolysis factor 1) in addition to a crude fraction of high molecular-weight (now known to contain the proteasome, see below) [143,144].

^{125}I-labeled APF-1 was converted to a higher molecular weight in an Mg^{2+} and ATP-dependent manner when incubated with the crude fraction. Additionally, this linkage was stable and covalent since it survived high pH and denaturation with 0.1 M NaOH. Examination of these higher species by SDS-PAGE revealed that APF-1 was conjugated to many different proteins [145]. APF-1 was subsequently identified as ubiquitin [146]. To show that this covalent attachment of ubiquitin was related to proteolysis, the authors showed that they could detect covalent attachment to various degradable proteins, such as lysozyme and globin. Importantly, they showed that the ubiquitin attachment occurs at a lysine residue, multiple ubiquitin attachments can occur on a single substrate protein using a processive enzymatic mechanism, and that depletion of ATP results in a return to un-modified protein, demonstrating the dynamic nature of this attachment [147]. From this work, a model was proposed that is still accurate today: ubiquitin is covalently attached to substrate proteins that are then delivered to a specific protease (proteasome), resulting in degradation and release of free ubiquitin (via the action of deubiquitinating enzymes).

Dr. Hershko and colleagues then determined that the mechanism of ubiquitin attachment requires the sequential action of three enzymes [148,149]. First, the C-terminal glycine residue of ubiquitin is activated in an ATP-dependent reaction that results in a thiol-ester linkage to a cysteine residue in the active site of the E1 activating

enzyme. This activated ubiquitin is then transferred to a cysteine residue of the E2 conjugating enzyme. Finally, the ubiquitin is linked in an iso-peptide bond to a lysine residue of a substrate protein specifically bound to an E3 ubiquitin ligase. This substrate linkage can occur via a direct transfer from the E2 or following an additional transfer to a cysteine residue of the E3. By successively adding ubiquitin moieties to the lysine residues of previously conjugated ubiquitin molecules, a polyubiquitin chain is formed. This chain may then be recognized by the 26S proteasome (reviewed in [150]). Drs. Avram Hershko, Aaron Ciechanover, and Irwin Rose were awarded the Nobel Prize in Chemistry in 2004 for their work on the basic functions and mechanism of ubiquitin-mediated proteolysis.

The 26S proteasome, a large cylindrical multi-subunit protein complex found in the cytoplasm and nucleus of all eukaryotes, recognizes substrate proteins tagged with ubiquitin and subsequently cleaves them into short polypeptide fragments. The 26S proteasome contains a 20S catalytic core particle (CP) composed of 4 rings of 7 subunits each, and either one or two 19S regulatory particles (RP) composed of 19 subunits. The 19S RP is further divided into a lid and base. The lid of the 19S RP recognizes ubiquitinated substrates and deubiquitinates them. The base contains ATPase subunits that interact with and open the gateway into the 20S CP, bind to and unfold substrate proteins, and translocate the substrate into the 20S CP. The proteolytic active sites are located on the inside surface of the 20S CP and consist of chymotrypsin-like, trypsin-like, and peptidylglutamyl-peptide hydrolyzing activities. In summary, the substrate is recognized by its ubiquitin chain by the lid, deubiquitinated and bound by protein-protein interactions in the base, unfolded, transferred into the 20S catalytic core, proteolytically

cleaved at the three protease active sites, and released through the other end as small peptides (reviewed in [151]).

Temporal regulation of protein destruction is a key aspect of cellular metabolism. Some proteins are very long-lived while others are quickly degraded. In yeast, there is a single ubiquitin activating enzyme (E1; Uba1p), thirteen ubiquitin conjugating enzymes (E2; Ubc1p-Ubc13p), and over eighty ubiquitin ligases (E3) [152]. The large number of E3s determines the exquisite sensitivity of substrate recognition, either alone or in conjunction with its partner E2. Here I will focus on one particular E3 ubiquitin ligase, the Anaphase Promoting Complex (APC), which has been studied in detail.

The anaphase promoting complex

The APC, also called the cyclosome, is a multi-subunit cullin-RING (really interesting new gene) E3 ubiquitin ligase. The APC is essential for cell cycle progression, regulating timely transit through mitosis and entry into S phase. To achieve this precise temporal regulation of the cell cycle, the substrates of the APC must be degraded at a specific time. This pattern of degradation is achieved by regulating both the recognition of these substrates and the timing of APC activity.

Subunit composition

In *S. cerevisiae,* the APC is composed of 13 core protein subunits (Apc1, Apc2, Apc3/Cdc27, Apc4, Apc5, Apc6/Cdc16, Apc8/Cdc23, Apc9, Apc10/Doc1, Apc11, Apc13/Swm1, Cdc26, and Mnd2). Additionally, two substrate specificity factors (Cdc20p and Cdh1p) also transiently associate with the complex. Apc2 (cullin;

scaffolding protein) and Apc11 (RING-finger; E2 interacting protein) make up the catalytic core of the complex, exhibiting robust *in vitro* ubiquitination activity but no substrate-specificity [153-155]. The majority of the core subunits are essential (8 of 13) making their characterization and determination of their arrangement in the complex difficult. To overcome this challenge, Dr. David Toczyski and colleagues engineered a yeast strain in which the APC was rendered non-essential. This strain was generated through the deletion of securin/*PDS1* and *CLB5,* and overexpression of the CDK inhibitor *SIC1*. In strains lacking APC activity, Clb/CDK activity continues to oscillate during the cell cycle even though Clb protein levels remain constant. This argues that oscillating Sic1 activity is sufficient to trigger the feedback loops necessary for bi-stable Clb/CDK activity. These results suggested that the APC has two obligatory substrates in yeast: securin, whose degradation is required for sister chromosome separation during mitosis, and mitotic B-type cyclins (Clb1p-Clb6p) [156].

The authors went on to utilize this strain for elucidating the subunit arrangement of the complex *in vivo*. By deleting subunits singly and monitoring which of the remaining subunits still associated, the authors were able to propose an architectural map of the *S. cerevisiae* APC (Figure 6). The largest subunit, Apc1p, acts as a scaffold protein, bridging two sub-complexes. One sub-complex contains proteins Apc2, Apc11, and Apc10/Doc1, with Apc2 independently tethering the other two to Apc1p. The second sub-complex contains the TPR proteins Apc6/Cdc16, Apc8/Cdc23 and Apc3/Cdc27, which associate with Apc1 via Apc4 and Apc5. This work also demonstrated that binding of the activator Cdh1p depends upon both Apc2p and Apc3/Cdc27p, and an internal motif called the C-box [157]. From other studies, it was

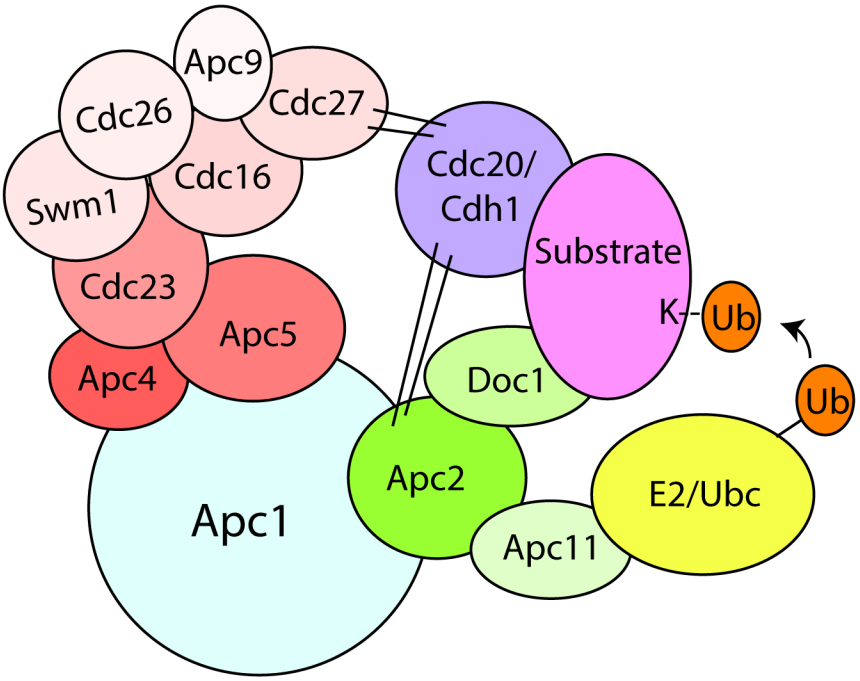

Figure 6. Schematic of the Anaphase Promoting Complex (APC).
The APC is composed of multiple protein subunits and the relative orientation of these subunits within the complex is depicted here. Apc1p (light blue) is a large scaffolding protein that bridges two sub-complexes: the TPR protein containing sub-complex (shades of red) and the substrate/E2 interacting sub-complex (shades of green). The activator protein (Cdc20/Cdh1; blue) interacts with the substrate protein (pink) through its degron motif and with the APC core through interactions with both Cdc27p and Apc2p. Apc11p associates with the E2 ubiquitin conjugating enzyme (Ubc). Doc1p interacts with the substrate protein and is necessary for the efficient transfer of ubiquitin (Ub) from the E2 onto the lysine residue(s) of the substrate protein or previously conjugated ubiquitin moieties.

shown that Apc9p is required for Apc3/Cdc27p association [158,159] and Apc13/Swm1p stabilizes the association of Apc3/Cdc27p, Apc6/Cdc16p, Apc9, and Cdc26 with the other complex subunits [160], suggesting that Apc9p and Swm1p associate with the TPR sub-complex, with Apc9p interacting with Cdc27p and Swm1p reinforcing the entire sub-complex. Mnd2p interacts with protein subunits Apc1, Apc5 and Apc8/Cdc23 *in vitro* [161]. Mnd2p inhibits premature activation of the APC in meiosis and mitosis, by interfering with the Ama1p meiotic activator [162,163].

Structure of the APC

The crystal structure of several protein subunits of the APC has been determined. The Apc10/Doc1 protein structure is composed of a Doc homology domain that forms a β-sandwich structure [164]. Mutations within this region perturb APC-activity on those substrates containing D-boxes (one of several sequences found in target proteins, see below), suggesting the Doc domain is important for substrate recognition [165]. The structure of an Apc6/Cdc16-Cdc26 complex showed that Apc6/Cdc16p forms a homo-dimer via its TPR motifs made from anti-parallel α-helices. Apc6/Cdc16p also interacts directly with Cdc26p to form a hetero-tetramer, generated through the interaction of their respective TPR motifs [166]. The crystal structure of the N-terminus of Apc3/Cdc27p revealed that, like Apc6/Cdc16p, this protein is able to form a homo-dimer via direct interactions between the TPR motifs. The C-terminal portion of Apc3/Cdc27p is also predicted to adopt an overall fold similar to that of Cdc16p [167]. These studies support findings that the TPR-containing subunits are present in multiple copies per complex [168-170].

The overall structure of the intact APC has been determined for *S. cerevisiae*, *S. pombe*, *X. laevis*, and humans using cryo-electron-microscopy (EM) [168-172]. The specific details of the structures differ amongst species, but the overall shape is triangular, with a cavity at the core. Though the cryo-EM structure revealed the overall shape of the enzyme, a more detailed analysis was used to determine the location of subunits within the intact complex. Using antibody labeling, nano-gold labeling, and/or subunit deletions, the location of some subunits within the complex has been determined [168-172]. In *S. cerevisiae*, these studies are in good agreement with the work from the Toczyski laboratory, discussed above [157]. For example, the catalytic core of the complex (Apc2 and Apc11) lies in close proximity to Apc1 within the intact structure, while the TPR-containing subunits (Apc6/Cdc16, Apc8/Cdc23, and Apc3/Cdc27) are present in multiple copies and are located peripherally in the complex (Figure 6) [170,171].

Substrate recognition and the role of co-activators

The APC utilizes two proteins, cell division cycle 20 (Cdc20p) and Cdc20-homolog 1 (Cdh1p), to activate the APC core complex. Without these activators, the APC is unable to bind most substrates. Therefore, the role of Cdc20p and Cdh1p is proposed to be substrate-recognition and recruitment to the APC core. The combination of purified APC complexes with *in vitro* transcribed/translated (IVT) activators results in a shift in size on native gels, indicating that a larger complex has been formed. Furthermore, addition of IVT-produced substrate results in a super-shift, indicating formation of a ternary complex [173].

APC-dependent degradation depends upon specific degradation motifs. The best characterized are the destruction box (D-box) and the KEN box motifs. The D-box was first identified in 1991 by Dr. Marc Kirschner's laboratory and has a consensus sequence of RxxLxxxxN (Arg-any two amino acids-Leu-any four amino acids-Asn) [174,175]. The 'R' and 'L' of this sequence are invariant amongst substrates, but the 'N' is much less conserved [176]. The KEN box motif was likewise discovered in Dr. Kirschner's lab [177]. Consistent with the hypothesis that co-activators bind to substrates, the ternary complex obtained from incubation of purified APC with IVT-produced activator and substrate depends upon an intact D-box or KEN box degron signal [159]. Furthermore, several substrates and degron-containing peptides have been shown to directly associate with the activator proteins [178-182]. These studies all suggest that the role of the activator is to physically associate with the substrate.

Several studies have also suggested that substrate recognition can be facilitated through direct association of the substrate with the APC core. These results involve the Apc10/Doc1p subunit. Mutation of *APC9/DOC1* reduces substrate binding and reaction processivity (the ability to add ubiquitin moieties) in a D-box dependent manner, but these mutations do not affect activator binding [165,183,184]. These results suggest that the substrate may contact both the activator and the APC core through the Apc10/Doc1p subunit. To explore this model of this multi-contact model for substrate binding, two groups independently determined the structure of the intact APC in complex with the activator subunit and substrate.

Dr. Jan-Michael Peters' laboratory used cryo-negative EM to determine the structure of an intact *S. cerevisiae* APC core bound to both Cdh1p and a fragment (~200

aa) of Hsl1p that contains the D-box and KEN-box degrons necessary for APC recognition [171]. To confirm the specificity of observed interactions, the authors also performed these analyses with a fragment containing mutated degrons and in the absence of Cdh1p. The authors found the binding of the Hsl1p fragment to the APC only occurred when the D-box was intact and that this interaction was greatly enhanced by the presence of Cdh1p. Furthermore, this fragment underwent ubiquitination, indicating this is a functional substrate. Comparison of the structures obtained both with and without substrate revealed a substrate-dependent density located between Cdh1p and Apc10/Doc1p, consistent with the role of both the activator and the Apc10/Doc1p subunit in substrate binding.

A similar technique was used by Dr. David Barford's laboratory to determine the substrate-binding sites [185]. The authors used cryo-EM and determined the structure of the APC in complex with *S. cerevisiae* Cdh1p and the same Hsl1p fragment used above. The results were similar: Cdh1p and Apc10/Doc1p are bridged by density that is dependent on addition of the substrate. However, these authors went further in their exploration into substrate-interactions by determining precisely how the degron motifs contributed to these changes. They repeated the cryo-EM using very short D-box peptides, ~18 nt in length, to serve as their 'substrate'. This peptide bound and generated very similar structural changes to the Hsl1p fragment, but the bridging between Apc10/Doc1p and Cdh1p was reduced, confirming that this density arises from the substrate peptide. As seen above, this binding was also eliminated upon mutation of the D-box within this peptide. Surprisingly, however, a KEN-box peptide does not bridge Apc10/Doc1p and Cdh1p, arguing that this is a D-box specific interaction. The authors

also showed by NMR that Apc10/Doc1p makes direct contact with the D-box but not KEN-box peptides. These two studies support the model in which the substrate makes multiple contacts within the APC, with the activator protein and the core subunit Apc10/Doc1p. The latter study further suggests that this model may specifically apply to D-box containing substrates.

Regulation of activity through the cell cycle by phosphorylation

APC activity is regulated through the cell cycle. The complex is active during mitosis through G1 phase. The phosphorylation state of both the APC core subunits and co-activators is the major mechanism of regulation. During mitosis, CDK activity is high, resulting in the phosphorylation of core subunits Apc6/Cdc16, Apc8/Cdc23, Apc3/Cdc27, and Apc1 [186-188]. Phosphorylation of the complex stimulates the association of Cdc20p, thus activating the ligase. However, at the same time, phosphorylation of Cdh1p prevents its association with the complex. This antagonistic phosphorylation stipulates the order in which the APC is activated: APC^{Cdc20p} in mitosis and APC^{Cdh1p} in G1 phase. The phosphatase that relieves Cdh1p phosphorylation, Cdc14p, is sequestered in the nucleolus for the majority of the cell cycle. Cdc14p is released upon signals from the FEAR (Cdc-fourteen early anaphase release) network or MEN (mitotic exit network) during anaphase, after chromosome separation (reviewed in [189]). MEN mutants arrest in mitosis with high CDK levels (such as *cdc15-2*), while mutants of the FEAR network delay mitotic exit but do not arrest, indicating that this pathway is not essential.

Direct phosphorylation of substrates can also regulate APC activity. Cdc6 degradation is inhibited by phosphorylation events near the D-box motif [190]. Likewise, securin is phosphorylated near its KEN and D-box motifs, preventing efficient APC-mediated ubiquitination; Cdc14p can release this inhibition [191]. Therefore, there are several levels of phosphorylation-mediated regulation on APC activity that ensure the precise timing of substrate degradation and cell cycle progression.

Significance of this Study

The human telomerase RNA (hTR) was cloned in 1995 and introduction of an inhibitory anti-sense hTR into HeLa cells resulted in telomere attrition and eventual cell death [44]. While this result indicated a correlation between telomere shortening and loss of cell proliferation in human cells, it was in 1998 that a causal relationship was demonstrated. In this pivotal work, the authors introduced the recently cloned catalytic subunit [35,36,192], human telomerase reverse transcriptase (hTERT), into normal telomerase-negative cells. These cells exhibited restored telomerase activity, elongated telomeres, normal proliferation rates, and increased lifespan [193]. The identification of telomerase activity in humans demonstrated the evolutionary conservation of this enzyme complex and highlighted its importance in cell proliferation and lifespan, making its study relevant to human disease.

Elucidating the mechanisms that regulate telomerase activity is important because of telomerase's role in both aging and cancer. Dyskeratosis congenita is a human disease that results from mutation of several genes that affect telomerase activity, most strikingly the telomerase RNA template, *hTR*, a homolog to *TLC1* RNA. This mutation results in

haploinsufficiency, a situation in which the presence of one copy of the template is not enough to maintain proper telomere length and chromosome stability. Therefore, individuals with this disease experience stem cell failure and are at greater risk for developing cancer [194].

Telomerase is active in germ cells but not in most somatic cells. Cells that do not express telomerase experience telomere shortening each replication cycle. This phenomenon has been implicated as a way for a cell to count the number of times it has divided. Therefore, telomeres may act as a tumor-suppression mechanism by limiting the number of replication cycles. However, telomerase is re-activated in about 90% of all human cancers (reviewed in [195]). Therefore, the understanding of telomerase regulation could benefit researchers in the development of cancer therapies to inhibit telomerase function.

My published work [196] presented in this dissertation (Chapter II and III) focuses on the regulated assembly of the telomerase complex through the temporal degradation of the recruitment subunit, Est1p. Since the fundamental aspects of telomeres and telomerase are evolutionarily conserved between *S. cerevisiae* and humans, and assembly is critical to telomerase activity, insight into how the human enzyme is regulated can be obtained using this model system.

[1]CHAPTER II

THE ANAPHASE PROMOTING COMPLEX CONTRIBUTES TO THE DEGRADATION OF THE *S. CEREVISIAE* TELOMERASE RECRUITMENT SUBUNIT EST1

Introduction

Telomeres are unique protein-DNA complexes found at the termini of linear eukaryotic chromosomes. These regions are critical for protecting chromosomes against nucleolytic digestion and for distinguishing normal chromosome ends from internal double-strand breaks. Loss of telomere function causes end-to-end fusions that result in anaphase bridge-breakage cycles and catastrophic genomic instability [195]. While the majority of the telomere is comprised of tandem G/T-rich double-stranded DNA repeats, the terminus exists as a short 3'-overhang throughout the cell cycle [110,111]. After passage of the replication fork in late S phase, the 3'-overhangs are transiently increased in length, at least in part due to exonucleolytic digestion of the 5'-strand [17,110-112]. Telomerase, a ribonucleoprotein complex, can extend these 3'-overhangs by reverse transcription, while the conventional lagging-strand DNA replication machinery is thought to fill in the 5'-gap [197].

[1] The work presented in this chapter is published in [196]: Ferguson JL, Chao WCH, Lee E, Friedman KL (2013) The Anaphase Promoting Complex Contributes to the Degradation of the *S. cerevisiae* Telomerase Recruitment Subunit Est1p. *PLoS ONE* 8(1): e55055. doi:10.1371/journal.pone.0055055

S. cerevisiae telomerase contains three dedicated protein subunits (Est1, Est2 and Est3) [33,38,198] and an intrinsic RNA (*TLC1*) containing the template for nucleotide addition [41]. The 1.2 kb *TLC1* RNA acts as a scaffold, providing separate binding sites for telomerase subunits Est1p and Est2p, the Sm protein complex, and the Ku heterodimer [47]. Association of the 7-member Sm complex is critical for RNA maturation [46], while Ku binding is important for nuclear retention of the RNA and efficient telomerase recruitment to telomeres [53-55]. Est2p, a reverse transcriptase [32], and *TLC1* RNA are sufficient for *in vitro* activity and are thus considered the catalytic core of the enzyme [199]. Both Est1p and Est3p are regulatory or accessory proteins since each is dispensable *in vitro* but required *in vivo* to maintain telomere length [33,38,198,199]. The Est3p regulatory subunit is recruited to the complex through direct interactions with Est1p and Est2p, and stimulates telomerase activity *in vitro* [63,81].

Est1p binds *TLC1* RNA via three secondary structural elements within sub-helix IVc: a pentanucleotide bulge, an adjacent internal loop, and a single-stranded region at the base of the sub-helix [51,52]. In addition to its interaction with the RNA, Est1p is also important for the recruitment of telomerase to the telomere through a direct interaction with the telomeric single-stranded DNA binding protein, Cdc13p [96-100]. The Est1 protein undergoes proteasome-dependent cell cycle-regulated destruction in G1 phase, thereby preventing telomerase complex assembly during G1 phase when telomerase is not active at telomeres [101].

Protein destruction by the proteasome is regulated through the attachment of the small polypeptide ubiquitin to target molecules. Such ubiquitin-dependent protein degradation is accomplished through a multi-step process: the ubiquitin moiety is

activated by an E1 activating enzyme, transferred to an E2 conjugating enzyme, and finally, covalently attached to lysine residues present within a target protein that is bound to an E3-ligase. Multiple rounds of this process result in polyubiquitinated proteins that are subsequently delivered to the 26S proteasome for degradation. Temporal coordination of ubiquitination and proteolysis of key regulatory proteins is critical for unidirectional progression of the cell cycle [200]. One of the well-studied poly-ubiquitinating E3 complexes with this role is the Anaphase Promoting Complex (APC).

The APC is a multi-subunit E3 ubiquitin ligase that is critical for transit through the cell cycle. Although the core subunits are constitutively expressed [161,201,202], APC functionality oscillates, exhibiting no activity in S and G2 phase, and high activity during mitosis and G1 phase [203]. The APC utilizes two evolutionarily conserved, WD40-domain containing activators, Cdc20p/Fizzy and Cdh1p/Hct1/Fizzy-related [204-206]. These activators bind directly to substrates via degradation motifs [173,178,181,182], the best characterized being the Destruction box (D-box: an arginine and leucine separated by any two amino acids, RxxL) and KEN-box [174,177,207]. The binding of these activators to the APC core particle is tightly regulated: Cdc20p associates when cyclin-dependent kinase (CDK/Cdc28p) activity is high in mitosis, while Cdh1p association is inhibited by phosphorylation and therefore occurs when CDK activity is low at the end of mitosis through G1 phase [208-210]. The direct binding of pseudosubstrate inhibitors and degradation of activator proteins also contribute to temporal regulation of APC activity [176]. APC^{Cdc20p} is critical during mitosis when specific recognition and subsequent destruction of the separase inhibitor (securin/Pds1p) results in cohesin cleavage, and thus sister-chromatid separation [206,211]. APC^{Cdh1p}

activity promotes exit from mitosis and ensures that CDK levels remain low, allowing for loading of replication origins with initiation proteins prior to the beginning of S phase, when CDK activity increases [176,212,213].

Est1p undergoes cell cycle-regulated degradation during G1 phase, thereby preventing Est3p recruitment and telomerase complex assembly [101]. Here I present evidence that Est1 protein levels oscillate during the cell cycle through an APC-dependent mechanism *in vivo*. Degradation requires three sequences in Est1p that match the D-box consensus, consistent with direct recognition of Est1p by the APC. However, recombinant Est1 protein is not degraded or ubiquitinated by the APC *in vitro*, suggesting that Est1p either lacks the necessary structure or modification(s) that influence APC recognition *in vivo* or is an indirect target of the APC. Because Est1p stimulates association of Est3p with the telomerase complex, these results shed light on the regulation of yeast telomerase biogenesis and demonstrate an additional connection between telomere maintenance and cell cycle regulation pathways.

Results and Discussion

Est1p is stabilized in early S phase

The telomerase recruitment protein, Est1p, undergoes degradation in G1 phase but not G2/M phase [101]. To more thoroughly examine the temporal regulation of Est1 protein levels, cells expressing MYC_{13}-tagged *EST1* from its endogenous locus were arrested at three points in the cell cycle: G1 with the mating pheromone, alpha-factor; early S with the ribonucleotide reductase inhibitor, hydroxyurea; and late G2/M with the

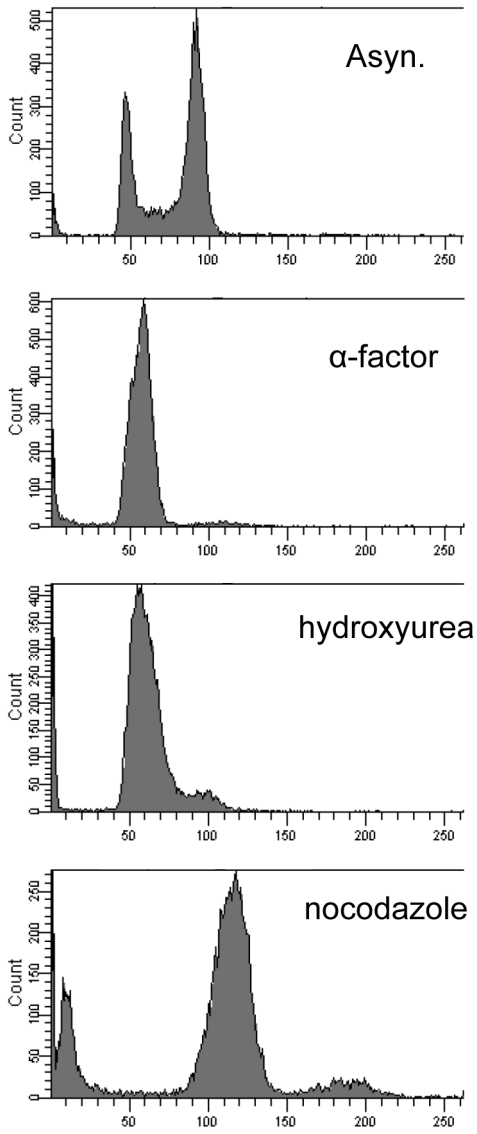

Figure 7. Flow cytometry of arrested cells.
Example of the typical flow cytometry histograms resulting from *S. cerevisiae* strains used in this study left untreated (asynchronous; Asyn.) or arrested as indicated. The profile of hydroxyurea-blocked cells is nearly indistinguishable from that observed upon treatment with α-factor, consistent with an early S phase arrest in the vast majority of cells.

microtubule destabilizing agent, nocodazole. The efficiency of arrest was confirmed to be greater than 95% in each experiment by flow cytometry (Figure 7) and observation of bud index (data not shown). As expected, Est1-MYC$_{13}$p was readily detected in whole-cell extract from asynchronously growing cells but not in the untagged control strain, indicating specificity of the MYC-antibody (Figure 8A, lanes 1 and 2). In agreement with previous observations [100,101], endogenously expressed Est1-MYC$_{13}$p was undetectable in G1 phase and abundant in G2/M-arrested cells (Figure 8A, compare lanes 3 and 5). Similar to G2/M-arrested cells, Est1-MYC$_{13}$p was readily detected from early S-arrested cells (Figure 8A, lane 4), suggesting that Est1 protein levels increase as cells enter S phase.

Although *EST1* transcript levels are ~3 fold lower in G1 phase than during G2/M [214,215], we have previously shown that differential protein stability is an important factor determining Est1p levels during the cell cycle [101]. To examine the kinetics of Est1p degradation at different points in the cell cycle, protein half-life was determined using a standard promoter shut-off assay. Following a brief induction of *HA$_3$-EST1* expression from the *GAL1*-promoter, both transcription and translation were inhibited and protein abundance was examined over time. As shown in Figure 8B, and in agreement with published work [101], HA$_3$-Est1p was rapidly degraded during a G1 phase arrest, but was more stable during a G2/M phase arrest [101]. In accordance with the steady state protein levels (Figure 8A), overexpressed HA$_3$-Est1p was also stable when cells were arrested in early S phase with hydroxyurea (Figure 8B, middle). Quantification of these assays confirmed a statistically significant increase in protein half-life during early S and G2/M phase as compared to G1 phase (Figure 8C;

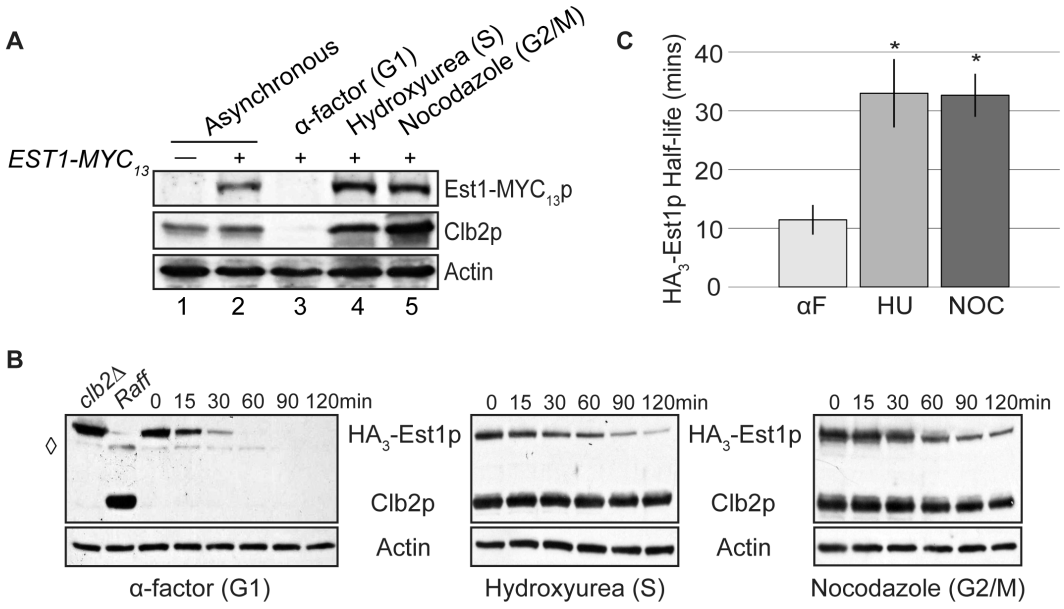

Figure 8. Est1p is unstable in G1 phase, but stable in early S and G2/M phases.
(A) Endogenously expressed Est1p-MYC$_{13}$p levels during cell cycle arrests. Strains YKF800 (untagged; lane 1) and YKF801 (*EST1-MYC$_{13}$*; lanes 2-5) were grown asynchronously at 30°C to mid-log phase and then left untreated (asynchronous) or arrested by addition of α-factor, hydroxyurea, or nocodazole, as indicated. When 95% of the population was arrested, as monitored by the bud-index, cells were harvested. Whole-cell extract was prepared and western blotted using anti-MYC, anti-Clb2p, and anti-Actin antibodies, as indicated.
(B) Half-life of HA$_3$-Est1p during cell cycle arrests. Strain YKF802 containing plasmid pVL242RtoA (*P$_{GAL1}$-HA$_3$-EST1*) was grown asynchronously at 30°C to mid-log phase and arrested with α-factor, hydroxyurea, or nocodazole, as indicated. When 95% of the population was arrested, as monitored by the bud-index, expression of *HA$_3$-EST1* was induced with addition of galactose and then subsequently repressed (after 1 hour) with glucose and cycloheximide (time 0). Samples from cells harvested at the indicated times were western blotted with anti-HA, anti-Clb2p and anti-Actin antibodies, as indicated. An induced asynchronous sample of strain YKF806 + pVL242RtoA (*clb2Δ*; left panel), served as a negative control for Clb2p and positive control for HA$_3$-Est1p detection. An uninduced asynchronous sample of strain YKF802 + pVL242RtoA (Raff; left panel) served as a positive control for Clb2p detection and negative control for HA$_3$-Est1p specificity. A non-specific background band is indicated by ✧.
(C) Quantification of data shown in (B), as described in Materials and Methods. The calculated half-lives were averaged from independent biological replicates: αF (α-factor), n=7; HU (hydroxyurea), n=4; NOC (nocodazole), n=4. Error bars are standard deviation from the mean. Both HU and NOC are statistically different from αF by two-tailed t-test (p-values 1.1 x10^{-5} and 1.1 x10^{-6}, respectively) as denoted by *.

p-values =$1.1x10^{-5}$ and $1.1x10^{-6}$, respectively). Together, these results suggest that Est1p is rapidly degraded during G1 phase, stabilizes in early S phase, and remains stable through G2/M phase.

Est1p is more stable in G1 phase when APC activity is compromised

The pattern of Est1p degradation during the cell cycle is reminiscent of that observed for targets of the E3-ubiquitin ligase complex, APC. As a comparison, levels of the B-type cyclin Clb2p, a known APC substrate [216,217], were monitored within the same extracts utilized for Est1p detection. As expected, Clb2p was undetectable in G1 and robustly detected in both S and G2/M arrested cells (Figure 8A and 8B). In addition to confirming the efficiency of cell cycle arrest, these results led me to hypothesize that Est1p degradation depends upon APC function.

I monitored the degradation rate of overexpressed HA_3-Est1p in alpha-factor arrested cells expressing the temperature-sensitive (ts) allele *cdc16-123*. This allele renders the APC non-functional at the restrictive temperature of 37°C and exhibits proteolysis defects with known APC substrates [216,217]. A strain harboring the *cdc16-123* allele was transformed with a complementing *CEN* vector expressing wild-type *CDC16* under control of its endogenous promoter (denoted *CDC16*) or an empty-vector (denoted *cdc16-123*). Using the promoter shut-off assay described above, the average half-life of overexpressed HA_3-Est1p was greater in the *cdc16-123* strain than in the complemented strain (Figure 9A and 9C) and trended toward significance with a p-value of 0.08. Therefore, I wanted to verify the relevance of this trend by examining other strains that compromise APC function *in vivo*.

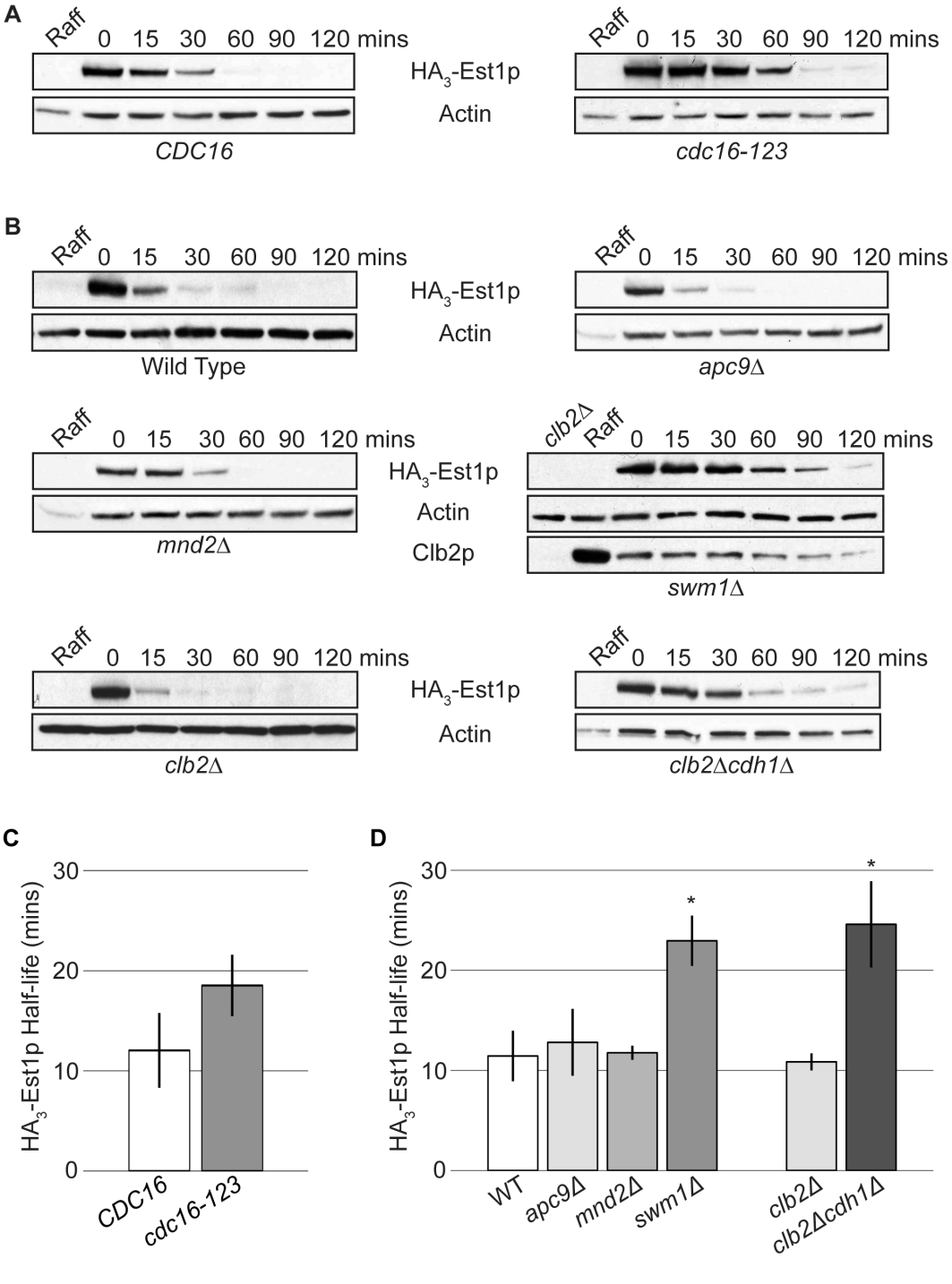
A
Raff
0 15 30 60 90 120 mins
HA3-Est1p
Actin
CDC16
cdc16-123
B
Wild Type
apc9Δ
mnd2Δ
clb2Δ
Clb2p
swm1Δ
clb2Δcdh1Δ
C
HA3-Est1p Half-life (mins)
30
20
10
0
CDC16
cdc16-123
D
WT
apc9Δ
mnd2Δ
swm1Δ
clb2Δ
clb2Δcdh1Δ
*

Figure 9. APC function is required for normal Est1p degradation during G1 phase.
(A) HA_3-Est1p stability increases when APC function is compromised. Western blots of Est1p stability assays from strain K4438 (*cdc16-123*) harboring pKF600 (*GAL1-HA_3-EST1*) plus either a complementing vector pRS416-*CDC16* (labeled "*CDC16*") or an empty vector pRS416 (labeled "*cdc16-123*") were conducted as described in Materials and Methods. An uninduced sample (Raff) served as a negative control for HA_3-Est1p specificity.
(B) HA_3-Est1p is stabilized in APC deletion mutants. Western blots of Est1p stability assays from strains YKF802 (Wild Type), YKF803 (*apc9Δ*), YKF804 (*mnd2Δ*), YKF805 (*swm1Δ*), YKF806 (*clb2Δ*) and YKF807 (*clb2Δcdh1Δ*) containing pVL242RtoA (P_{GAL1}-*HA_3-EST1*) were conducted as described in Materials and Methods. For YKF805 (*swm1Δ*), an uninduced asynchronous sample (Raff) served as a positive control for Clb2p detection and negative control for HA_3-Est1p specificity, while an uninduced asynchronous sample of strain YKF806 (*clb2Δ*) served as a negative control for Clb2p detection.
(C) Quantification of results shown in (A). Bars represent the average HA_3-Est1p half-life from three independent biological replicates. Error bars are standard deviation of the mean (p-value = 0.08 by two-tailed t test).
(D) Quantification of results shown in (B). Bars represent the average HA_3-Est1p half-life from independent biological replicates: n=3 for all strains except *clb2Δcdh1Δ*, where n=4. Error bars are standard deviation from the mean. By two-tailed paired t-test, there is a significant difference between the control (WT) and *swm1Δ* (p-value 0.0002) but not between WT and *apc9Δ* (p-value 0.49) or *mnd2Δ* (p-value 0.83). There is a significant difference between the control (*clb2Δ*) and *clb2Δcdh1Δ* strains (p-value 0.003). Significant differences are denoted by *.

Although APC activity is critical for cell viability, several subunits of this large E3 ubiquitin ligase are encoded by non-essential genes (*e.g.* Apc9p, Mnd2p, and Swm1p). Proteolysis of known APC substrates is minimally compromised in *apc9Δ* and *mnd2Δ* cells, suggesting that these two subunits exhibit substrate-specific effects or have minor contributions to full APC function. However, proteolysis of known APC substrates securin/Pds1p, Clb2p, Cdc5p, and Ase1p is decreased in *swm1Δ* cells, indicating a greater contribution to full APC activity [160,218]. Using the promoter shut-off assay, the half-life of overexpressed HA_3-Est1p was determined in *apc9Δ*, *mnd2Δ,* or *swm1Δ* cells arrested in G1 phase with alpha-factor (Figure 9B and 9D). HA_3-Est1p was significantly more stable during G1 phase in *swm1Δ* cells than in wild-type cells (p-value = 0.0002), while the rate of degradation was unaffected by the deletion of either *apc9* or *mnd2* (p-values = 0.49 and 0.84, respectively). Endogenously expressed Clb2p was detected in the same *swm1Δ* samples, but was undetectable from *apc9Δ* or *mnd2Δ* samples (Figure 9B and data not shown), confirming the predicted phenotype of these strains. Thus, like known APC targets, normal Est1p degradation during G1 phase requires Swm1p function.

During G1 phase, the APC is associated with the activator protein Cdh1p. Like *SWM1*, *CDH1* is non-essential, most likely because securin and B-type cyclins, essential substrates of the APC, are sufficiently targeted by the mitotic activating factor, Cdc20p [156]. I examined the protein half-life of Est1p in *cdh1Δ* cells arrested in alpha-factor. Since deletion of *cdh1* results in cyclin accumulation that leads to bypass of the alpha-factor arrest [205,212,219], these analyses were performed in a *clb2Δ* background to prevent cells from moving into S phase. Consistent with the results obtained in *swm1Δ*

cells, overexpressed HA_3-Est1p was significantly stabilized in *clb2Δcdh1Δ* cells arrested in G1 phase (p-value = 0.003; Figure 9B and 9D, compare to *clb2Δ*). While clearly increased in comparison to the wild-type strain, the half-life of Est1p in alpha-factor arrested *swm1Δ* ($T_{1/2}$ = 23 +/- 2.5 mins) or *clb2Δcdh1Δ* ($T_{1/2}$ = 25 +/- 4.3 mins) strains was lower than that of the corresponding WT strain arrested with hydroxyurea ($T_{1/2}$ = 33 +/- 5.8 mins; p-values 0.04 and 0.06, respectively) or nocodazole ($T_{1/2}$ = 33 +/- 3.7 mins; p-values 0.01 and 0.03, respectively). These differences are consistent with the retention of partial APC activity in these viable strains. Collectively, these experiments support the hypothesis that the APC plays a role in the G1-specific degradation of Est1p.

CDH1 is required for the cell-cycle oscillation of Est1 protein levels

The loss of Est1p during an alpha-factor arrest (Figure 8A) could be over-emphasized due to the artificial length of G1 phase. To confirm the kinetics with which Est1p levels fluctuate as cells enter and traverse an unperturbed G1 phase, I examined levels of endogenously expressed Est1-MYC_{13}p after release of *cdc15-2* cells from mitotic arrest. *CDC15* encodes a protein kinase required for mitotic exit and incubation of *cdc15-2* cells at the restrictive temperature of 37°C results in cell cycle arrest in late anaphase/telophase [220]. Because CDK activity is elevated and the Cdc14p phosphatase is sequestered in the nucleolus and unable to dephosphorylate Cdh1p [189,208-210], APC^{Cdh1p} is not active during the *cdc15-2* arrest. In contrast, the observation that *cdc15-2* arrested cells have separated chromosomes indicates that APC^{Cdc20p} is active and able to mediate Pds1p proteolysis prior to the arrest point. *cdc15-2* cells were incubated at the restrictive temperature until 95% of the population was arrested with the characteristic

"dumbbell" morphology and then released from the arrest by shifting back to the permissive temperature of 23°C. Samples were harvested every 20 mins following release. Synchrony of the release was monitored by analysis of Clb2p levels, observation of the bud index (Figure 10), and flow cytometry (data not shown).

In agreement with published reports, endogenous Clb2p levels decreased upon release from the *cdc15-2* arrest [205,221,222], with the lowest point of expression at 40 to 60 mins Figure 11A). Approximately 50% of cells show the first evidence of bud formation 60 mins after release (Figure 10), consistent with the interpretation that the trough of Clb2 expression corresponds to G1 phase. Examination of Est1-MYC_{13}p levels within these same samples revealed a similar pattern; the lowest point of expression occurred 40-60 mins after release from the *cdc15-2* block (Figure 11A). Four independent biological replicates were done to demonstrate the reproducibility of this G1 phase decrease for both Clb2p and Est1-MYC_{13}p (Figure 11A). The expression of both proteins at 40 and 60 mins after release was significantly decreased from the protein levels observed at the *cdc15-2* arrest (p-values for Clb2p: $6.0x10^{-5}$ and $1.7x10^{-4}$, respectively; p-values for Est1-MYC_{13}p: $3.7x10^{-4}$ and $1.9x10^{-4}$, respectively).

Although the pattern with which Clb2p and Est1p declined in abundance after *cdc15-2* release was very similar, only Clb2p showed a large increase in expression at the end of the time course (100 mins) compared to the starting protein level. I attribute this behavior to the previous observation that a fraction of Clb2p undergoes APC^{Cdc20p}-dependent degradation [222], which would be expected to have occurred prior to the *cdc15-2* arrest. Therefore, the starting protein levels observed for Clb2p at the *cdc15-2* arrest may already be partially reduced, with additional degradation attributable to

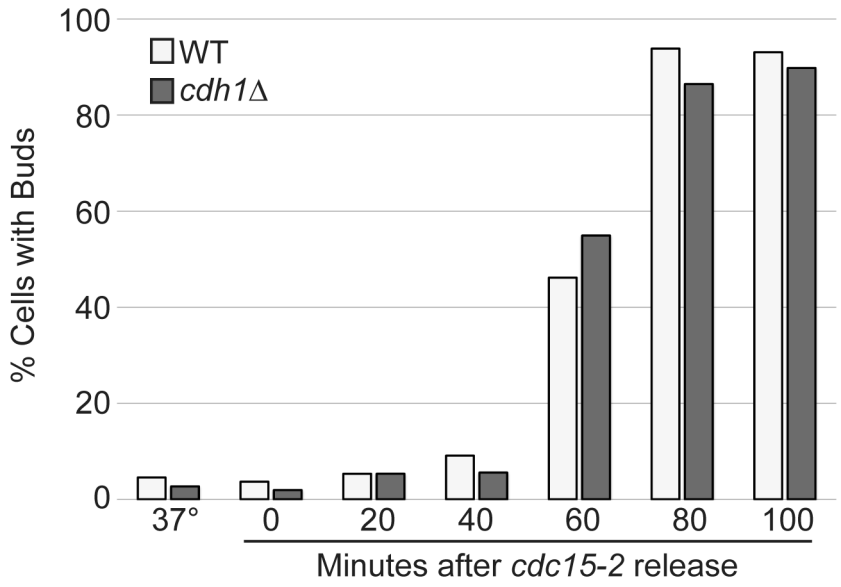

Figure 10. Cells released from the *cdc15-2* arrest proceed synchronously into the next cell cycle.
Budding index of cells collected at the indicated times after release from the *cdc15-2* arrest (Figure 11). Results are from a single WT (light) and *cdh1Δ* (dark) assay and indicate the percentage of cells with visible buds. This result is representative of the pattern observed from the *cdc15-2* arrest and release assays.

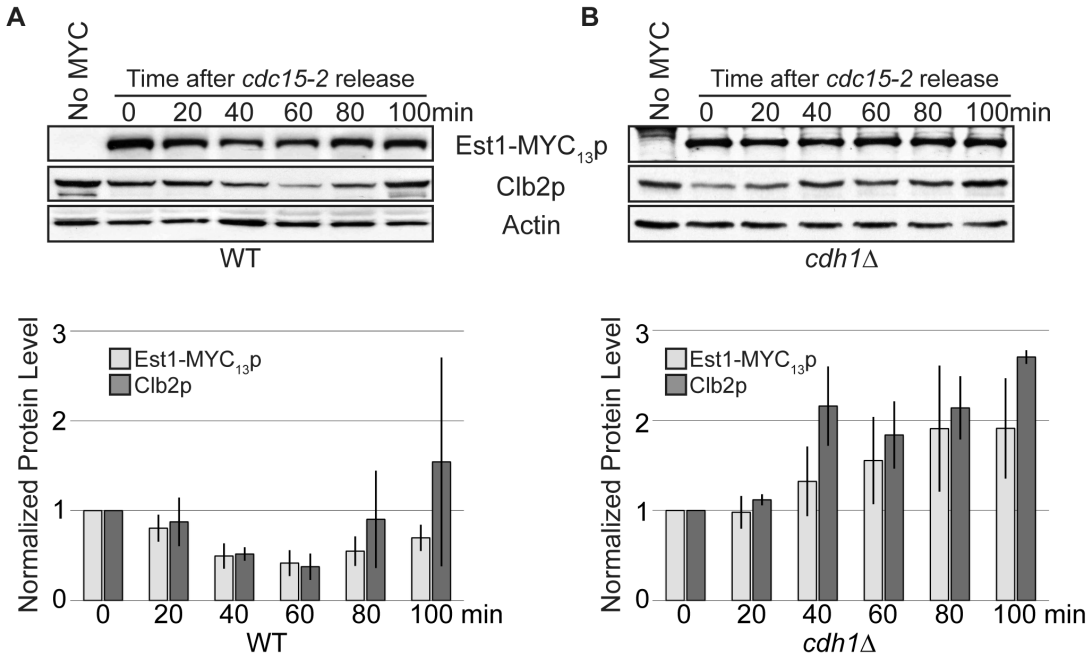

Figure 11. Cell-cycle oscillation of Est1p requires Cdh1p.
(A) Est1 protein levels oscillate through the cell cycle. Strain YKF808 (*cdc15-2 EST1-MYC$_{13}$)* was grown asynchronously at 23°C to mid-log phase and shifted to the restrictive temperature (37°C) for 3.5 hrs. When 95% of the cells were arrested, as monitored by bud-index (Figure 10), the culture was returned to the permissive temperature (23°C; time 0). Whole-cell extract was prepared from samples harvested every 20 mins following release and western blotted using anti-MYC, anti-Clb2p, and anti-Actin antibodies, as indicated. YCM191 (*cdc15-2*) served as the untagged (No MYC) control for Est1-MYC$_{13}$p and was harvested following the 37°C incubation period. Est1-MYC$_{13}$p and Clb2p intensity at each time were normalized to input (actin) and starting amount (time 0). Bars represent the average of four independent biological replicates for Est1-MYC$_{13}$p (light) and Clb2p (dark); error bars are standard deviation of the mean.
(B) Deletion of *CDH1* perturbs the oscillation of Est1-MYC$_{13}$p through the cell cycle. Strain YKF809 (*cdc15-2 cdh1Δ EST1-MYC$_{13}$*) was treated as in (A), except the bars represent the average of three independent biological replicates.

APC^{Cdh1p} activity. The failure of Est1p to accumulate above the starting amount by the end of the time course suggests that Est1p may not undergo degradation in late mitosis, prior to the *cdc15-2* arrest point.

Since Cdh1p plays a role in Est1p degradation during G1 phase (Figure 9B and 9D), I hypothesized that deletion of this APC-activator would abrogate the protein oscillation pattern observed from cells released from a *cdc15-2* arrest. A *cdh1Δ cdc15-2* strain was incubated at restrictive temperature until >95% of the cells were arrested and then released by lowering the temperature. As monitored by both the bud index (Figure 10) and flow cytometry (data not shown), the cells proceeded into the next cell cycle similarly to wild type, with the emergence of small buds beginning at 60 mins after release. Consistent with published work, Clb2p levels no longer decreased during transit through G1 phase in *cdh1Δ* cells (Figure 11B; [205]). Importantly, Est1-MYC_{13}p also did not exhibit a decline in protein levels as cells proceeded through G1 phase following release from the *cdc15-2* arrest (compare Figure 11A and 11B). Based on the preceding analysis of protein levels as cells exit mitosis and enter the following S phase, I conclude that Est1p likely undergoes proteolysis solely during G1 phase, stabilizes as cells transit through S phase, and remains stable through mitosis. Furthermore, APC^{Cdh1p} is the primary regulator of the G1 phase-specific proteolysis of Est1p.

As the *cdh1Δ cdc15-2* cells proceeded through the later timepoints of the release, the protein levels of both Est1-MYC_{13}p and Clb2p increased over their respective starting amounts (time 0). This has been reported for Clb2p [205,222] and may result from the combination of lack of degradation and additional transcription/translation as cells exit the arrest [101,214,215,223,224]. As mentioned above, APC^{Cdc20p} also degrades a pool

of Clb2p during mitosis [222], prior to the *cdc15-2* arrest point, leading to a partially reduced starting amount. However, since this experiment depends upon a dramatic temperature shift (23° to 37°), I also cannot eliminate artifacts resulting simply from the temperature change. Though the temperature is slowly raised to prevent heat-shock effects [225], it remains possible that the high temperature causes a drop in the transcript level that then recovers following release at permissive temperature. If a Northern Blot of transcript levels confirms this hypothesis, a simple modification of the experiment could eliminate these concerns: a nocodazole block and release of wild-type yeast. Furthermore, the experiment could be done by arresting at the restrictive temperature for *cdc15-2* and then inducing expression of wild-type *CDC15* using an inducible promoter, eliminating the need for a return to the permissive temperature to release the arrested cells into a synchronous cell cycle.

Mutation of *cis*-acting sequences stabilizes Est1p in G1 phase

The data presented thus far demonstrate that the APC influences the G1 phase-specific degradation of Est1p. However, these experiments do not address whether Est1p is a direct substrate of the APC. Substrates of the APC are recognized through specific degron motifs such as the Destruction box (D-box: sequence RxxL) and KEN box [174,177,207]. If Est1p is a direct target of APC^{Cdh1p}, I would predict *EST1* to encode specific degron(s) important for the recognition and subsequent proteolysis of Est1p. Examination of the amino acid sequence of Est1p revealed the presence of six putative D-boxes positioned in pairs throughout the protein (Figure 12A). To test if any of these putative D-boxes has a role in Est1p degradation during G1 phase, I mutated the

important arginine (R) and leucine (L) residues of each consensus sequence to alanine (A) and determined protein half-life using a promoter shut-off assay in cells arrested with alpha-factor. Individual mutation of putative D-boxes 1, 2, and 4 stabilized the protein during G1 phase while no significant increase in half-life was observed upon mutation of putative D-boxes 3, 5, or 6 (Figure 12B and Figure 13A; data not shown). Because the degron motifs occurred in pairs, I also asked whether mutating each pair of putative D-boxes (1+2, 3+4, or 5+6) would further inhibit proteolysis. Consistent with the single D-box data, combined mutation of 1+2 or 3+4 resulted in stabilization of the protein, but the effect was not additive. No stabilization was observed upon mutation of D boxes 5+6 (Figure 12B and Figure 13A). The extent to which the half-life increased for either the single or combined mutations was not statistically different from the half-life observed during a nocodazole (G2/M phase) arrest, suggesting that the loss of a single D-box motif is sufficient to stabilize the protein in G1 phase.

To corroborate the results obtained with the specific point mutations described above, I also monitored the half-life of several deletion variants of Est1p. Deletion of the C-terminal 300 amino acids (denoted CΔ300 in Figure 12A) removes putative D-boxes 5 and 6, previously shown not to contribute to Est1p degradation during G1 phase (Figure 12B). Consistent with that conclusion, the half-life of Est1p$^{C\Delta300}$ remained unchanged compared to the full-length protein, suggesting that putative D-boxes 5 and 6 are not degron motifs (Figure 12C and Figure 13B). A larger C-terminal deletion (CΔ500) did not express well; I was therefore unable to examine the stability of an Est1p peptide containing only D-boxes 1 and 2 (data not shown). I next generated systematic deletions from the N-terminus of *EST1* to assess the influence of D-boxes 1 and 2 on Est1p

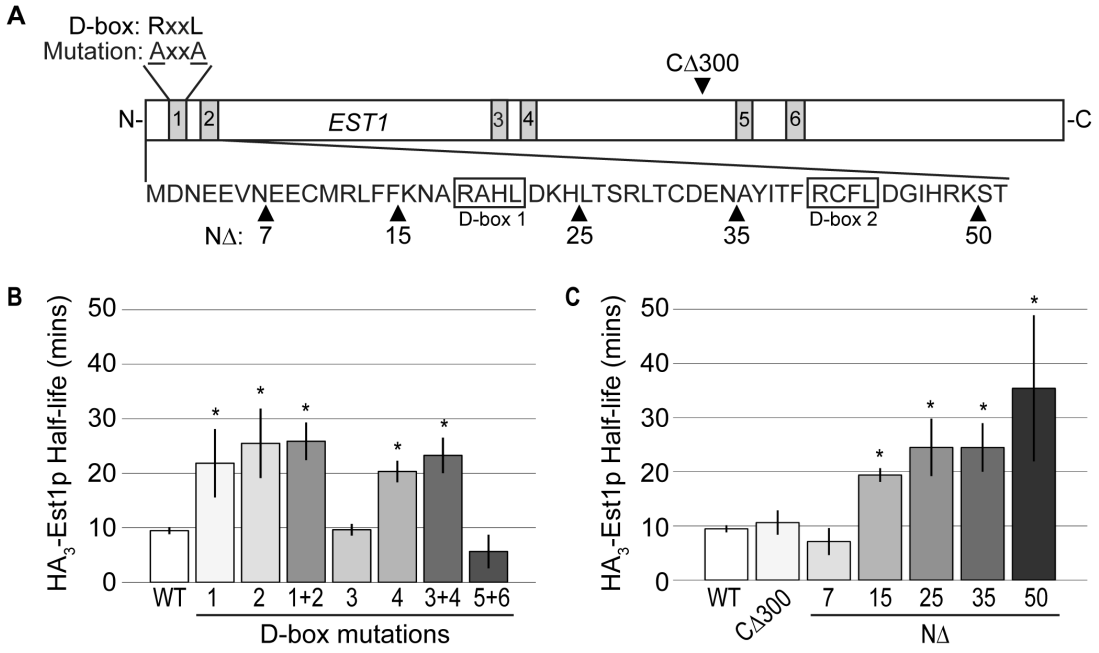

Figure 12. Est1p degradation in G1 phase requires three destruction boxes (D-boxes).

(A) Schematic of *EST1* shown to scale. *EST1* contains six putative D-boxes with sequence RxxL (boxes labeled 1-6). Deletion of the C-terminal 300 amino acids (CΔ300) results in a truncated protein that removes putative D-boxes 5 and 6. The N-terminal 52 amino acids are shown, with putative D-boxes 1 and 2 outlined. Upward pointing black triangles represent the position of the indicated N-terminal deletion.

(B) D-boxes 1, 2, and 4 contribute to Est1p degradation. YKF802 containing pKF600 (*GAL1-HA$_3$-EST1*) plasmids expressing either wild-type *EST1* (WT) or the D-box (DB) mutated (RxxL to AxxA) *est1* alleles indicated were treated as in Figure 8B, except strains were arrested with α-factor. Bars represent the average HA$_3$-Est1p half-life for three independent biological replicates; error bars are the standard deviation of the mean. Using a two-tailed t-test, there is no significant difference from WT for D-box 3 (p-value 0.833) or D-boxes 5+6 (p-value 0.104). D-box 1 (p-value 0.027), D-box 2 (p-value 0.012), D-boxes 1+2 (p-value 0.001), D-box 4 (p-value 0.001) and D-boxes 3+4 (p-value 0.002) are significantly different than WT, denoted by *.

(C) Deletion of D-box 1 or 2 stabilizes Est1p during G1 phase. YKF802 containing pKF600 plasmids expressing either wild-type *EST1* (WT) or the *est1* deletion variants indicated (CΔ300, NΔ7, NΔ15, NΔ25, NΔ35 or NΔ50) were treated as in (A). Bars represent the average HA$_3$-Est1p half-life for independent biological replicates: n=3 for each variant except NΔ50, where n=4. Error bars are standard deviation from the mean; significance is denoted by *. By a two-tailed t-test, there is no significant difference between WT and CΔ300 (p-value 0.445) or NΔ7 (p-values 0.188). The half-lives observed for NΔ15 (p-value 0.0003), NΔ25 (p-value 0.008), NΔ35 (p-value 0.005) and NΔ50 (p-value 0.02) are significantly different from WT.

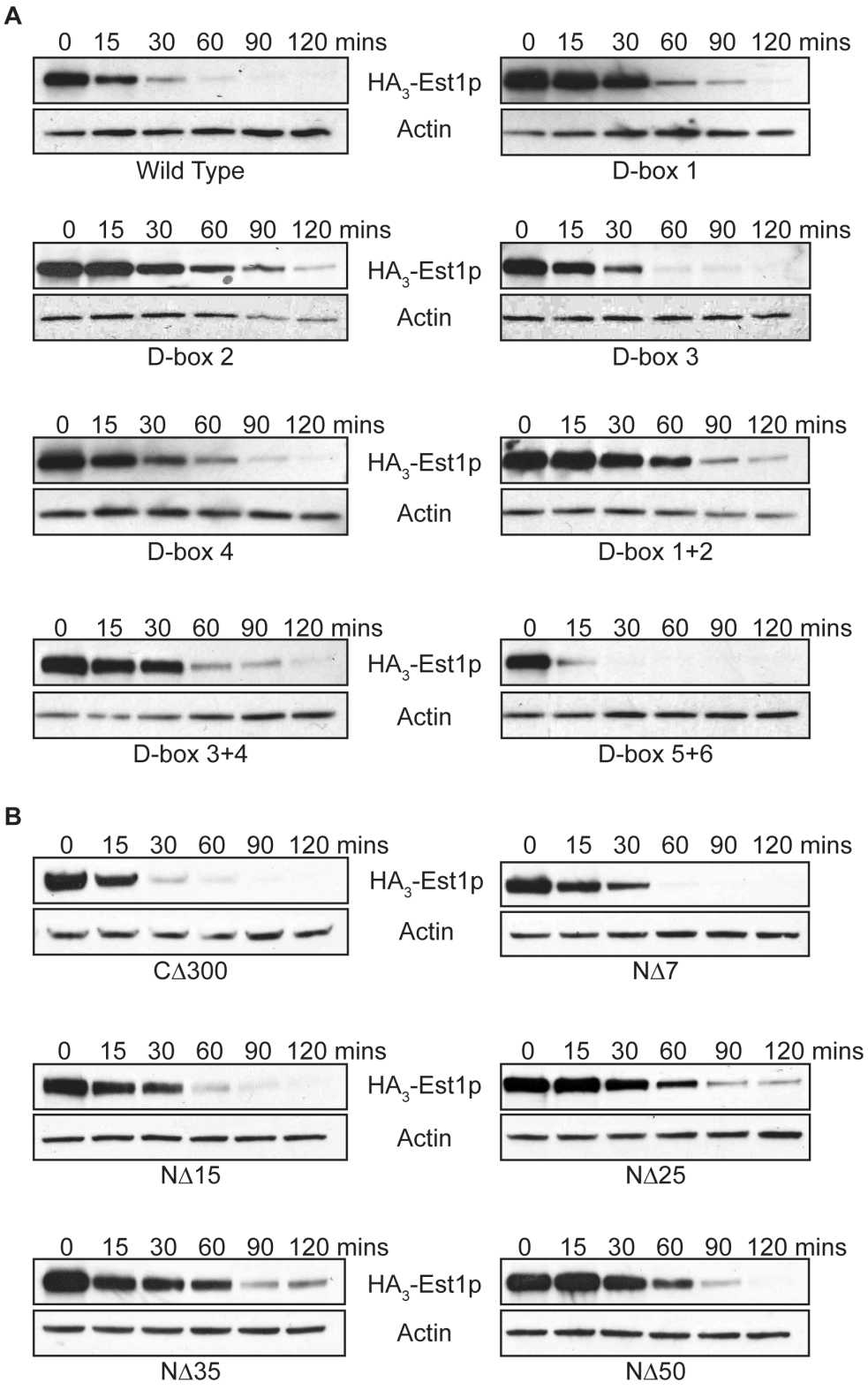
A
0 15 30 60 90 120 mins
HA3-Est1p
Actin
Wild Type
D-box 1
D-box 2
D-box 3
D-box 4
D-box 1+2
D-box 3+4
D-box 5+6
B
CΔ300
NΔ7
NΔ15
NΔ25
NΔ35
NΔ50

Figure 13. Est1p degradation in G1 phase depends upon specific degron motifs.
(A) Western blots of Est1p stability assays from strain YKF802 containing pKF600 (*GAL1-HA$_3$-EST1*) plasmids expressing the D-box (DB) mutated (RxxL to AxxA) *est1* alleles indicated (DB1; DB2; DB1+2; DB3; DB4; DB3+4; DB5+6), treated as in Figure 8B (α-factor).
(B) Strain YKF802 containing pKF600 plasmids expressing the deletion variants indicated (CΔ300, NΔ7, NΔ15, NΔ25, NΔ35 or NΔ50) were treated as in (A).
Results are quantified in Figure 12.

degradation. The N-terminal boundaries of D-boxes 1 and 2 are located at amino acid 19 and 41, respectively (Figure 12A). I constructed five N-terminal deletions: *est1*$^{N\Delta 7}$, *est1*$^{N\Delta 15}$, *est1*$^{N\Delta 25}$, *est1*$^{N\Delta 35}$, and *est1*$^{N\Delta 50}$. Examination of the protein half-life via promoter shut-off assay revealed no stabilization with the smallest deletion (Est1p$^{N\Delta 7}$), but the half-lives of Est1p$^{N\Delta 25}$, Est1p$^{N\Delta 35}$, and Est1p$^{N\Delta 50}$ were increased (Figure 12C and Figure 13B). Again consistent with the lack of additivity previously observed, loss of putative D-box 1 (Est1p$^{N\Delta 25}$ and Est1p$^{N\Delta 35}$) was equivalent in effect to loss of both putative D-boxes 1 and 2 (Est1p$^{N\Delta 50}$). The extent of stabilization observed in the deletion variants was similar to that observed with the point mutations (compare Figure 12B and 12C). Est1p$^{N\Delta 15}$ was more stable than the full-length protein even though no portion of a predicted D-box was deleted with this construct (Figure 12C and Figure 13B). Since this deletion retains only 3 amino acids N-terminal to the beginning of D-box 1, I attribute this stabilization to misfolding of D-box 1 and disrupted recognition by APC^{Cdh1p}. However, it is possible that a novel degron motif exists between amino acids 7 and 15. These results are consistent with Est1p being a direct substrate of the APC and suggest that *EST1* encodes three degron motifs (D-boxes 1, 2, and 4) important for recognition and subsequent degradation during G1 phase.

Neither proteolysis nor ubiquitination of recombinant Est1p by the APC occurs *in vitro*

The analyses described above suggest that Est1p undergoes G1-specific degradation that is dependent upon direct recognition of degron motifs within the protein by APC^{Cdh1p}. To examine the direct effect of APC^{Cdh1p} on Est1p, I monitored degradation

of recombinant Est1p using *Xenopus laevis* egg extracts either without (APC inactive) or with (APC active) human Cdh1 supplementation. Recombinant *Drosophila* cyclin B served as a positive control for APC-mediated degradation, while firefly luciferase served as the negative control. As expected, luciferase remained stable while cyclin B was efficiently degraded in the presence of Cdh1 (Figure 14A). However, there was no observed degradation of recombinant Est1p when Cdh1 was added (Figure 14A).

To eliminate the possibility of cross-species incompatibility, I collaborated with William Chao, a graduate student in David Barford's laboratory in London, UK. Using my supplied plasmids, William tested whether Est1p is ubiquitinated by APC^{Cdh1p} *in vitro* when all components of the assay are either purified from *S. cerevisiae* or are recombinant proteins of *S. cerevisiae* origin. ^{35}S-labeled substrates synthesized in rabbit reticulocyte lysate (RRL) were incubated with methylated-ubiquitin and recombinant Cdh1p in the presence (+) or absence (−) of purified *S. cerevisiae* APC complexes (Figure 14B). Methylated-ubiquitin prevents poly-ubiquitin chain formation; thus, substrate ubiquitination results in two observable changes: 1) loss of signal corresponding to the unmodified protein and 2) appearance of a ladder of higher molecular weight bands indicative of covalent attachment of a single ubiquitin moiety to individual lysines. *S. cerevisiae* securin/Pds1p, previously shown to undergo APC^{Cdh1p}-dependent ubiquitination *in vitro* [226], served as a positive control. As expected, Pds1p was ubiquitinated in a manner dependent upon addition of both purified APC and recombinant Cdh1p [indicated by the ladder of higher molecular weight species and loss of the unmodified signal (Figure 14B, lane 2)]. In contrast, Est1p was not detectably ubiquitinated in this assay (Figure 14B, compare lanes 3 and 4).

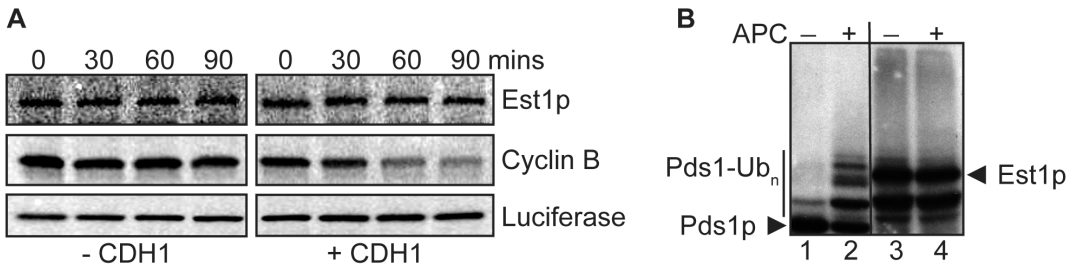

Figure 14. Est1p is not a target of the APC *in vitro*.
(A) Est1p is not degraded by the APC *in vitro*. *X. laevis* egg extract (− CDH1) was activated by the addition of *in vitro* transcribed human Cdh1 to obtain APC-activated extract (+ CDH1). ^{35}S-labeled substrate proteins (*S. cerevisiae* Est1p, *D. melanogaster* Cyclin B, or firefly luciferase) were incubated with either inactive (− CDH1) or activated extract (+ CDH1) as described in Materials and Methods. Samples were removed at the indicated times, separated by gel-electrophoresis and exposed to a phosphor-imager screen.
(B) Est1p is not ubiquitinated *in vitro*. ^{35}S-labeled substrates (*S. cerevisiae* Est1p and Pds1p) were incubated with Ubc4p (E2 ligase), recombinant *S. cerevisiae* Cdh1p, and methylated-ubiquitin in the absence (− ; lanes 1 and 3) or presence (+ ; lanes 2 and 4) of purified *S. cerevisiae* APC complexes. Reactions were separated by gel electrophoresis and detected by autoradiography film. Black arrows indicate the unmodified protein. The vertical line indicates the region where ubiquitin-conjugated forms of Pds1p migrate. This experiment was performed by William Chao.

Experiments designed to detect substrate ubiquitination *in vivo* are challenging because the ubiquitinated forms represent a small fraction of the total protein, are rapidly degraded by the proteasome, and are acted on by deubiquitinating enzymes (Dubs). Despite using techniques designed to limit these concerns [227,228], I have not detected ubiquitination of overexpressed Est1p *in vivo* (data not shown). However, these analyses have not been exhaustive and do not rule out the possibility that a critical pool of Est1p undergoes ubiquitination *in vivo*.

The lack of APC^{Cdh1p}-dependent ubiquitination or degradation of Est1p *in vitro* using two different assays contrasts with our identification of degradation motifs in Est1p that resemble those utilized by APC^{Cdh1p} in other substrates and that are required for Est1p degradation during G1 phase (Figure 12). One possibility is that modifications of Est1p influence recognition by APC^{Cdh1p} *in vivo* and that these modification(s) are not appropriately mimicked upon expression of Est1p in RRL. Although much of the regulation of APC-mediated degradation occurs through direct modulation of APC activity, post-translational modification of substrate molecules has been found to affect recognition by the APC in several cases including Cdc6, securin, and Aurora A [176,190,191,229,230]. While it was recently reported that Est1p is not detectibly phosphorylated *in vivo* [81], the presence of other post-translation modifications has not been addressed. I also cannot exclude the possibility that recombinant Est1p is mis-folded, precluding recognition by APC^{Cdh1p} in the *in vitro* assays.

An alternate possibility is that the amino acids required for Est1p degradation *in vivo* (Figure 12) do not mediate direct interaction with APC^{Cdh1p}, but are instead required for recognition by a currently unidentified ubiquitin ligase or protease. Because our

results provide strong evidence that Est1p degradation depends upon APC^{Cdh1p} function (Figure 9 and Figure 11), I would need to postulate that the effect of the APC is indirect. For example, Est1p may be targeted for degradation via a mechanism that itself is under positive regulation by the APC, reminiscent of cohesin cleavage by separase after Pds1/securin degradation via APC^{Cdc20p} [231].

Previous work has shown that Est1p regulates the assembly of the telomerase complex *in vivo*. However, even in the presence of abundant Est1 protein and telomerase complex assembly, telomerase is unable to elongate telomeres during G1 phase [101]. This observation suggests that additional regulatory mechanisms prevent inappropriate telomerase activity. A role for the Rif2 protein in G1-specific telomerase inhibition was recently reported [232]. However, these results do not rule out an additional regulatory role for Est1p degradation during G1 phase. In this light, it is intriguing that all of the D-box stabilizing mutations (Figure 12) cause telomere shortening when expressed under control of the endogenous promoter in *est1Δ* cells (Figure 15). While this observation suggests that the stabilization of Est1p during G1 phase may be deleterious, I cannot rule out the possibility that the mutations affect other aspects of Est1p function.

In summary, our *in vivo* results are most consistent with a model in which Est1p levels oscillate through the cell cycle, undergoing G1-specific degradation that is dependent upon APC^{Cdh1p}-mediated recognition of specific degron motifs within the protein. Reduced Est1p levels during G1 phase are in turn predicted to restrict the assembly of the active telomerase complex [101]. Although I cannot rule out misfolding of the recombinant protein as an explanation for the lack of Est1p degradation *in vitro*,

these results raise the intriguing possibility that additional regulatory events modulate Est1p abundance in a manner that depends upon APC function.

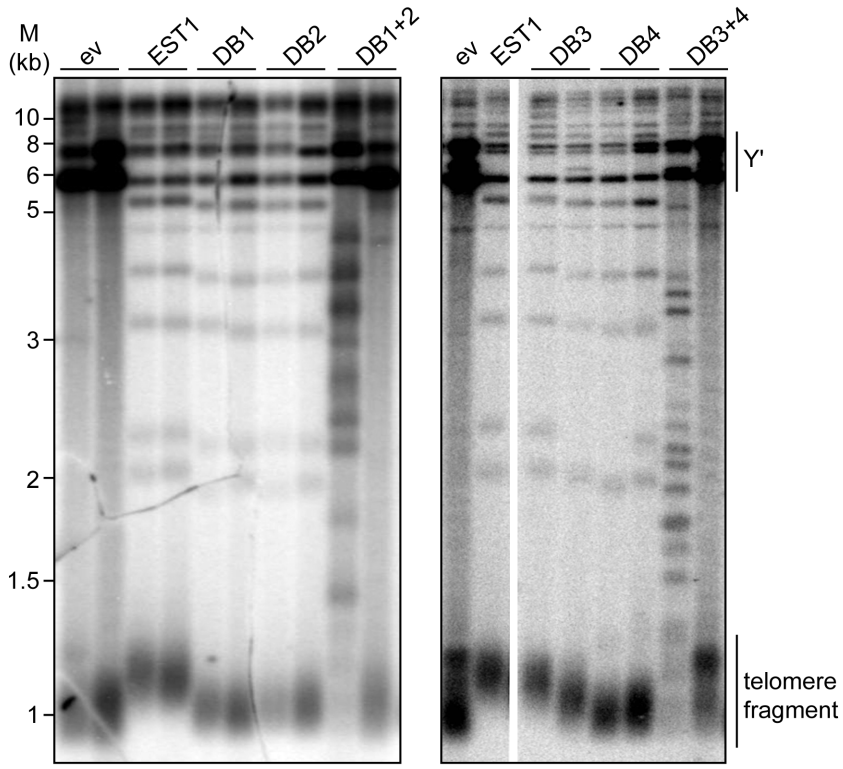

Figure 15. Stabilized alleles of Est1p fail to complement an *est1* deletion.
Independent isolates from strain YKF810 (*est1Δ*) harboring plasmids pRS416 (empty vector: ev), pRS416-*EST1* (EST1), or the *est1* alleles indicated (DB1; DB2; DB1+2; DB3; DB4; DB3+4) were propagated for >100 generations. DNA was extracted, digested with *Xho*I, Southern blotted, and probed with a randomly labeled telomeric DNA probe. Y′-elements and telomere fragments from Y′-containing chromosomes are indicated. Positions of molecular weight markers (M) are indicated in kilobases (kb). Alleles partially compromised for function have telomere fragments that are shorter than the wild-type control while severely compromised alleles result in the formation of telomerase-negative survivors characterized by Y′-element amplification and/or heterogeneous telomere length (smears throughout the lane).

CHAPTER III

THE CONSEQUENCE OF STABILIZED EST1

Introduction

Telomeres are the unique protein-DNA regions at the ends of linear eukaryotic chromosomes that are critical for protecting chromosomes against deleterious events such as nucleolytic digestion and recognition as internal double-strand breaks. Telomerase is the reverse transcriptase responsible for maintaining telomeres (reviewed in [197]). *S. cerevisiae* telomerase activity is regulated in the cell cycle; extension occurs in late S and G2/M phases but not in G1 phase [136,137], even though the catalytic core of the complex (Est2p and *TLC1* RNA) is found to associate with the telomere during G1 phase in a manner dependent upon the *TLC1*-yKu interaction [54,55]. Est1p undergoes APC-dependent degradation during G1 phase (Chapter II) that prevents its association with the telomere and telomerase complex. Since Est1p is necessary and sufficient for the recruitment of Est3p to the telomere and into the complex, Est3p also does not robustly associate during G1 phase [81,101], though a small peak of telomere association has been observed [81]. The primary regulatory role for Est1p is to recruit telomerase to the site of action. This recruitment function is accomplished through the direct protein-protein interaction between Est1p and the ssDNA binding protein Cdc13p [96-100].

In Chapter II, I demonstrated that the APC is involved in the degradation of Est1p during G1 phase. The APC is a multi-subunit E3 ubiquitin ligase that is critical for transit through the cell cycle. Although the core subunits are constitutively expressed

[161,201,202], APC functionality oscillates due to phosphorylation states [208-210], exhibiting no activity in S and G2 phase, and high activity during mitosis and G1 phase [203]. The APC uses two evolutionarily conserved, WD40-domain containing activators, Cdc20p/Fizzy and Cdh1p/Hct1/Fizzy-related [204-206]. These activators bind directly to substrates via degradation motifs [173,178,181,182], the best characterized being the Destruction box (D-box: an arginine and leucine separated by any two amino acids, RxxL) and KEN-box [174,177,207]. One significant aspect of my research was examining the contribution of putative D-boxes (consensus RxxL) to Est1p half-life during G1 phase. Six predicted D-boxes were systematically examined by disruption with alanine substitutions targeted to the conserved R and L of the consensus motif (AxxA; Figure 12). When mutated, three of these D-boxes (1, 2 and 4) stabilized Est1p during G1 phase, arguing that these regions are important for degradation (Figure 12 and 13). However, each of these mutants failed to complement an *est1Δ* strain for telomere length, suggesting these alleles are compromised for an essential function of Est1p (Figure 15). In this chapter, I characterize additional Est1p D-box mutants and demonstrate that there is no detectible consequence to stabilizing Est1p.

Results and Discussion

Stabilized alleles of *est1* have short telomeres

Three of the six putative D-boxes (1, 2 and 4) stabilized Est1p during G1 phase when mutated (RxxL → AxxA), but each of these mutants failed to complement an *est1Δ* strain for telomere length, suggesting these alleles are compromised for an essential

function of Est1p (Figure 15). To identify *est1* mutants that retained telomere maintenance, I tested a variety of other D-box mutations. I made more modest substitutions in which the conserved Arg was changed to Lys to preserve the amino acid charge and expressed these changes either as a single mutant (KxxL or R→K) or with the conserved Leu simultaneously mutated (KxxA or R→K,L→A). As shown in Figure 16, the charge-preserving substitutions of R→K (lanes 3 and 19) maintained nearly wild-type telomere length. Though the combination with the L→A mutation showed telomere shortening (lane 4 and 20), this decrease was not as severe as that observed from the original (AxxA) mutations (lanes 7, 8, and 14), suggesting the charge of the residue is important for telomerase function. Simultaneously mutating different D-boxes (lanes 9, 11 and 15) results in constructs that are unable to complement the *est1Δ* (Figure 16), suggesting the four amino acids involved in the substitutions (AxxA + AxxA) are important residues for function and that the deleterious defects are additive.

It became apparent that there is a strong negative correlation between stability and function in telomere length maintenance: mutation of predicted D-box 3 results in telomeres with near wild-type length, but the same mutations in D-box 1, 2, or 4 results in very short telomeres (Figure 17). Furthermore, combining D-box 3 (AxxA) with D-box 2 (AxxA) does not compromise telomere length more than that observed with the single D-box 2 mutations (Figure 16, compare lanes 8 and 10). This result is consistent with D-box 3 exhibiting a wild-type half-life in G1 phase (Figure 12), suggesting it is not a true degron motif. Therefore, I hypothesized that stabilization of Est1p was detrimental to telomere length maintenance.

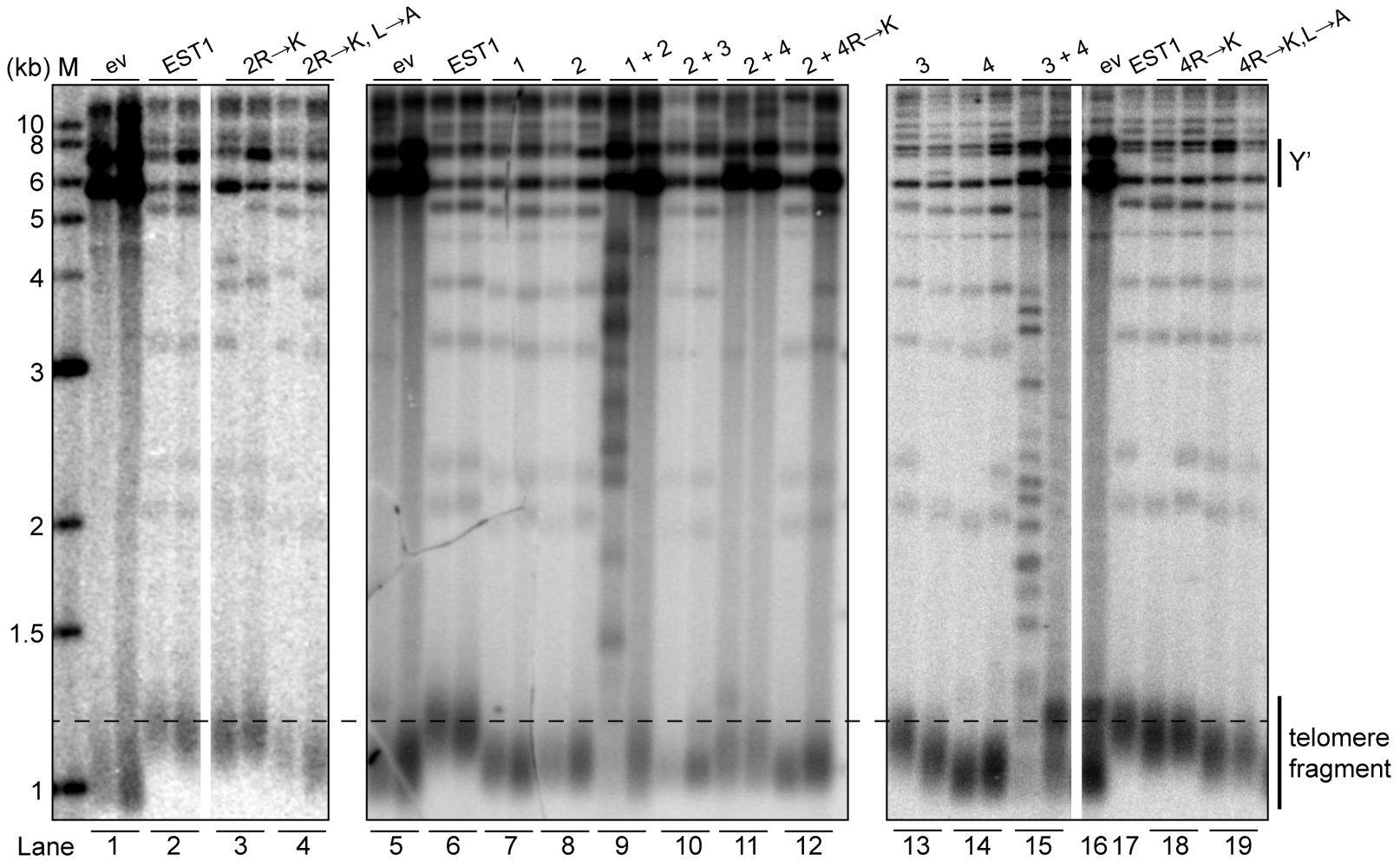
(kb) M
ev
EST1
2R→K
2R→K, L→A
ev
EST1
1
2
1 + 2
2 + 3
2 + 4
2 + 4R→K
3
4
3 + 4
ev
EST1
4R→K
4R→K,L→A
10
8
6
5
4
3
2
1.5
1
Y'
telomere
fragment
Lane
1
2
3
4
5
6
7
8
9
10
11
12
13
14
15
16
17
18
19

Figure 16. Mutation of Est1p D-boxes compromises telomere length.
Independent isolates from strain YKF810 (*est1Δ*) harboring plasmids pRS416 (empty vector: ev), pRS416-*EST1* (EST1), or the *est1* D-box alleles indicated were propagated for >100 generations. DNA was extracted, digested with *Xho*I, Southern blotted, and probed with a randomly labeled telomeric DNA probe. Y′-elements and telomere fragments from Y′-containing chromosomes are indicated. Positions of molecular weight markers (M) are indicated in kilobases (kb). The horizontal dashed line indicates wild-type telomere length. Alleles partially compromised for function have telomere fragments that are shorter than the wild-type control while severely compromised alleles result in the formation of telomerase-negative survivors characterized by Y′-element amplification and/or heterogeneous telomere length (smears throughout the lane). Shown are three separate gels; irrelevant lanes have been removed and are represented by thin white spaces.

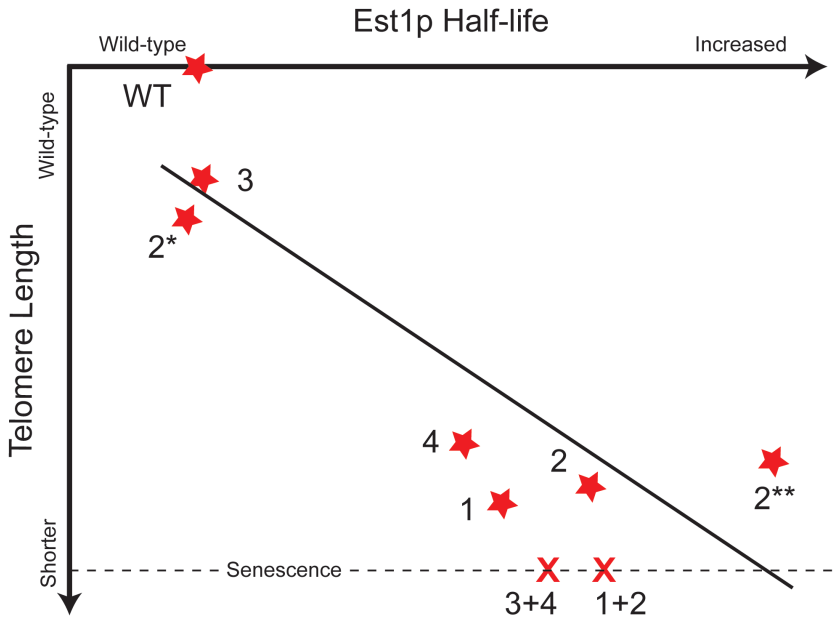

Figure 17. Negative correlation between Est1p half-life and telomere length. Telomere lengths were quantified from independent isolates of strain YKF810 (*est1Δ*) harboring plasmids pRS416-*EST1* (WT) or the *est1* D-box alleles indicated. The mean change in telomere length compared to WT was determined and plotted against the average protein half-life. A line of best fit is shown and demonstrates that as Est1p stability increases, telomere length decreases. Two *est1* D-box alleles (1+2 and 3+4) are represented by a red "X" at the value of their protein half-life (Figure 13); a telomere length measurement is uninformative due to survivor formation and maintenance of telomeres using a telomerase-independent mechanism (Figure 16, lanes 9 and 15). However, since these mutants result in survivor formation, the length can be interpreted to be shorter than that of any other mutant shown. * indicates DB2KxxL and ** indicates DB2KxxA.

If this hypothesis is correct, the wild-type length conferred by D-box 2 (KxxL) should be associated with a wild-type protein half-life in G1 phase, and the D-box 2 (KxxA) mutation should have an increased half-life, since it shortens telomeres. The protein half-life of these alleles measured with the promoter shut-off assay was consistent with this hypothesis (Figure 18). However, the correlation is not absolute. The D-box 2 (KxxA) mutation stabilizes the protein similarly to the more severe mutation (AxxA) that shortens telomeres to a greater extent. It is also important to note that the half-lives of alleles with mutations of the Arg residue only (AxxL or KxxL) are not significantly different from wild type. These results suggest that mutation of the D-box 2 leucine residue is required to escape degradation, but I did not confirm this by mutation of the conserved Leu residue alone. While most studies have examined simultaneous mutation of the Arg and Leu residues to test for D-box function, cyclin B can be stabilized with mutation of the Arg residue alone *in vitro* [175] and *in vivo* [233]. Therefore, I cannot exclude the possibility that the stabilization gained from these mutations is independent of degron recognition by the APC.

The experiments presented above were conducted using a 2μ P_{GAL1}-HA_3-*EST1* plasmid (pKF600). However, a plethora of experiments were conducted examining the contribution of these D-boxes to Est1p degradation using a different 2μ plasmid (pRS423-*GAL1*-HA_3-*EST1*). Although the *EST1* ORF is identical on these two plasmids, I discovered that Est1p degradation is not regulated in the endogenous manner when expressed from the pRS423 plasmid: the protein is unstable throughout the cell cycle (Figure 8). A number of additional D-box mutations were tested for effects on protein stability in G1 phase in the context of the pRS423 vector before the anomalous

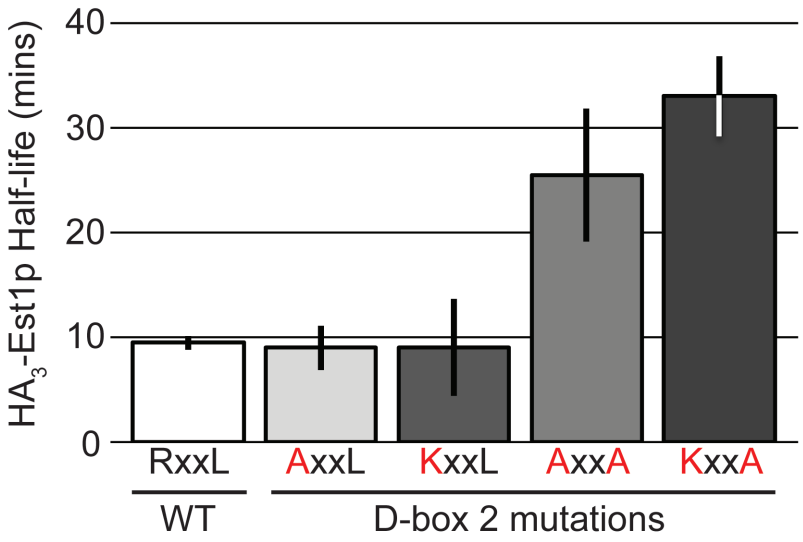

Figure 18. Degradation of Est1p requires the conserved leucine residue in D-box 2. Quantification of promoter shut-off assays, as described in Figure 12. Alleles shown here are *est1-DB2* (AxxA; described in Chapter II); *est1-DB2R→A* (AxxL); *est1-DB2R→K* (KxxL); and *est1-DB2R→K,L→A* (KxxA). Differences from the wild-type (WT) *EST1* sequence are depicted in red. Two distinct alleles of D-box 2 result in stabilization of the protein during G1 phase. This stabilization depends upon simultaneous disruption of both conserved residues. Bars represent the average half-life from three independent experiments; error bars are the deviation from the mean. DB2 (AxxL) and DB2 (KxxL) are not statistically different from WT (p-values = 0.73 and 0.88, respectively). DB2 (KxxA) and DB2 (AxxA) are statistically different from WT (p-values = 0.0005 and 0.012, respectively).

degradation pattern of this protein was discovered. Although many of these constructs had effects consistent with results later obtained in pKF600, these data were not used in these studies. The reason for the different behavior of the pRS423-expressed protein is unknown.

Fusion of the *CLB2* D-box to stabilized *est1* alleles rescues telomere length

If reduced degradation of Est1p during G1 phase is the cause of telomere shortening, I would expect telomere length to be rescued if the mutated protein was rendered unstable. D-box motifs are transportable, conferring degradation to a normally stable protein [174,175,217]. Therefore, I fused the D-box from *CLB2* (RLALNNVTN) to the N-terminus of the *est1* alleles and examined the ability of the constructs expressing these alleles to maintain telomere length in an *est1Δ* background. As shown in Figure 19, fusion of the *CLB2* D-box to $est1^{DB2\underline{A}xx\underline{A}}$ or $est1^{DB2\underline{K}xx\underline{A}}$ rescued telomere length (compare lanes 11 and 19 with 10 and 18, respectively). This rescue was specific to those mutations within D-box 2, since no rescue was achieved with fusion to $est1^{DB1}$ (lanes 5 and 6), $est1^{DB1+2}$ (lanes 13 and 14), $est1^{DB4}$ (lanes 21 and 22) or $est1^{DB3+4}$ (26 and 27). Likewise, there was no telomere elongation when fused to wild-type *EST1* (lanes 2 and 3). These results suggest that the telomere length defect can be rescued by restoring the presence of a D-box (and presumably degradation).

To determine if this rescue depends upon the function of the *CLB2* D-box, I mutated the conserved Arg, Leu, and Asn to Ala (RLALNNVTN→<u>A</u>LL<u>A</u>NNVT<u>A</u>) and examined telomere length maintenance in an *est1Δ* strain. As expected, the mutated fusion no longer rescued the D-box 2 alleles (Figure 19, lanes 12 and 20), arguing that an

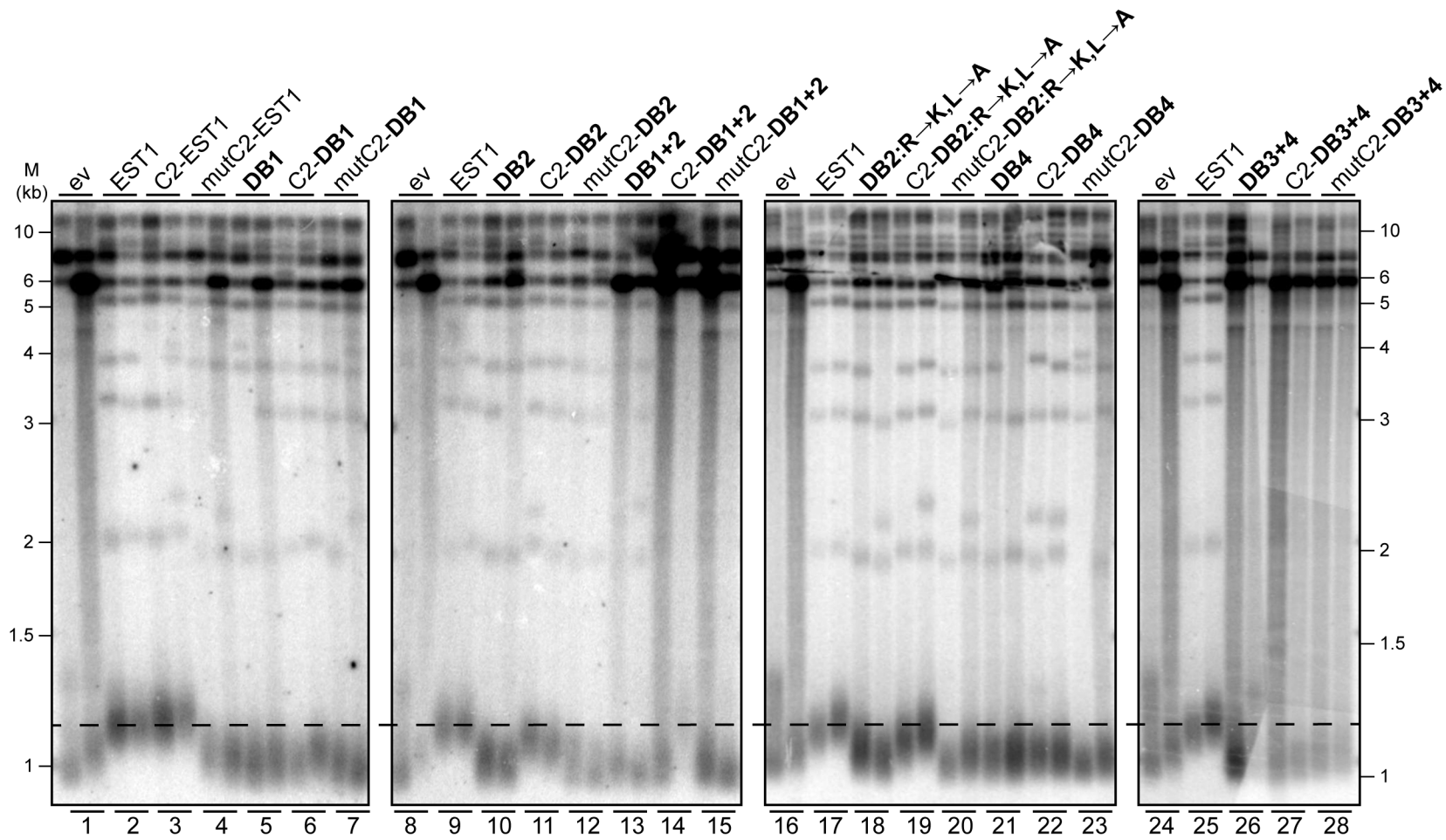
M
(kb)
ev
EST1
C2-EST1
mutC2-EST1
DB1
C2-DB1
mutC2-DB1
ev
EST1
DB2
C2-DB2
mutC2-DB2
DB1+2
C2-DB1+2
mutC2-DB1+2
ev
EST1
DB2:R→K,L→A
C2-DB2:R→K,L→A
mutC2-DB2:R→K,L→A
DB4
C2-DB4
mutC2-DB4
ev
EST1
DB3+4
C2-DB3+4
mutC2-DB3+4
10
6
5
4
3
2
1.5
1
1 2 3 4 5 6 7 8 9 10 11 12 13 14 15 16 17 18 19 20 21 22 23 24 25 26 27 28

Figure 18. Fusion of the D-box from *CLB2* rescues the telomere length of Est1^{DB2} alleles.
Independent isolates from strain YKF810 (*est1Δ*) harboring plasmids pRS416 (empty vector: ev), pRS416-*EST1* (EST1), or the *est1* D-box alleles indicated. Also shown are these alleles fused to either the wild-type (RLALNNVTN) or mutant (ALLANNVTA) *CLB2* D-box (denoted C2 or mutC2, respectively). Isolates were propagated for >100 generations. DNA was extracted, digested with *Xho*I, Southern blotted, and probed with a randomly labeled telomeric DNA probe. Positions of molecular weight markers (M) are indicated in kilobases (kb). The horizontal dashed line indicates wild-type telomere length. Alleles partially compromised for function have telomere fragments that are shorter than the wild-type control while severely compromised alleles result in the formation of telomerase-negative survivors characterized by Y′-element amplification and/or heterogeneous telomere length (smears throughout the lane).

intact D-box is necessary. However, interpretation of this result is complicated by the observation that telomere shortening also occurs with fusion of the mutated *CLB2* D-box to wild-type *EST1*, despite the lack of effect from the WT *CLB2* D-box sequence. This shortening was specific to the mutated *CLB2* D-box sequence (lanes 2-4). I re-examined this effect using a less severe mutation of the *CLB2* D-box, substituting only the Arg and Leu residues, but this construct also compromised telomere length when fused to wild-type *EST1* (data not shown).

To confirm that the *CLB2* D-box restored regulated degradation when fused to D-box 2 mutants, I determined the half-life of the fusion proteins using the promoter shut-off assay. I also monitored the stability of the wild-type *EST1* fusion, which was expected to show the same stability as Est1p alone. Fusion of the *CLB2* D-box to the *est1* allele mutated in D-box 4 did not restore telomere length, so the half-life of this fusion protein was determined as well. As an additional control, I monitored the half-life of each protein when fused to the mutant *CLB2* D-box. Unexpectedly, the fusion of the *CLB2* D-box sequence to the D-box 2 mutant protein did not lessen the protein half-life (Figure 20). The half-life was also similarly unchanged for wild-type Est1p and D-box 4 fusions. Although the half-life remained unchanged when the mutated *CLB2* D-box was fused to each of these proteins, this result is uninformative in light of the failure of the WT *CLB2* D-box to promote protein degradation. These results suggest that the telomere shortening observed upon stabilization of Est1p in the D-box 2 variants is not a simple consequence of Est1p overexpression or stability in G1 phase, since the fusion protein retains a long half-life yet exhibits a return to wild-type telomere length. Perhaps the mutations in D-box 2 compromise Est1 protein folding that the fusion of the WT *CLB2*

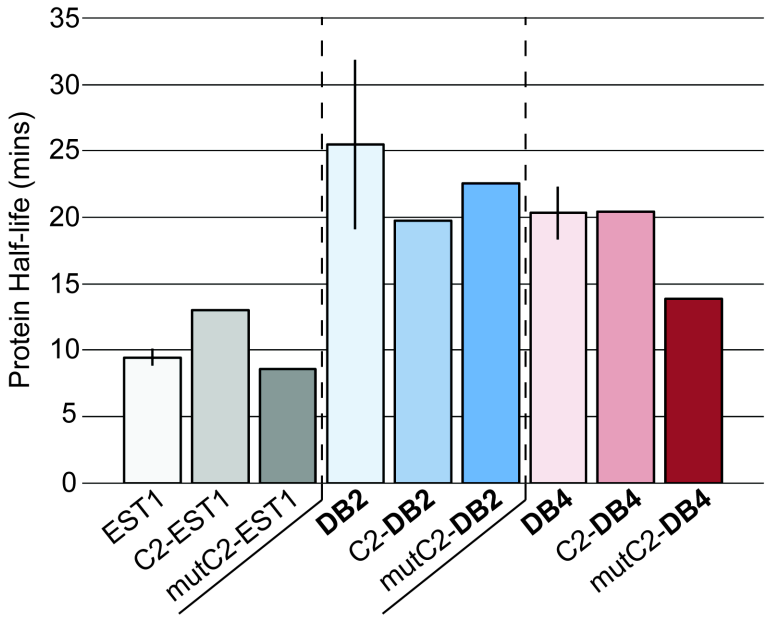

Figure 20. Fusion of the *CLB2* D-box does not change protein half-lives.
YKF802 containing pKF600 (*GAL1-HA$_3$-EST1*) plasmids expressing either wild-type *EST1* (WT) or the D-box (DB) mutated (RxxL to AxxA) *est1* alleles indicated were treated as in Figure 8B, except strains were arrested with α-factor. Also tested were alleles fused to either the wild-type (RLALNNVTN) or mutant (ALLANNVTA) *CLB2* D-box (denoted C2 or mutC2, respectively) at the N-terminus of the *EST1* ORF. Values for EST1, DB2 and DB4 represent the average half-life for three independent biological replicates; error bars are the standard deviation of the mean. Values for the fusion constructs are from a single experiment.

D-box helps restore. If so, the *est1* alleles that failed to be rescued (Figure 19) may be more severely unfolded or compromised for an essential Est1p function.

Overexpression of wild-type *EST1* does not compromise telomere length

Telomere length is compromised when D-boxes are mutated and the Est1 protein is stabilized against degradation in G1 phase. However, while I was able to rescue telomere length with fusion of the *CLB2* D-box to Est1-DB2 mutants (Figure 19), the protein remained stabilized (Figure 20), suggesting that the stabilized protein is not the cause of telomere shortening. Since increased resistance of a protein to degradation will result in increased steady-state levels of that protein, overproducing the protein may mimic the consequences of inappropriate stabilization. Therefore, I examined the telomere length of strains that constitutively expressed *EST1* under control of the *ADH1*, *TEF*, or *GAL1* promoters to achieve different levels of overexpression. As shown in Figure 21, introduction of a *CEN* vector expressing *EST1* under control of the endogenous promoter did not change telomere length as compared to the empty vector control (lanes 1 and 2). Introduction of a *CEN* vector expressing *EST1* under the control of *ADH1*, *TEF*, or *GAL1* promoters did not result in telomere shortening (lanes 3, 4, and 5). In fact, telomeres appear to have elongated. Taken together, these data suggest there is no adverse consequence to preventing Est1p degradation during the cell cycle. A discussion of the implication of these findings is in Chapter V.

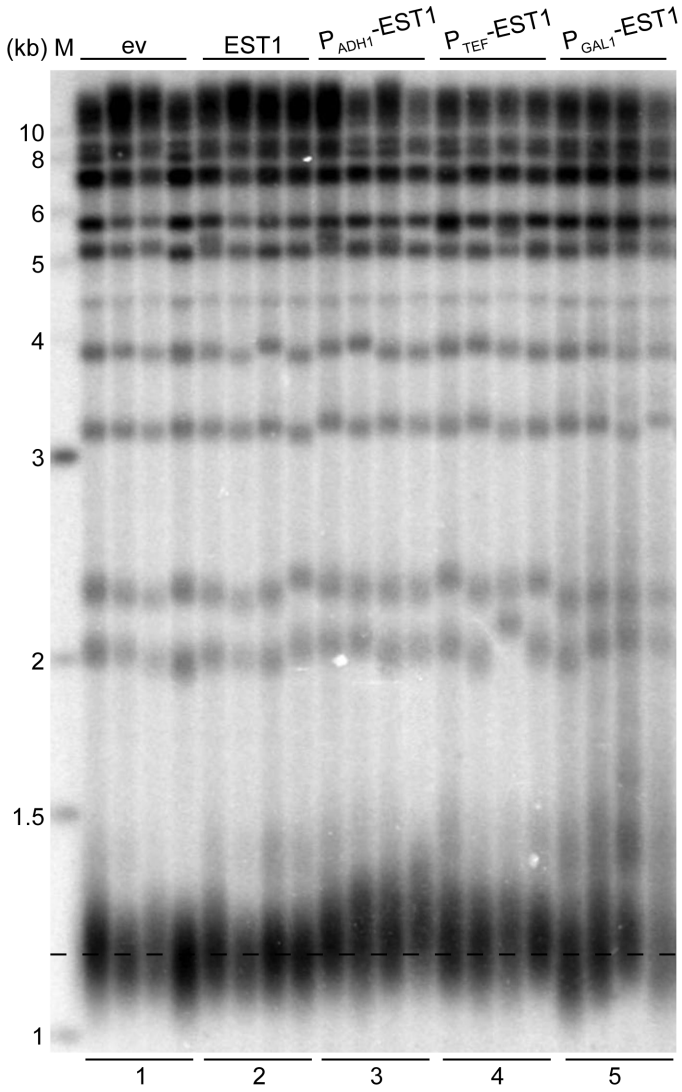

Figure 21. Overexpression of *EST1* does not compromise telomere length maintenance.

Four independent isolates from strain YKF802 (*EST1*) harboring pRS416 (empty vector: ev), pRS416-*EST1* (EST1), or plasmids expressing *EST1* under control of the overexpression promoters, *ADH1*, *TEF*, or *GAL1*. Isolates were propagated for >100 generations on glucose media, except for *GAL1* which was propagated on galactose containing media. DNA was extracted, digested with *Xho*I, Southern blotted, and probed with a randomly labeled telomeric DNA probe. Positions of molecular weight markers (M) are indicated in kilobases (kb). The horizontal dashed line indicates the average wild-type telomere length. Note the smears do not decrease in length, indicating no telomere shortening occurred.

CHAPTER IV

MATERIALS AND METHODS

Ethics Statement

All work with *Xenopus laevis* was approved by the Institutional Animal Care and Use Committee (IACUC) at Vanderbilt University Medical Center (protocol #M/07/143) and was carried out in accordance with their policies and guidelines. *Xenopus laevis* were maintained by the Division of Animal Care (DAC) at Vanderbilt University's Animal Care Facility, which provides both veterinary and husbandry services. Animals were monitored on a daily basis by the DAC for signs of morbidity (e.g. lethargy, open sores, and excessive skin shedding). Animals with these symptoms were subsequently euthanized by anaesthetic overdose with 0.05% Benzocaine absorbed through the skin, consistent with recommendations from the Panel on Euthanasia of the American Veterinary Medical Association.

Yeast Strains and Plasmids

S. cerevisiae strains used in this study are summarized in Table 1. All gene disruptions were generated using PCR-mediated gene disruption [234]; primer sequences are shown in Table 2. The *bar1Δ::hisG* in K1534 [212] was replaced by amplification of the *bar1Δ::kanMX4* cassette from the yeast knockout collection [235] (Open Biosystems) to yield YKF800 using primer pair Bar1for/Bar1rev. The *bar1Δ::hisG* of K1534,

MAY6810 and MAY6812 [217] was replaced by amplifying (primer pair Bar1::Hyg/Bar1::Hyg) the *hphMX4* cassette from pAG32 [236] to yield YKF802, YKF806, and YKF807, respectively. YKF803, YKF804, and YKF805 were constructed by amplification of the *apc9*, *mnd2* and *swm1* gene disruption cassettes (*xxx::kanMX4*) from the yeast knockout collection and integrated into YKF802, using primer pairs Apc9for/Apc9rev; Mnd2for/Mnd2rev; and Swm1for/Swm1rev, respectively. A MYC_{13} epitope tag was incorporated at the C terminus of the endogenous *EST1* locus using plasmid pRS416-*EST1-MYC$_{13}$-hphNT1* [derived from pFA6a-13MYC-kanMX6 [237], pYM16 (*hphNT1*) [238] (Euroscarf), and pRS416 [239]; details of plasmid construction available by request]. Digestion of this plasmid with *Sac*I and *Kpn*I yielded a linear DNA molecule containing homology upstream and downstream of the *EST1* chromosomal locus to allow one-step gene replacement. Transformation of this fragment into strains YKF800 and YCM191 yielded YKF801 and YKF808, respectively. YKF809 was generated by PCR-amplification of the *cdh1Δ::KAN^R* allele from MAY6812 and introduction into YKF808 by one-step gene replacement. To yield YKF810, the endogenous *EST1* locus was deleted in YKF802 by PCR-based gene deletion using plasmid pFA6a-kanMX6 [237].

Plasmids used in this study are summarized in Table 3. Plasmid pKF600 is derived from pVL242RtoA [101] and differs by the arrangement of restriction sites to facilitate cloning of mutant alleles. Individual D-box mutations (RxxL → AxxL, KxxL, KxxA or AxxA) were constructed by site-directed mutagenesis using the SOEing method (Figure 22) [240] and cloned into pKF600 using *Bam*HI and *Sph*I to yield the indicated pKF600-DB plasmids. Simultaneous mutation of D-boxes 1+2, 2+3, 2+4, 3+4,

2+4R→K, or 5+6 was achieved by site-directed mutagenesis using a single mutant plasmid as the template in the PCR reaction. Deletion alleles of *EST1* were generated by PCR amplification of a portion of *EST1* followed by insertion into pKF600 using primers M1209 + delta300; and E1Ndel7, E1Ndel15, E1Ndel25, E1Ndel35 or E150D + M1212. Plasmid pRS416-EST1 was generated by PCR amplifying the *EST1* upstream promoter region, ORF, and downstream terminator region and cloning into pRS416. Mutant *est1* alleles were introduced by subcloning from the pKF600 vector series, to yield the indicated pRS416-DB plasmids. To generate *CLB2* D-box fusion plasmids, *EST1* was amplified using primer pair (Clb2Dboxinsert and EST1R264AL267Arev) or (Clb2mutDboxins and EST1R264AL267Arev) and cloned into pRS416-EST1 using *Bam*HI and *Pfl*MI; this region was then subcloned into the pRS416-DB plasmids using *Hpa*I. The *CDC16* complementing plasmid was generated in two steps: one primer pair (CDC16for + CDC16intrev) amplified the promoter region and first-half of the *CDC16* ORF while a second primer pair (CDC16intfor + CDC16rev) amplified the second-half of the *CDC16* ORF and terminator. These two fragments were sequentially cloned into pRS416 using *Xho*I/*Cla*I and *Cla*I/*Sac*I to yield the complementing vector, pRS416-CDC16. This construct complemented the *cdc16-123* ts allele for growth at 37°C. The promoter region of pYM-N6 (ADH1), pYM-N18 (TEF) or pYM-N22 (GAL1) [238] was digested with *Sac*I and *Xba*I, and cloned into pRS416; the *EST1* ORF from pRS416-EST1 was subcloned downstream of the promoter using *Bam*HI and *Kpn*I digestion to yield the pRS416-Promoter-EST1 plasmids. To generate plasmid pKF601, the *EST1* ORF was PCR-amplified (Est1Fsefor + Est1Ascrev) and cloned into pCS2FA2R [derivative of pCS2; gift from Laurie Lee] at restriction sites *Fse*I and *Asc*I. The *EST1*

ORF was PCR-amplified (M1209 + yEst1XbaRev) and cloned into pcDNA3.1-Hygro (Invitrogen) at restriction sites *Bam*HI and *Xba*I to yield pKF602.

Table 1. *S. cerevisiae* strains used in this study.

Name	[a] Relevant Genotype	Source
K1534	*bar1Δ::hisG*	[212]
YKF800	*bar1Δ::kanMX4*	This study
YKF801	YKF800 *EST1-MYC$_{13}$* [*hphNT1*]	This study
YKF802	*bar1Δ::hphMX4*	This study
K4438	K1534 *cdc16-123*	[212]
YKF803	YKF802 *apc9Δ::kanMX4*	This study
YKF804	YKF802 *mnd2Δ::kanMX4*	This study
YKF805	YKF802 *swm1Δ::kanMX4*	This study
MAY6810	*bar1Δ::hisG clb2Δ::URA3*	[217]
YKF806	*bar1Δ:: hphMX4 clb2Δ::URA3*	This study
MAY6812	*bar1Δ::hisG clb2Δ::URA3 cdh1Δ:: KAN^R*	[217]
YKF807	*bar1Δ::hphMX4 clb2Δ::URA3 cdh1Δ::KAN^R*	This study
YCM191	*bar1Δ::URA3 cdc15-2*	Gift from C. Hardy
YKF808	YCM191 *EST1-MYC$_{13}$ [hphNT1]*	This study
YKF809	YKF808 *cdh1Δ::KAN^R*	This study
YKF810	YKF802 *est1Δ::kanMX6*	This study

[a] All strains are derivatives of W303: *MATa ade2-1 trp1-1 can1-100 leu2-3,112 his3-11,15 ura3 ssd1 GAL*

Table 2. Primers used in this study.

Primer Name	[a] Primer Sequence 5' → 3'
Bar1::Hyg forward	CATACCAAAATAAAAAGAGTGTCTAGAAGGGTCATATAGGCGCGCCA GATCTGTTTAG
Bar1::Hyg reverse	GATATTTATATGCTATAAAGAAATTGTACTCCAGATTTCATCGATGAA TTCGAGCTCG
Bar1for	GTTTATAGATAACGGCTCTTGC
Bar1rev	CGTTTGGTTAGTTCAGCTAGG
M1209	ACTAGGATCCTAATGGATAATGAAGAAGTTAACGAAG
M1212	CCCTCACCATTACTTGTTCTCGCATGCTCAAGTAGGAGTATCTGGC
E1DB1RL2Afor-ext	CAAGAACGCTGCAGCGCATGCGGATAAACATCTAACATC
E1DB1RL2Arev-ext	GATGTTAGATGTTTATCCGCATGCGCTGCAGCGTTCTTG
E1DB2rightFor	GCATATATCACGTTCGCTTGCTTCGCGGATGGTATACATTGCAAATCT AC
E1DB2rightRev	GTAGATTTGCAATGTATACCATCCGCGAAGCAAGCGAACGTGATATAT GC
DB2R2Kfor	GCATATATCACGTTTAAATGCTTCCTGG
DB2R2Krev	CCAGGAAGCATTTAAACGTGATATATGC
DB2R2KL2Afor	GCATATATCACGTTTAAATGCTTCGCGGATGGAATACATTGC
DB2R2KL2Arev	GCAATGTATTCCATCCGCGAAGCATTTAAACGTGATATATGC
EST1R264AL267Afor	CTGTATTTTTTTGAATTAGTAGCAGGAGCTGCAGTAAGGATTCCG
EST1R264AL267Arev	CGGAATCCTTACTGCAGCTCCTGCTACTAATTCAAAAAAATACAG
E1DB4RL2Afor-ext	CTCCTAATTTTCCGGAAGCAAGACGTGCGATGAAAAAATTGGC
E1DB4RL2Arev-ext	GCCAATTTTTTCATCGCACGTCTTGCTTCCGGAAAATTAGGAG
E1DB4R2Kfor	CCTAATTTTCCGGAAAAAAGACGGCTGATGAAAAAATTGG
E1DB4R2Krev	CCAATTTTTTCATCAGCCGTCTTTTTTCCGGAAAATTAGG
E1DB4R2KL2Afor	CCTAATTTTCCGGAAAAAAGACGTGCGATGAAAAAATTGG
E1DB4R2KL2Arev	CCAATTTTTTCATCGCACGTCTTTTTTCCGGAAAATTAGG
E1DB5RL2ADMfor	GATTAAGTCATATGCATCTATTGCGCAGTACACTC
E1DB5RL2ADMrev	GAGTGTACTGCGCAATAGATGCATATGACTTAATC
E1DB6RL2Afor-ext	GCCACAGGCCGAAAGCTAGCTATGCTTTTAGAGAAGATATTATTTTCA GG
E1DB6RL2Arev-ext	CCTGAAAATAATATCTTCTCTAAAAGCATAGCTAGCTTTCGGCCTGTG GC
Clb2Dboxinsert	CACATGCCACCGGATCCTAATGAGATTGGCTTTGAACAACGTTACTAA TGATAATGAAGAAG

Table 2, continued

Primer Name	[a] Primer Sequence 5' → 3'
Clb2mutDboxinsert	CACATGCCACCGGATCCTAATGGCATTGGCTGCCAACAACGTTACTGC TGATAATGAAGAAG
Est1 Fse for	GATTGGGGCCGGCCATGGATAACGAAGAAGTTAACGAAG
Est1 Asc rev	GATTGGGGCGCGCCTCAAGTAGGAGTATCTGGCAC
yEst1XbaRev	GGACTCTAGATCAAGTAGGAGTATCTGGCACTTG
CDC16for	GCTCCTCGAGCGCTATGCGATGAAAGCATTG
CDC16intfor	CCTTCTGTCGCATCGATTAGCGGAAAC
CDC16intrev	GTTTCCGCTAATCGATGCGACAGAAGG
CDC16rev	GGACGAGCTCGGGAAAGAAGAACGGCAAGGAG
Apc9 forward	GAACAGGGAACTAGGTTTGGAAG
Apc9 reverse	GTATAGAAAACGCATATCAACTG
Mnd2 forward	CTGTGCTACGCCACATCAGAATAC
Mnd2 reverse	CTAAGCACTTTTGGTGCACTTGTG
Swm1 forward	CGTGAGAGAAGGGAGAATAATATC
Swm1 reverse	GTGCATAGTACCCATACACCAC
delta300	GTCCGCATGCTCAATCGAAACTTCCCATTGTGGC
E1Ndel7	GCTAAGGATCCTAGAAGAATGTATGAGATTATTTTTC
E1Ndel15	GCTAAGGATCCTAAAGAACGCTCGTGCGCATCTG
E1Ndel25	GCTAAGGATCCTAACATCAAGGTTGACATGCGATG
E1Ndel35	GCTAAGGATCCTAGCATATATCACGTTCAGATGC
E150D	GCTAAGGATCCTAGCGACTAGGTTTCTCGAAGAGC

[a] Underlined sequence indicates restriction enzyme recognition site.

Table 3. Plasmids used in this study.

Name	Relevant Sequence or description	Source
pVL242RtoA	P_{GAL1}-*HA*$_3$-*EST1 [LEU2 2μ]*	[101]
pKF600	P_{GAL1}-*HA*$_3$-*EST1 [LEU2 2μ]*	This study
pKF600-DB1	P_{GAL1}-*HA*$_3$-*est1*$^{D\text{-}box\ 1\ (RAHL \rightarrow \underline{A}AH\underline{A})}$	This study
pKF600-DB2	P_{GAL1}-*HA*$_3$-*est1*$^{D\text{-}box\ 2\ (RCFL \rightarrow \underline{A}CF\underline{A})}$	This study
pKF600-DB3	P_{GAL1}-*HA*$_3$-*est1*$^{D\text{-}box\ 3\ (RGAL \rightarrow \underline{A}GA\underline{A})}$	This study
pKF600-DB4	P_{GAL1}-*HA*$_3$-*est1*$^{D\text{-}box\ 4\ (RRRL \rightarrow \underline{A}RR\underline{A})}$	This study
pKF600-DB1+2	P_{GAL1}-*HA*$_3$-*est1*$^{D\text{-}box\ 1+2}$	This study
pKF600-DB3+4	P_{GAL1}-*HA*$_3$-*est1*$^{D\text{-}box\ 3+4}$	This study
pKF600-DB5+6	P_{GAL1}-*HA*$_3$-*est1*$^{D\text{-}box\ 5+6\ (RSIL \rightarrow \underline{A}SI\underline{A}\ and\ RSYL \rightarrow \underline{A}SY\underline{A})}$	This study
pKF600-C300	P_{GAL1}-*HA*$_3$-*est1*$^{C\Delta 300}$	This study
pKF600-N7	P_{GAL1}-*HA*$_3$-*est1*$^{N\Delta 7}$	This study
pKF600-N15	P_{GAL1}-*HA*$_3$-*est1*$^{N\Delta 15}$	This study
pKF600-N25	P_{GAL1}-*HA*$_3$-*est1*$^{N\Delta 25}$	This study
pKF600-N35	P_{GAL1}-*HA*$_3$-*est1*$^{N\Delta 35}$	This study
pKF600-N50	P_{GAL1}-*HA*$_3$-*est1*$^{N\Delta 50}$	This study
pKF600-DB2R2A	P_{GAL1}-*HA*$_3$-*est1*$^{D\text{-}box\ 2\ (RCFL \rightarrow \underline{A}CFL)}$	This study
pKF600-DB2R2K	P_{GAL1}-*HA*$_3$-*est1*$^{D\text{-}box\ 2\ (RCFL \rightarrow \underline{K}CFL)}$	This study
pKF600-DB2R2KL2A	P_{GAL1}-*HA*$_3$-*est1*$^{D\text{-}box\ 2\ (RCFL \rightarrow \underline{K}CF\underline{A})}$	This study
pKF600-C2	P_{GAL1}-*HA*$_3$-*Clb2DB-EST1*	This study
pKF600-C2-DB2	P_{GAL1}-*HA*$_3$-*Clb2DB- est1*$^{D\text{-}box\ 2}$	This study
pKF600-C2-DB4	P_{GAL1}-*HA*$_3$-*Clb2DB- est1*$^{D\text{-}box\ 4}$	This study
pKF600-mutC2	P_{GAL1}-*HA*$_3$-*Clb2db-EST1*	This study
pKF600-mutC2-DB2	P_{GAL1}-*HA*$_3$-*Clb2db- est1*$^{D\text{-}box\ 2}$	This study
pKF600-mutC2-DB4	P_{GAL1}-*HA*$_3$-*Clb2db- est1*$^{D\text{-}box\ 4}$	This study
pRS416	Empty vector *[URA3 CEN]*	[239]
pRS416-EST1	P_{EST1}-*EST1*	This study
pRS416-DB1	P_{EST1}- *est1*$^{D\text{-}box\ 1\ (RAHL \rightarrow \underline{A}AH\underline{A})}$	This study
pRS416-DB2	P_{EST1}- *est1*$^{D\text{-}box\ 2\ (RCFL \rightarrow \underline{A}CF\underline{A})}$	This study
pRS416-DB3	P_{EST1}- *est1*$^{D\text{-}box\ 3\ (RGAL \rightarrow \underline{A}GA\underline{A})}$	This study
pRS416-DB4	P_{EST1}- *est1*$^{D\text{-}box\ 4\ (RRRL \rightarrow \underline{A}RR\underline{A})}$	This study
pRS416-DB1+2	P_{EST1}- *est1*$^{D\text{-}box\ 1+2}$	This study
pRS416-DB3+4	P_{EST1}- *est1*$^{D\text{-}box\ 3+4}$	This study
pRS416-DB2R2K	P_{EST1}- *est1*$^{D\text{-}box\ 2\ (RCFL \rightarrow \underline{K}CFL)}$	This study
pRS416-DB2R2KL2A	P_{EST1}- *est1*$^{D\text{-}box\ 2\ (RCFL \rightarrow \underline{K}CF\underline{A})}$	This study
pRS416-DB2+3	P_{EST1}- *est1*$^{D\text{-}box\ 2+3}$	This study
pRS416-DB2+4	P_{EST1}- *est1*$^{D\text{-}box\ 2+4}$	This study
pRS416-DB2+4R2K	P_{EST1}- *est1*$^{D\text{-}box\ 2+4\ (RRRL \rightarrow \underline{K}RRL)}$	This study
pRS416-DB4R2K	P_{EST1}- *est1*$^{D\text{-}box\ 4\ (RRRL \rightarrow \underline{K}RRL)}$	This study
pRS416-DB4R2KL2A	P_{EST1}- *est1*$^{D\text{-}box\ 4\ (RRRL \rightarrow \underline{K}RR\underline{A})}$	This study
pRS416-C2-EST1	P_{EST1}- *Clb2DB-EST1*	This study
pRS416-C2-DB1	P_{EST1}- *Clb2DB-est1*$^{D\text{-}box\ 1}$	This study

Table 3, continued

Name	Relevant Sequence or description	Source
pRS416-C2-DB2	P_{EST1}- *Clb2DB-est1*$^{D\text{-}box\ 2}$	This study
pRS416-C2-DB1+2	P_{EST1}- *Clb2DB-est1*$^{D\text{-}box\ 1+2}$	This study
pRS416-C2-DB2R2KL2A	P_{EST1}- *Clb2DB-est1*$^{D\text{-}box\ 2\ (RCFL \rightarrow \underline{K}CF\underline{A})}$	This study
pRS416-C2-DB4	P_{EST1}- *Clb2DB- est1*$^{D\text{-}box\ 4}$	This study
pRS416-C2-DB3+4	P_{EST1}- *Clb2DB-est1*$^{D\text{-}box\ 3+4}$	This study
pRS416-mutC2-EST1	P_{EST1}- *Clb2db-EST1*	This study
pRS416-mutC2-DB1	P_{EST1}- *Clb2db-est1*$^{D\text{-}box\ 1}$	This study
pRS416-mutC2-DB2	P_{EST1}- *Clb2db-est1*$^{D\text{-}box\ 2}$	This study
pRS416-mutC2-DB1+2	P_{EST1}- *Clb2db-est1*$^{D\text{-}box\ 1+2}$	This study
pRS416-mutC2-DB2R2KL2A	P_{EST1}- *Clb2db-est1*$^{D\text{-}box\ 2\ (RCFL \rightarrow \underline{K}CF\underline{A})}$	This study
pRS416-mutC2-DB4	P_{EST1}- *Clb2db-est1*$^{D\text{-}box\ 4}$	This study
pRS416-mutC2-DB3+4	P_{EST1}- *Clb2db-est1*$^{D\text{-}box\ 3+4}$	This study
pRS416-ADH-EST1	P_{ADH1}-*EST1*	This study
pRS416-TEF-EST1	P_{TEF}-*EST1*	This study
pRS416-GAL1-EST1	P_{GAL1}-*EST1*	This study
pRS416-CDC16	P_{CDC16}-*CDC16*	This study
pKF601	P_{Sp6}-*EST1*	This study
pCS2FA2R-Cyclin B	P_{Sp6}-*CycB*	Gift from L. Lee
pKF602	P_{T7}-*EST1*	This study
pRSET-PDS1	P_{T7}-*PDS1*	[159]

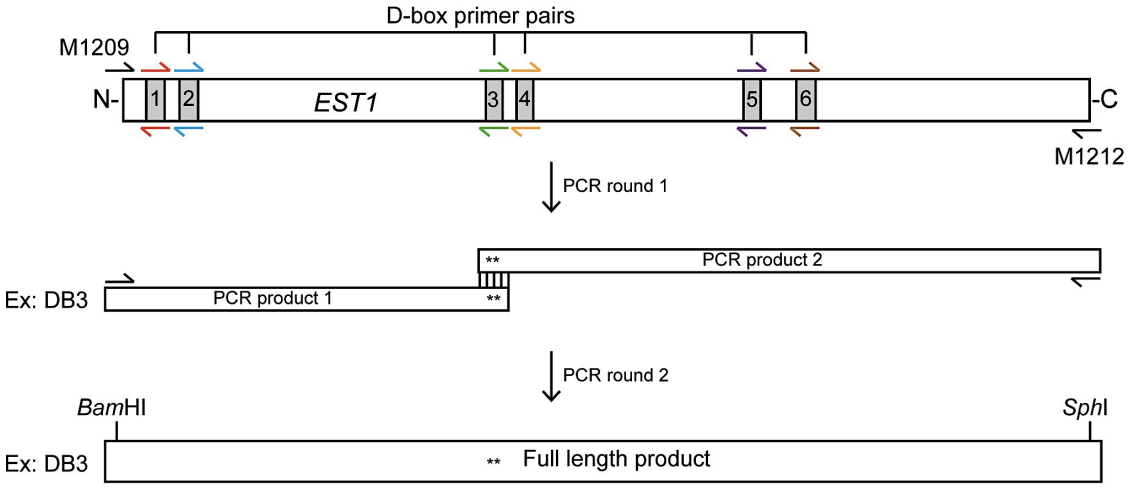

Figure 22. Construction of *est1* D-box mutant alleles by SOEing PCR.
To introduce site-directed mutations within the six putative *EST1* D-boxes, complementary primer pairs were designed (colored arrows). PCR round 1 consists of two reactions 1) outer forward primer (M1209) and inner reverse D-box primer, and 2) inner forward D-box primer and outer reverse primer (M1212). The second round of PCR uses the two outer primers (M1209 and M1212) and the two DNA products from round 1, which anneal via their complementary region. The end product is the mutated (asterisks) full-length 'stitched' product, which was then cloned into pKF600 using *Bam*HI and *Sph*I restriction enzyme sites. *est1-DB3* is shown as an example. The primer pairs used were: E1DB1RL2A; E1DB2right; DB2R2K; DB2R2KL2A; EST1R264AL267A (DB3); DB4RL2A; DB4R2K; DB4R2KL2A; E1DB5RL2ADM; E1DB6RL2A, shown in Table 2.

Determination of Est1p Steady-State Levels During Cell Cycle Arrest

Strains YKF800 (*bar1Δ*) and YKF801 (*bar1Δ EST1-MYC$_{13}$*) were grown asynchronously at 30°C to $OD_{600} \approx 0.5$ and either left untreated (asynchronous) or treated with α-factor (0.5 μM final concentration; Zymo Research), hydroxyurea (15 mg/ml) final concentration; Sigma Aldrich), or nocodazole (10 mg/ml nocodazole in DMSO to a final concentration of 10μg/ml; Sigma Aldrich) for a minimum of 2.5 hrs. When 95% of the population exhibited the characteristic morphologies, cells were harvested and whole-cell extract prepared as described [61]; protein concentrations were determined by Bradford assay (Bio-Rad). Equal amount of protein extract (100-150μg) were separated by 10% Tris-Glycine (Bio-Rad) and 7% NuPAGE Bis-Tris (Invitrogen) gels and transferred to Hybond P (GE Healthcare). Each membrane was blocked with 5% milk/phosphate-buffered saline pH 7.4 with 0.05% Tween (PBS-T) followed by incubation with primary antibodies overnight at 4°C. Antibody dilutions were as follows: Clb2-1:6000 dilution rabbit polyclonal y-180 (Santa Cruz); Actin-1:1200 goat polyclonal C-11 (Santa Cruz); 1:1000 mouse monoclonal mAbcam8224 (Abcam); and MYC-1:333 murine monoclonal Ab.1 (OP10L, EMD Biosciences). Bis-Tris gels were utilized for Est1-MYC$_{13}$p detection because the protein co-migrated with a background band that could not be resolved using the 10% Tris-glycine gels. Secondary antibodies were 1:10000 dilutions of peroxidase-conjugated goat anti-mouse [Millipore], goat anti-rabbit [Millipore], and donkey anti-goat [sc-2020; Santa Cruz]. ECL Plus Western Blotting Detection system (GE Healthcare) was used for detection.

For flow cytometry analysis, cells were treated as described in [241], except that samples were digested overnight with RNase A at 37°C instead of pepsin. Fluorescence

and light scattering were monitored for 10,000 cells using a 5-laser BD LSRII. To eliminate any size-bias, samples were not gated and all events are plotted in the histograms presented.

Overexpressed Est1p Stability Assays and Half-Life Quantification

Strains YKF802 (wild type), YKF803 (*apc9Δ*), YKF804 (*mnd2Δ*), YKF805 (*swm1Δ*) containing plasmid pVL242RtoA (*GAL1-HA$_3$-EST1*) or variants of pKF600 (*GAL1-HA$_3$-EST1*: WT; DB1; DB2; DB2R→A; DB2R→K; DB2R→K,L→A; DB1+2; DB3; DB4; DB3+4; DB5+6; CΔ300; NΔ7; NΔ15; NΔ25; NΔ35; NΔ50) were assayed as described in [101], except using hydroxyurea (15 mg/ml final concentration; Sigma Aldrich) where indicated. Also examined were constructs with either the wild-type (RLALNNVTN) or mutant (ALLANNVTA) *CLB2* D-box fused to the N-terminus of the WT, DB2 or DB4 gene. For temperature-sensitive experiments, K4438 (*cdc16-123*) containing plasmid pKF600 and either a complementing vector (pRS416-*CDC16*) or empty vector (pRS416) were assayed as in [101], except for growth in 2% (w/v) raffinose media lacking leucine and uracil (-Leu -Ura) and a shift to the restrictive temperature (37°C) at the time of galactose addition. Samples were separated on 10% tris-glycine SDS-PAGE gels (Bio-Rad) and transferred to Hybond P (GE Healthcare). Membranes were blocked with 5% milk/phosphate-buffered saline pH 7.4 with 0.05% Tween (PBS-T) followed by incubation with primary antibodies (HA: 1:500 dilution [murine monoclonal HA.11; Covance]; Clb2 and Actin, as above) overnight at 4°C. Secondary antibodies and detection system are as described above. For half-life determination, the signal obtained for HA$_3$-Est1p at each time point was corrected for input (actin),

normalized to the starting amount (time 0), base-*e* log-transformed, and plotted against time. The slope was determined using a linear best-fit line and used to calculate the half-life by $T_{1/2} = \ln(2)/\text{slope}$, as described in [242].

cdc15-2 Block and Release

1000 ml cultures of strains YKF808 (*cdc15-2 EST1-MYC$_{13}$*) and YKF809 (*cdc15-2 cdh1Δ EST1-MYC$_{13}$*) were grown asynchronously at 23°C to $OD_{600} \approx 0.4$ and then shifted to the restrictive temperature (37°C) in an air incubator for 3.5 hrs or until >95% of the population was arrested in mitosis, as determined by observation of the bud index. Cultures were released from the *cdc15-2* arrest by rapid cooling in an ice water bath to 23°C (time 0) and returned to a 23°C air incubator for the remainder of the experiment. Samples (125 ml) were harvested at 20 min intervals following release and whole-cell extract was prepared as described [61]. Synchrony of the release was monitored by bud-index and flow cytometry. YCM191 (untagged; *cdc15-2*) was grown as above and harvested following incubation at 37°C. Equal amounts of protein (120 μg), as determined by Bradford assay (Bio-Rad), were analyzed by Western blotting as described above. Est1-MYC$_{13}$p and Clb2p signal intensity at each time point was normalized to protein input (actin) and starting amount (time 0). Samples from each assay were analyzed by Western blot two to three times and the quantified results were averaged to give yield a value for that independent assay. Averages determined from the independent biological replicates (WT = 4, *cdh1Δ* = 3) were subsequently averaged to yield the values reported in Figure 11. Standard deviation of the mean was determined across the independent biological replicates.

In vitro Assays of Est1p Stability/Ubiquitination

Xenopus laevis egg extracts were prepared in a manner similar to that previously described [177,243]. Briefly, eggs from Human chorionic gonadotropin (HCG)-injected, pregnant mare serum gonadotropin (PMSG)-primed frogs were collected and washed in 1x Marc's modified ringer (MMR) solution. Eggs were dejellied with 2% cysteine and then washed into extract buffer (XB) and XB containing protease inhibitors. A 30 sec packing spin at 1000 rpm at 2°C was performed, followed by a crushing spin at 13,000 rpm for 5 min at 2°C. The cytoplasmic layer was collected and subjected to a clarifying spin also at 13,000 rpm for 5 min at 2°C. The clarified cytoplasmic layer was collected. After addition of protease inhibitors, energy mix [243] and cytochalasin B, extracts were either frozen in liquid nitrogen (− CDH1) or activated with addition of *in vitro* transcribed human Cdh1-MYC_6 RNA (+ CDH1) for 2 hrs at room temperature prior to flash freezing, and stored in liquid nitrogen. An anti-MYC Western blot confirmed successful translation of Cdh1-MYC_6 RNA. ^{35}S-labeled substrates (*S. cerevisiae* Est1p, *Drosophila* Cyclin B, and firefly luciferase) were produced using the TNT Sp6 Quick coupled *in vitro* transcription/translation (IVT) kit (Promega). Additional Cdh1-MYC_6 protein was produced using the TNT Sp6 High-Yield Wheat Germ Protein Expression System (Promega), added (2 μL) to thawed + CDH1 extract, and incubated at room temperature for 15 mins. Inactive (− CDH1) and active (+ CDH1) extracts (10 μL) were incubated at room temperature with 1-2 μL recombinant substrates, energy mix, and ubiquitin (Sigma). Samples (2 μL) were taken at 0, 30, 60 and 90mins and frozen in liquid nitrogen. Samples were separated on 10% Tris-glycine (Bio-Rad) SDS-PAGE gels, fixed, dried and exposed to a phosphor-imager screen.

APC/C ubiquitination assays were adopted and modified from [244]. ^{35}S-labeled substrates and unlabeled *S. cerevisiae* Cdh1 were prepared using TNT T7 Quick coupled *in vitro* transcription/translation (IVT) (Promega). Each ubiquitination reaction contained approximately 10 ng of APC, 1 μl of ^{35}S-labeled substrate, and 2 μl of Cdh1 in a 10 μl reaction volume with 40 mM Tris-HCl pH 7.5, 10 mM $MgCl_2$, 0.6 mM DTT, 2.7 mM ATP, 6.6 μg of methyl-ubiquitin, 500 ng of Ubc4, 200 ng of ubiquitin aldehyde (Enzo Life Science), 2 mM LLnL (N-acetyl-Leu-Leu-Norleu-aldehyde; Sigma). Reactions were incubated at room temperature for 60 mins and were analyzed by 8% SDS-PAGE. Gels were fixed and stained with Coomassie Blue followed by drying and exposure to BioMax MR Film (Kodak).

Southern Blotting

For complementation tests, strain YKF810 (*est1Δ*) containing pRS416-EST1 was grown in non-selective media, plated on 5-fluroorotic acid (5-FoA) to select for loss of the complementing plasmid, and then transformed using the standard lithium acetate method with an empty vector (pRS416), complementing plasmid (pRS416-EST1), or variants of pRS416 expressing mutant *est1* alleles (DB1; DB2; DB2R→K; DB2R→K,L→A; DB1+2; DB3; DB4; DB4R→K; DB2+4R→K; DB4R→K,L→A; DB3+4; DB2+3, DB2+4). Also examined were constructs with either the wild-type (RLALNNVTN) or mutant (ALLANNVTA) *CLB2* D-box fused to the N-terminus, including wild-type; DB1; DB2; DB1+2; DB2R→K,L→A; DB4; and DB3+4. Independent transformants were restreaked three times on selective media and then grown in liquid culture. DNA was extracted by glass bead lysis [245], digested with

*Xho*I, and Southern blotted as described in [62]. Mean telomere restriction fragment length was calculated from densitometric scans by Image J software and a linear log curve derived from the molecular weight markers. To determine the difference in length, mutant lengths were compared to the WT control run on the same gel.

For analysis of telomere length upon overexpression of *EST1*, strain YKF802 (wild type) was transformed with an empty vector (pRS416) or plasmids expressing *EST1* under various promoter strengths, including the endogenous *EST1* promoter (pRS416-EST1), *ADH1* promoter (pRS416-ADH-EST1), TEF promoter (pRS416-TEF-EST1), or *GAL1* promoter (pRS416-GAL-EST1). Independent transformants were treated as above, except for the pRS416-GAL1-EST1 isolates which were cultured with media containing 2% raffinose + 1% galactose to induce expression. As a control, this media treatment was tested on the control strain (pRS416) and did not affect telomere length (data not shown).

CHAPTER V

CONCLUSIONS AND FUTURE DIRECTIONS

Telomeres are critical for the maintenance of genome integrity, ensuring the faithful replication of chromosomes and protecting chromosome ends from damage. Telomerase activity is temporally regulated; telomere extension only occurs during late S and G2/M phases [137]. One mechanism that contributes to this restriction is the regulation of complex assembly. During G1 phase, Est1 protein levels are regulated through a proteasome-dependent pathway [101], arguing that the amount of Est1p fluctuates due to protein degradation. Though Est3p levels do not decrease during G1 phase, the protein does not associate with the telomerase complex or telomeres [81,101]. The regulated assembly of Est3p with other telomerase subunits depends upon Est1p, since *EST1* overexpression during G1 phase is sufficient to recruit Est3p [101]. Likewise, Est1p is necessary for Est3p association with the telomere [81]. Since complex assembly is necessary for *in vivo* activity, understanding how these subunits assemble is critical. Therefore, in this thesis, I focused on the regulation of telomerase assembly by determining the mechanism that targets Est1p for degradation during G1 phase (Chapters II and III).

Est1p Undergoes Regulated Degradation

Est1p levels fluctuate during the cell cycle

Though it was known that Est1p levels are low during G1 phase as compared to G2/M phase [101], the remainder of the cell cycle was unexamined. Since telomere replication and extension occur during late S phase, I was interested in determining when Est1p levels begin to increase. Therefore, I monitored Est1p levels throughout the cell cycle following a release from a mitotic arrest using the *cdc15-2* ts allele. Est1p levels rose as cells began transit through S phase (Figure 11), suggesting that complex assembly may occur near the G1/S phase transition, prior to telomere elongation (late S phase). However, previous work had shown that assembly of the telomerase complex is not the sole determinant of telomerase activity [101]. One possibility is that the telomere is inaccessible to telomerase during G1 phase. Therefore, it would be informative to determine if the telomerase protein subunits (Est1-3) associate with the telomere by ChIP when Est1p levels are artificially increased during G1 phase. To increase Est1p levels, the protein can be overexpressed using a constitutive (*ADH1* or *TEF*) or inducible (*GAL1*) promoter. Likewise, overexpression can also be achieved by using a stabilized allele of Est1p (see below).

The mechanism of Est1p degradation

Since the timing of Est1p degradation is similar to the known APC-substrate Clb2p (Figure 8), I investigated the contribution of the APC to Est1p degradation. I found that deletion of non-essential subunits or perturbation of APC activity using ts

alleles increased the half-life of overexpressed Est1p (Figure 9). Likewise, endogenously expressed Est1p was not degraded once released from the *cdc15-2* arrest when the APC-activator *CDH1* was deleted (Figure 11). These results strongly argue that the APC contributes to Est1p degradation. In support of the hypothesis that the APC recognizes Est1p directly, I found that several APC degron motifs (D-boxes) within *EST1* are necessary for protein degradation (Figures 12 and 13). However, when I expressed Est1 in RRL and monitored degradation in *Xenopus* egg extract that had been activated with exogenously added Cdh1 protein, no degradation was detected over a 60min time-course (Figure 14A). In collaboration with David Barford's laboratory, it was also demonstrated that Est1p is not ubiquitinated by the *S. cerevisiae* APC *in vitro* (Figure 14B). Collectively, the *in vitro* results suggest that Est1p is not directly recognized by the APC, a finding that appears inconsistent with the identification of D-box sequences that influence Est1p stability *in vivo*. In the following sections I will elaborate on the evidence supporting each possibility (Est1p either is or is not a direct target of the APC) and propose further experiments that may offer clarity between the two interpretations.

Possibility #1: Est1p is a direct target of the APC

If Est1p is a direct target of the APC, then one must postulate that it is the negative results in the *in vitro* assays that are misleading. One possibility is that the recombinant Est1 protein produced in RRL is not recognized by the APC because either the folding and/or modifications of the protein are non-native. While I have not shown that the recombinant Est1 protein produced in RRL is either active or folded, there is evidence that an unfolded structure can nevertheless be recognized by APC machinery.

A fragment of human Cyclin B and *S. cerevisiae* Pds1p/securin that contains the degron motif recognized by the APC was purified from *E. coli* and found to natively exist in an unstructured state [246]. These and similar fragments are ubiquitinated and/or degraded in an APC-dependent manner [175,246,247], suggesting these unfolded structures are sufficiently recognized. Likewise, the structure of APC^{Cdh1p} in complex with a short peptide containing the D-box or KEN-box degrons of known substrates was determined by electron microscopy (EM) [171,185]. These data suggest the degron regions can exist in an extended or relatively unfolded conformation; therefore, unfolding of Est1p may not be a significant concern.

A more likely possibility is that the RRL-produced Est1p does not mimic appropriate post-translational modification(s) necessary for APC-mediated recognition and subsequent degradation/ubiquitination *in vitro*. Phosphorylation of critical residues located near the D-box of mammalian Cdc6 protein [190] and yeast Pds1p/securin [191] disrupts recognition by the activator subunits (Cdc20p and Cdh1p), therefore inhibiting APC-dependent degradation. Likewise, an N-terminal region termed the A-box (sequence: RILGPSNVPQRV) in the eukaryotic mitotic kinase Aurora A must be de-phosphorylated at mitotic exit to allow destruction in a D-box and APC-dependent manner [229]. On the other hand, acetylation of mammalian cyclin A [248] and BubR1 [249] or farnesylation of the kinetochore protein Cenp-F [250] promotes APC-mediated degradation. These examples highlight the recent observations that post-translational modifications can play important positive and negative regulatory roles in APC-mediated degradation. The cell-free RRL system is capable of some post-translational activity, including phosphorylation, farnesylation, isoprenylation, acetylation, and adenylation

(Promega; [251]). Therefore, the RRL produced Est1p may exhibit inhibitory modifications that normally undergo regulated removal *in vivo*, or lack necessary modifications for degradation. To examine these possibilities, the RRL-produced Est1p can be pre-treated with enzymes capable of producing (kinases, farnesyltransferases, acetyltransferases, etc.) or removing (phosphatases, inhibitors, etc.) these modifications and re-tested in the *in vitro* degradation/ubiquitination assays (although there is always the caveat that the modifications may not be on the appropriate residue).

Another approach to address this issue is to utilize Est1p protein that has been purified from yeast. Although the human homolog of Est1p has been successfully produced in RRL [252,253], there are no published reports of recombinant *S. cerevisiae* Est1p being produced in RRL or *E. coli*. However, several groups [81,94,100] have successfully purified Est1p from *S. cerevisiae*, and demonstrated that the protein thus isolated stimulates telomerase activity [94], directly associates with the ssDNA binding protein Cdc13p [100], and interacts with Est3p *in vitro* [81]. The *in vitro* ubiquitination/degradation assays could be repeated with Est1p purified from yeast because this protein is likely to be folded correctly and contain native modifications.

It is important to note, however, that Est1p reportedly does not undergo phosphorylation. These experiments utilized the Phos-tag technique wherein a chemical is added to the gel to retard the mobility of phosphorylated proteins [81]. However, a more thorough approach would be to perform 2-dimensional gel electrophoresis, stable isotope labeling by amino acids in cell culture (SILAC) and mass spectrometry (MS), or subject immunoprecipitated Est1p to *in vitro* kinase assays using purified kinases. Candidates to examine include the cyclin-CDK/Cdc28p and DDK (Cdc7/Dbf4) kinase

complexes, since these are active when Est1p levels are elevated and inactive at the time of Est1p degradation [254]. Since there have been no published reports examining other post-translational modifications on Est1p, the modification state of Est1p could be an intriguing avenue to explore since it could regulate telomerase complex assembly.

Possibility #2: Est1p is an indirect target of the APC

The alternative explanation posits that the *in vitro* results are robust and that Est1p cannot be directly recognized by the APC. In this model, APC activity must be necessary for the degradation of an unknown substrate that in turn affects the stability of Est1p. Possible steps at which this indirect effect could be manifested are discussed below. Of the evidence that I have presented for a role of the APC in Est1p stability *in vivo*, the results that argue for direct recognition of Est1p are those in which potential D-box sequences were identified.

I mutated six putative D-boxes and examined the effect of these mutations on the half-life of Est1p during G1 phase. Mutations in D-boxes 1, 2, and 4 stabilized Est1p, consistent with the idea that Est1p is a direct APC substrate and that these regions are necessary for recognition by the APC. However, other explanations for these effects are plausible. Charlene Hawkins, a graduate student in our lab, recently identified a nuclear localization sequence (NLS) that includes the residues of D-box 4. When these residues are mutated to alanine, nuclear import of Est1p is compromised and telomeres shorten. However, nuclear localization and telomere shortening can be nearly fully rescued by the fusion of the SV40-NLS sequence, arguing that the cause of telomere shortening is mis-localization (unpublished). Since the APC is localized to the nucleus [203,255],

stabilization that results from mutation of these residues may be due to sequestration of Est1p in the cytoplasm, away from the degradation machinery. If true, the half-life of Est1-DB4 mutants should be restored to wild type when the mutant protein is fused to the SV40-NLS. Consistent with this hypothesis, the Cin8p spindle motor protein requires nuclear localization for APC-mediated degradation [217]. While defects in nuclear localization may account for the effect of mutations in putative D-box 4, the stabilization of mutations in D-boxes 1 and 2 cannot be attributed to mislocalization based on the known NLS sequences (Hawkins and Friedman, unpublished data).

The experiments presented here to monitor the stability of Est1 variants with D-box mutations were done using promoter shut-off assays in which Est1p is expressed at levels much higher than those encountered endogenously. Although such experiments are commonly used in the field, there is a concern that mechanisms leading to degradation of highly overexpressed protein may differ from those acting upon native Est1p (this issue is discussed in more detail below). I attempted to address this issue by re-expressing the mutated Est1 proteins from the endogenous *EST1* locus. Contrary to expectation, I did not observe any accumulation of Est1 protein in G1 phase arrested cells (data not shown). While this result could indicate that the D-boxes identified using overexpressed constructs are not important at endogenous expression levels, there are some concerns with the interpretation of this result as well. When endogenous protein levels are examined in G1 phase, cells are held at the G1 arrest for several hours, as compared to a normal G1 phase transit time of no more than 30 minutes. Therefore, stabilized protein with a half-life that increases from 10 mins to 20-30 mins may undergo several rounds of degradation during the incubation period, significantly depleting the

protein pool. A similar finding has been reported for Clb2p. Using a promoter shut-off assay, Clb2p is stabilized when *SWM1* is deleted. However, endogenously expressed Clb2p is not detectible in G1 arrested *swm1Δ* cells [196,218]. Upon release from a G1 arrest in *swm1Δ* cells, Clb2p does not oscillate during the subsequent cell cycle as seen in wild-type cells [218]. This data suggests the elongated G1 phase may overemphasize the amount of protein decline, even if the protein half-life is significantly longer. Therefore, I suggest that monitoring the oscillation patterns following synchronous release from an arrest is a more informative experiment. In this type of experiment, the cells proceed through a normally timed cell cycle and decreases/increases in protein steady-state levels should not be artificially affected.

Potential Mechanisms Through Which the APC Could Indirectly Affect Est1p Expression

I have presented evidence that the APC affects Est1p degradation *in vivo*, though it remains possible that this is through an indirect mechanism. The APC could degrade a protein that is in turn responsible for regulated Est1p protein stability. This possibility has a precedent in the literature. At the metaphase-to-anaphase transition, APC^{Cdc20p} ubiquitinates Pds1p/securin, releasing Esp1p/separase to cleave Scc1p/cohesin and initiate sister-chromatid separation (reviewed in [176]). The Scc1p cleavage product then undergoes rapid degradation through the N-end rule pathway [256]. Perturbation of the APC using the temperature-sensitive allele *cdc23-1* increases the half-life of the Scc1 protein [257], through an indirect effect of preventing Pds1p/securin degradation. In such a case, Est1p would therefore not be considered a direct target of the APC, but would still

be degraded in an APC-dependent pathway. This conclusion is supported by both the *in vitro* and *in vivo* data. To identify the true protease responsible for Est1p degradation, a genetic screen of known E3 ubiquitin ligases could be used.

A second possibility is that the APC affects expression of Est1p at the RNA level. The *cdc15-2* block and release experiment shows a reproducible decrease in Est1 and Clb2 protein as cells proceed through G1 phase. However, since Est1p transcript levels also decrease during G1 phase (at least during an arrest) [101], the decrease in protein could be affected by decreasing RNA levels. One possibility is that the APC degrades a protein that in turn affects Est1p RNA expression or stability. If this is the case, Northern blot analysis of samples taken after release from the *cdc15-2* block will show that the Est1p RNA is stabilized through G1 phase in the absence of *CDH1*.

A Proposed Role For Est1p Degradation

It is intriguing that each of the stabilized variants of Est1p fails to maintain normal length telomeres in an *est1Δ* background. However, while I observed rescue of telomere length with fusion of the *CLB2* D-box sequence for the *est1* D-box 2 mutants, the half-life of the protein was not decreased, arguing an indirect effect. I hypothesize that this small sequence supports proper protein structure, and thus active Est1p, in a manner dependent upon the Arg and Leu residues since mutation to Ala failed to rescue telomere length. Furthermore, overexpression of *EST1* for >100 generations did not result in a telomere length or cell viability defect. In fact, the telomeres were elongated under these conditions, as has been recently reported [104]. These data suggest there is

no detrimental effect from stabilizing Est1p and pose the question: what is the reason for Est1p degradation?

In each cell cycle, only 10% of telomeres are elongated. Furthermore, telomerase preferentially and more substantially extends the shortest telomere ends [130]. This elongation coincides with the preferential association of the telomerase complex (Est2p and Est1p) with short telomeres in a Tel1p and Xrs2-dependent manner [133,134]. Additionally, Tel1p does not preferentially associate with the shortest telomeres in the absence of Rif2p [133]. Since the number of Est1p molecules is predicted to be <50 [255] and one critically short telomere is sufficient to cause cellular senescence [258], it is logical to target the telomerase complex to the shortest ends. Perhaps the degradation of Est1p is important for resetting the 'mark' on the shortest telomeres for elongation. For example, the shortest telomeres that are elongated are most likely not going to be the shortest in the following cell cycle; therefore, Est1p may be critical for re-establishing the association with the appropriate telomere end. This hypothesis can be tested using the STEX assay discussed above. If degradation of Est1p is critical for re-setting the selection of shortest telomeres, overexpression from a high-expression promoter or use of a non-degradable allele could alter the pattern of telomere extension and result in hyper-elongation of telomeres if monitored for multiple cell cycles. Consistent with this hypothesis, telomerase remains tightly associated to its reaction products *in vitro* [76]; however this has not been addressed *in vivo* due to the technical limitations of distinguishing if the same telomerase complex is bound to a particular end following elongation. Therefore, Est1p degradation may be important for removing the telomerase complex from the telomere *in vivo* and/or marking the shortest ends for elongation.

The lack of telomere shortening upon *EST1* overexpression does not exclude the possibility that a pool of Est1p retains regulated degradation in a manner that is important for telomere maintenance. Since Est1p is localized to the nucleus upon overexpression ([259], Charlene Hawkins, unpublished), regulated degradation could be APC-dependent. As hypothesized above, if the reason Est1p is degraded is to re-mark the appropriate telomeres for elongation, a subset of molecules may be sufficiently degraded, such as those associated with the telomere at the end of S phase. Unfortunately, a direct test of this hypothesis is difficult.

Examining the Usefulness of Standard Techniques

The standard assays for determining the contribution of the APC to protein degradation rely heavily upon protein overexpression. However, as I have discussed above, overexpressed proteins can exhibit degradation patterns that are different than endogenously expressed protein. Overexpressed protein could potentially overwhelm the degradation machinery or cause proteolysis through an unnatural pathway. Overexpression could also overwhelm necessary pathways for protein modification. Monitoring of the half-life by promoter shut-off assay of proteins containing specific point mutations is the standard technique for identifying the sequences required for protein degradation. However, it can be difficult to determine if the stabilization observed is a direct effect of preventing recognition by the degradation machinery or if it results from an indirect effect. Stabilization of proteins can occur for many reasons, including mis-localization and aggregation. Protein aggregates are generally difficult to unfold or degrade and are associated with neurodegenerative diseases such as

Alzheimer's (reviewed in [260,261]). Monitoring proteins for appropriate localization and the absence of aggregated protein by immunofluorescence or through fusion to green fluorescent protein (GFP) can begin to address these concerns. Additionally, since APC degron motifs (D-boxes and KEN-boxes) are portable, demonstrating that the wild-type sequence identified renders a heterologous protein unstable while a mutated version does not, is another established technique that should be utilized to demonstrate that these sequences are true degron motifs.

This type of experiment gets more complicated when examining the effect of inhibiting APC activity using ts alleles, such as *cdc16-123* or *cdc23-1*. To evaluate the effect of the APC on endogenously expressed protein, cells must be arrested at the time of degradation (G1 phase for instance) and then shifted to the restrictive temperature. If the G1 arrest is not done first, the shift to the restrictive temperature will result in a mitotic arrest, where a subset of APC substrates are stable, including Est1p and Clb2p. On the other hand, since the APC regulates cyclin degradation, cyclins begin to accumulate when the APC is inactivated, resulting in release of the G1 arrest. To prevent this release from G1 phase, overexpression of the CDK inhibitor, *SIC1*, or deletion of the cyclin *CLB2* is used [212,216]. Cells can then be held at the restrictive temperature and, if the APC contributes to the protein degradation, the protein should accumulate over time during the arrest. However, since mRNA levels of substrates can also be cell-cycle regulated, like *EST1* and cyclins [101,215,224,262], accumulation may not occur due to insufficient translation. Therefore, the negative result may be uninformative. Furthermore, an alpha-factor block and release experiment examining the pattern of degradation through the ensuing cell cycle in the presence of an APC ts allele is also not

feasible because cells continue to accumulate substrate protein during transit through S and G2/M phases, but do not enter a subsequent G1 phase in which degradation could be observed [212]. Collectively, I propose that the cell-cycle regulated protein degradation field re-evaluate their methodology and begin reporting more results using endogenously expressed proteins, when possible.

Summary

Yeast telomerase activity is cell cycle regulated in part due to the regulated degradation of the Est1 protein subunit during G1 phase. In this thesis, I have demonstrated that the APC regulates the degradation of Est1p during G1 phase in a D-box dependent manner. Though *in vitro* experiments failed to demonstrate a direct-dependence on the APC, I suggest that the inconsistency with my *in vivo* work may be due to an inactive Est1 protein produced in RRL. Mutations that result in Est1p stabilization shorten telomeres, but overexpression of wild-type *EST1* does not. These results suggest that there is no detrimental consequence to overproducing or stabilizing Est1p. Therefore, I suggest that the degradation of Est1p is important for the preferential association of telomerase with short telomeres, a function that may be important for telomere length regulation but may not be essential for telomere maintenance. Understanding the regulation of telomerase complex assembly is essential for complete understanding of how telomerase is activated.

REFERENCES

1. Müller HJ (1938) The remaking of chromosomes. The Collecting Net 13: 181-195, 198.

2. McClintock B (1931) Cytological observations of deficiencies involving known genes, translocations and an inversion in *Zea mays*. Missouri Agricultural Experiment Research Station Research Bulletin 163: 4-30.

3. Watson JD, Crick FH (1953) The structure of DNA. Cold Spring Harb Symp Quant Biol 18: 123-131.

4. Bessman MJ, Kornberg A, Lehman IR, Simms ES (1956) Enzymic synthesis of deoxyribonucleic acid. Biochim Biophys Acta 21: 197-198.

5. Bessman MJ, Lehman IR, Simms ES, Kornberg A (1958) Enzymatic synthesis of deoxyribonucleic acid. II. General properties of the reaction. J Biol Chem 233: 171-177.

6. Lehman IR, Bessman MJ, Simms ES, Kornberg A (1958) Enzymatic synthesis of deoxyribonucleic acid. I. Preparation of substrates and partial purification of an enzyme from *Escherichia coli*. J Biol Chem 233: 163-170.

7. Okazaki R, Okazaki T, Sakabe K, Sugimoto K (1967) Mechanism of DNA replication possible discontinuity of DNA chain growth. Jpn J Med Sci Biol 20: 255-260.

8. Olovnikov AM (1971) Principle of marginotomy in template synthesis of polynucleotides. Doklady Akademii Nauk SSSR 201: 1496-1499.

9. Watson J (1972) Origin of concatameric T4 DNA. Nature New Biol 239: 197-201.

10. Olovnikov AM (1973) A theory of marginotomy. JTheorBiol 41: 181-190.

11. Hayflick L (1965) The limited *in vitro* lifetime of human diploid cell strains. Exp Cell Res 37: 614-636.

12. Todaro GJ, Wolman SR, Green H (1963) Rapid transformation of human fibroblasts with low growth potential into established cell lines by SV40. J Cell Physiol 62: 257-265.

13. Hall SS (2003) Merchants of immortality : chasing the dream of human life extension. Boston: Houghton Mifflin. vi, 439 p. p.

14. Harley CB, Futcher AB, Greider CW (1990) Telomeres shorten during ageing of human fibroblasts. Nature 345: 458-460.

15. Klobutcher LA, Swanton MT, Donini P, Prescott DM (1981) All gene-sized DNA molecules in four species of hypotrichs have the same terminal sequence and an unusual 3' terminus. ProcNatlAcadSciUSA 78: 3015-3019.

16. Henderson ER, Blackburn EH (1989) An overhanging 3' terminus is a conserved feature of telomeres. MolCellBiol 9: 345-348.

17. Wellinger RJ, Wolf AJ, Zakian VA (1993) *Saccharomyces* telomeres acquire single-strand TG1-3 tails late in S phase. Cell 72: 51-60.

18. Price C (2006) Ciliate telomeres. In: de Lange T, Lundblad V, Blackburn EH, editors. Telomeres. 2nd ed. Cold Spring Harbor, New York: Cold Spring Harbor Laboratory Press. pp. 465-493.

19. Blackburn EH, Gall JG (1978) A tandemly repeated sequence at the termini of the extrachromosomal ribosomal RNA genes in *Tetrahymena*. JMolBiol 120: 33-53.

20. Kirk KE, Blackburn EH (1995) An unusual sequence arrangement in the telomeres of the germ-line micronucleus in *Tetrahymena thermophila*. Genes Dev 9: 59-71.

21. Szostak JW, Blackburn EH (1982) Cloning yeast telomeres on linear plasmid vectors. Cell 29: 245-255.

22. Shampay J, Szostak JW, Blackburn EH (1984) DNA sequences of telomeres maintained in yeast. Nature 310: 154-157.

23. Greider CW, Blackburn EH (1985) Identification of a specific telomere terminal transferase activity in *Tetrahymena* extracts. Cell 43: 405-413.

24. Greider CW, Blackburn EH (1987) The telomere terminal transferase of *Tetrahymena* is a ribonucleoprotein enzyme with two kinds of primer specificity. Cell 51: 887-898.

25. Greider CW, Blackburn EH (1989) A telomeric sequence in the RNA of *Tetrahymena* telomerase required for telomere repeat synthesis. Nature 337: 331-337.

26. Yu G-L, Bradley JD, Attardi LD, Blackburn EH (1990) *In vivo* alteration of telomere sequences and senescence caused by mutated *Tetrahymena* telomerase RNAs. Nature 344: 126--132.

27. Zahler AM, Prescott DM (1988) Telomere terminal transferase activity in the hypotrichous ciliate *Oxytricha nova* and a model for replication of the ends of linear DNA molecules. Nucleic Acids Res 16: 6953-6972.

28. Shippen-Lentz D, Blackburn EH (1989) Telomere terminal transferase activity from *Euplotes crassus* adds large numbers of TTTTGGGG repeats onto telomeric primers. MolCellBiol 9: 2761-2764.

29. Morin GB (1989) The human telomere terminal transferase enzyme is a ribonucleoprotein that synthesizes TTAGGG repeats. Cell 59: 521-529.

30. Shippen-Lentz D, Blackburn EH (1990) Functional evidence for an RNA template in telomerase. Science 247: 546-552.

31. Lingner J, Hendrick LL, Cech TR (1994) Telomerase RNAs of different ciliates have a common secondary structure and a permuted template. Genes Dev 8: 1984-1998.

32. Lingner J, Hughes TR, Shevchenko A, Mann M, Lundblad V, et al. (1997) Reverse transcriptase motifs in the catalytic subunit of telomerase. Science 276: 561-567.

33. Lendvay TS, Morris DK, Sah J, Balasubramanian B, Lundblad V (1996) Senescence mutants of *Saccharomyces cerevisiae* with a defect in telomere replication identify three additional EST genes. Genetics 144: 1399-1412.

34. Greenberg RA, Allsopp RC, Chin L, Morin GB, DePinho RA (1998) Expression of mouse telomerase reverse transcriptase during development, differentiation and proliferation. Oncogene 16: 1723-1730.

35. Nakamura TM, Morin GB, Chapman KB, Weinrich SL, Andrews WH, et al. (1997) Telomerase catalytic subunit homologs from fission yeast and human. Science 277: 955-959.

36. Meyerson M, Counter CM, Eaton EN, Ellisen LW, Steiner P, et al. (1997) hEST2, the putative human telomerase catalytic subunit gene, is up-regulated in tumor cells and during immortalization. Cell 90: 785-795.

37. Bryan TM, Sperger JM, Chapman KB, Cech TR (1998) Telomerase reverse transcriptase genes identified in *Tetrahymena thermophila* and *Oxytricha trifallax*. Proc Natl Acad Sci USA 95: 8479-8484.

38. Lundblad V, Szostak JW (1989) A mutant with a defect in telomere elongation leads to senescence in yeast. Cell 57: 633-643.

39. Nugent CI, Hughes TR, Lue NF, Lundblad V (1996) Cdc13p: A single-strand telomeric DNA binding protein with a dual role in yeast telomere maintenance. Science 274: 249-252.

40. Gottschling DE, Aparicio OM, Billington BL, Zakian VA (1990) Position effect at *S. cerevisiae* telomeres: reversible repression of Pol II transcription. Cell 63: 751-762.

41. Singer MS, Gottschling DE (1994) TLC1: template RNA component of *Saccharomyces cerevisiae* telomerase. Science 266: 404-409.

42. Xie M, Mosig A, Qi X, Li Y, Stadler PF, et al. (2008) Structure and function of the smallest vertebrate telomerase RNA from teleost fish. J Biol Chem 283: 2049-2059.

43. Blasco MA, Funk W, Villeponteau B, Greider CW (1995) Functional characterization and developmental regulation of mouse telomerase RNA. Science 269: 1267-1270.

44. Feng J, Funk WD, Wang S-S, Weinrich SL, Avilion AA, et al. (1995) The RNA component of human telomerase. Science 269: 1236-1241.

45. Chen J-L, Greider CW (2006) Telomerase biochemistry and biogenesis. In: de Lange T, Lundblad V, Blackburn EH, editors. Telomeres. 2nd ed. Cold Spring Harbor, New York: Cold Spring Harbor Laboratory Press. pp. 49-79.

46. Seto AG, Zaug AJ, Sabel SG, Wolin SL, Cech TR (1999) *Saccharomyces cerevisiae* telomerase is an Sm small nuclear ribonucleoprotein particle. Nature 401: 177-180.

47. Zappulla DC, Cech TR (2004) Yeast telomerase RNA: a flexible scaffold for protein subunits. Proc Natl Acad Sci U S A 101: 10024-10029.

48. Livengood AJ, Zaug AJ, Cech TR (2002) Essential regions of *Saccharomyces cerevisiae* telomerase RNA: separate elements for Est1p and Est2p interaction. Mol Cell Biol 22: 2366-2374.

49. Chappell AS, Lundblad V (2004) Structural elements required for association of the *Saccharomyces cerevisiae* telomerase RNA with the Est2 reverse transcriptase. Mol Cell Biol 24: 7720-7736.

50. Zappulla DC, Goodrich KJ, Cech TR (2005) A miniature yeast telomerase RNA functions *in vivo* and reconstitutes activity *in vitro*. Nat Struct Mol Biol 12: 1072-1077.

51. Seto AG, Livengood AJ, Tzfati Y, Blackburn EH, Cech TR (2002) A bulged stem tethers Est1p to telomerase RNA in budding yeast. Genes Dev 16: 2800-2812.

52. Lubin JW, Tucey TM, Lundblad V (2012) The interaction between the yeast telomerase RNA and the Est1 protein requires three structural elements. RNA 18: 1597-1604.

53. Gallardo F, Olivier C, Dandjinou AT, Wellinger RJ, Chartrand P (2008) TLC1 RNA nucleo-cytoplasmic trafficking links telomerase biogenesis to its recruitment to telomeres. EMBO J 27: 748-757.

54. Fisher TS, Taggart AK, Zakian VA (2004) Cell cycle-dependent regulation of yeast telomerase by Ku. Nat Struct Mol Biol 11: 1198-1205.

55. Pfingsten JS, Goodrich KJ, Taabazuing C, Ouenzar F, Chartrand P, et al. (2012) Mutually exclusive binding of telomerase RNA and DNA by Ku alters telomerase recruitment model. Cell 148: 922-932.

56. Lingner J, Cech TR (1996) Purification of telomerase from *Euplotes aediculatus*: requirement of a primer 3' overhang. Proc Natl Acad Sci USA 93: 10712-10717.

57. Aigner S, Lingner J, Goodrich KJ, Grosshans CA, Shevchenko A, et al. (2000) *Euplotes* telomerase contains an La motif protein produced by apparent translational frameshifting. EMBO J 19: 6230-6239.

58. Witkin KL, Collins K (2004) Holoenzyme proteins required for the physiological assembly and activity of telomerase. Genes Dev 18: 1107-1118.

59. Qiao F, Cech TR (2008) Triple-helix structure in telomerase RNA contributes to catalysis. Nat Struct Mol Biol 15: 634-640.

60. Lebo KJ, Zappulla DC (2012) Stiffened yeast telomerase RNA supports RNP function *in vitro* and *in vivo*. RNA 18: 1666-1678.

61. Friedman KL, Cech TR (1999) Essential functions of amino-terminal domains in the yeast telomerase catalytic subunit revealed by selection for viable mutants. Genes Dev 13: 2863-2874.

62. Friedman KL, Heit JJ, Long DM, Cech TR (2003) N-terminal domain of yeast telomerase reverse transcriptase: recruitment of Est3p to the telomerase complex. Mol Biol Cell 14: 1-13.

63. Talley JM, DeZwaan DC, Maness LD, Freeman BC, Friedman KL (2011) Stimulation of yeast telomerase activity by the ever shorter telomere 3 (Est3) subunit is dependent on direct interaction with the catalytic protein Est2. J Biol Chem 286: 26431-26439.

64. Yen WF, Chico L, Lei M, Lue NF (2011) Telomerase regulatory subunit Est3 in two *Candida* species physically interacts with the TEN domain of TERT and telomeric DNA. Proc Natl Acad Sci U S A 108: 20370-20375.

65. Bryan TM, Goodrich KJ, Cech TR (2000) Telomerase RNA bound by protein motifs specific to telomerase reverse transcriptase. Mol Cell 6: 493-499.

66. Lue NF, Peng Y (1998) Negative regulation of yeast telomerase activity through an interaction with an upstream region of the DNA primer. Nucl Acids Res 26: 1487-1494.

67. Lue NF (2005) A physical and functional constituent of telomerase anchor site. J Biol Chem 280: 26586-26591.

68. Jacobs SA, Podell ER, Cech TR (2006) Crystal structure of the essential N-terminal domain of telomerase reverse transcriptase. Nat Struct Mol Biol 13: 218-225.

69. Bairley RCB, Guillaume G, Vega LR, Friedman KL (2011) A mutation in the catalytic subunit of yeast telomerase alters primer-template alignment while promoting processivity and protein-DNA binding. Journal of Cell Science 124: 4241-4252.

70. Gillis AJ, Schuller AP, Skordalakes E (2008) Structure of the *Tribolium castaneum* telomerase catalytic subunit TERT. Nature 455: 633-637.

71. Peng Y, Mian IS, Lue NF (2001) Analysis of telomerase processivity: mechanistic similarity to HIV-1 reverse transcriptase and role in telomere maintenance. Mol Cell 7: 1201-1211.

72. Lue NF, Lin Y-C, Mian IS (2003) A conserved telomerase motif within the catalytic domain of telomerase reverse transcriptase is specifically required for repeat addition processivity. Mol Cell Biol 23: 8440-8449.

73. Hossain S, Singh S, Lue NF (2002) Functional analysis of the C-terminal extension of telomerase reverse transcriptase. A putative "thumb" domain. J Biol Chem 277: 36174-36180.

74. Huard S, Moriarty TJ, Autexier C (2003) The C terminus of the human telomerase reverse transcriptase is a determinant of enzyme processivity. Nucleic Acids Res 31: 4059-4070.

75. Banik SS, Guo C, Smith AC, Margolis SS, Richardson DA, et al. (2002) C-terminal regions of the human telomerase catalytic subunit essential for *in vivo* enzyme activity. Mol Cell Biol 22: 6234-6246.

76. Prescott J, Blackburn EH (1997) Functionally interacting telomerase RNAs in the yeast telomerase complex. Genes & Development 11: 2790-2800.

77. Beattie TL, Zhou W, Robinson MO, Harrington L (2001) Functional multimerization of the human telomerase reverse transcriptase. Mol Cell Biol 21: 6151-6160.

78. Seimiya H, Sawada H, Muramatsu Y, Shimizu M, Ohko K, et al. (2000) Involvement of 14-3-3 proteins in nuclear localization of telomerase. EMBO J 19: 2652-2661.

79. Arai K, Masutomi K, Khurts S, Kaneko S, Kobayashi K, et al. (2002) Two independent regions of human telomerase reverse transcriptase are important for its oligomerization and telomerase activity. J Biol Chem 277: 8538-8544.

80. Morris DK, Lundblad V (1997) Programmed translational frameshifting in a gene required for yeast telomere replication. Curr Biol 7: 969-976.

81. Tuzon CT, Wu Y, Chan A, Zakian VA (2011) The *Saccharomyces cerevisiae* telomerase subunit Est3 binds telomeres in a cell cycle- and Est1-dependent manner and interacts directly with Est1 *in vitro*. PLoS Genet 7: e1002060.

82. Lee J, Mandell EK, Tucey TM, Morris DK, Lundblad V (2008) The Est3 protein associates with yeast telomerase through an OB-fold domain. Nat Struct Mol Biol 15: 990-997.

83. Yu EY, Wang F, Lei M, Lue NF (2008) A proposed OB-fold with a protein-interaction surface in *Candida albicans* telomerase protein Est3. Nat Struct Mol Biol 15: 985-989.

84. Lei M, Podell ER, Cech TR (2004) Structure of human POT1 bound to telomeric single-stranded DNA provides a model for chromosome end-protection. Nat Struct Mol Biol 11: 1223-1229.

85. Loayza D, De Lange T (2003) POT1 as a terminal transducer of TRF1 telomere length control. Nature 423: 1013-1018.

86. Liu D, Safari A, O'Connor MS, Chan DW, Laegeler A, et al. (2004) PTOP interacts with POT1 and regulates its localization to telomeres. Nat Cell Biol 6: 673-680.

87. Wang F, Podell ER, Zaug AJ, Yang Y, Baciu P, et al. (2007) The POT1-TPP1 telomere complex is a telomerase processivity factor. Nature 445: 506-510.

88. Latrick CM, Cech TR (2010) POT1-TPP1 enhances telomerase processivity by slowing primer dissociation and aiding translocation. Embo J.

89. Xin H, Liu D, Wan M, Safari A, Kim H, et al. (2007) TPP1 is a homologue of ciliate TEBP-beta and interacts with POT1 to recruit telomerase. Nature 445: 559-562.

90. Tejera AM, Stagno d'Alcontres M, Thanasoula M, Marion RM, Martinez P, et al. (2010) TPP1 is required for TERT recruitment, telomere elongation during nuclear reprogramming, and normal skin development in mice. Dev Cell 18: 775-789.

91. Abreu E, Aritonovska E, Reichenbach P, Cristofari G, Culp B, et al. (2010) TIN2-tethered TPP1 recruits human telomerase to telomeres *in vivo*. Mol Cell Biol 30: 2971-2982.

92. Lee J, Mandell EK, Rao T, Wuttke DS, Lundblad V (2010) Investigating the role of the Est3 protein in yeast telomere replication. Nucleic Acids Res.

93. Evans SK, Lundblad V (2002) The Est1 subunit of *Saccharomyces cerevisiae* telomerase makes multiple contributions to telomere length maintenance. Genetics 162: 1101-1115.

94. DeZwaan DC, Freeman BC (2009) The conserved Est1 protein stimulates telomerase DNA extension activity. Proc Natl Acad Sci USA 106: 17337-17342.

95. Virta-Pearlman V, Morris DK, Lundblad V (1996) Est1 has the properties of a single-stranded telomere end-binding protein. Genes & Dev 10: 3094--3104.

96. Evans SK, Lundblad V (1999) Est1 and Cdc13 as comediators of telomerase access. Science 286: 117-120.

97. Pennock E, Buckley K, Lundblad V (2001) Cdc13 delivers separate complexes to the telomere for end protection and replication. Cell 104: 387-396.

98. Bianchi A, Negrini S, Shore D (2004) Delivery of yeast telomerase to a DNA break depends on the recruitment functions of Cdc13 and Est1. Mol Cell 16: 139-146.

99. Li S, Makovets S, Matsuguchi T, Blethrow JD, Shokat KM, et al. (2009) Cdk1-dependent phosphorylation of Cdc13 coordinates telomere elongation during cell-cycle progression. Cell 136: 50-61.

100. Wu Y, Zakian VA (2011) The telomeric Cdc13 protein interacts directly with the telomerase subunit Est1 to bring it to telomeric DNA ends *in vitro*. Proc Natl Acad Sci U S A 108: 20362-20369.

101. Osterhage JL, Talley JM, Friedman KL (2006) Proteasome-dependent degradation of Est1p regulates the cell cycle-restricted assembly of telomerase in *Saccharomyces cerevisiae*. Nat Struct Mol Biol 13: 720-728.

102. Rhodes D (2006) The structural biology of telomeres. In: De Lange T, Lundblad V, Blackburn EH, editors. Telomeres. 2nd ed. Cold Spring Harbor, New York: Cold Spring Harbor Laboratory Press. pp. 317-343.

103. Taggart AKP, Teng S-C, Zakian VA (2002) Est1p as a cell cycle-regulated activator of telomere-bound telomerase. Science 297: 1023-1026.

104. Zhang M-L, Tong X-J, Fu X-H, Zhou BO, Wang J, et al. (2010) Yeast telomerase subunit Est1p has guanine quadruplex-promoting activity that is required for telomere elongation. Nat Struct Mol Biol 17: 202-209.

105. Tong X-J, Li Q-J, Duan Y-M, Liu N-N, Zhang M-L, et al. (2011) Est1 protects telomeres and inhibits subtelomeric y'-element recombination. Mol Cell Biol 31: 1263-1274.

106. Reichenbach P, Höss M, Azzalin CM, Nabholz M, Bucher P, et al. (2003) A human homolog of yeast Est1 associates with telomerase and uncaps chromosome ends when overexpressed. Curr Biol 13: 568-574.

107. Forstemann K, Lingner J (2001) Molecular basis for telomere repeat divergence in budding yeast. Mol Cell Biol 21: 7277-7286.

108. Ji H, Adkins CJ, Cartwright BR, Friedman KL (2008) Yeast Est2p affects telomere length by influencing association of Rap1p with telomeric chromatin. Mol Cell Biol 28: 2380-2390.

109. Wellinger RJ, Zakian VA (2012) Everything you ever wanted to know about *Saccharomyces cerevisiae* telomeres: beginning to end. Genetics 191: 1073-1105.

110. Dionne I, Wellinger RJ (1996) Cell cycle-regulated generation of single-stranded G-rich DNA in the absence of telomerase. Proc Natl Acad Sci U S A 93: 13902-13907.

111. Larrivee M, LeBel C, Wellinger RJ (2004) The generation of proper constitutive G-tails on yeast telomeres is dependent on the MRX complex. Genes Dev 18: 1391-1396.

112. Dionne I, Wellinger RJ (1998) Processing of telomeric DNA ends requires the passage of a replication fork. Nucleic Acids Res 26: 5365-5371.

113. Diede SJ, Gottschling DE (2001) Exonuclease activity is required for sequence addition and Cdc13p loading at a *de novo* telomere. Curr Biol 11: 1336-1340.

114. Bertuch AA, Lundblad V (2004) EXO1 contributes to telomere maintenance in both telomerase-proficient and telomerase-deficient *Saccharomyces cerevisiae*. Genetics 166: 1651-1659.

115. Maringele L, Lydall D (2002) EXO1-dependent single-stranded DNA at telomeres activates subsets of DNA damage and spindle checkpoint pathways in budding yeast yku70Delta mutants. Genes & Development 16: 1919-1933.

116. Huertas P, Cortes-Ledesma F, Sartori AA, Aguilera A, Jackson SP (2008) CDK targets Sae2 to control DNA-end resection and homologous recombination. Nature 455: 689-692.

117. Bonetti D, Martina M, Clerici M, Lucchini G, Longhese MP (2009) Multiple pathways regulate 3' overhang generation at *S. cerevisiae* telomeres. Molecular Cell 35: 70-81.

118. Frank CJ, Hyde M, Greider CW (2006) Regulation of telomere elongation by the cyclin-dependent kinase CDK1. Molecular Cell 24: 423-432.

119. Vodenicharov MD, Wellinger RJ (2006) DNA degradation at unprotected telomeres in yeast is regulated by the CDK1 (Cdc28/Clb) cell-cycle kinase. Molecular Cell 24: 127-137.

120. Grandin N, Reed SI, Charbonneau M (1997) Stn1, a new *Saccharomyces cerevisiae* protein, is implicated in telomere size regulation in association with Cdc13. Genes Dev 11: 512-527.

121. Grandin N, Damon C, Charbonneau M (2001) Ten1 functions in telomere end protection and length regulation in association with Stn1 and Cdc13. EMBO J 20: 1173-1183.

122. Petreaca RC, Chiu HC, Eckelhoefer HA, Chuang C, Xu L, et al. (2006) Chromosome end protection plasticity revealed by Stn1p and Ten1p bypass of Cdc13p. Nat Cell Biol 8: 748-755.

123. Petreaca RC, Chiu HC, Nugent CI (2007) The role of Stn1p in *Saccharomyces cerevisiae* telomere capping can be separated from its interaction with Cdc13p. Genetics 177: 1459-1474.

124. Sun J, Yu EY, Yang Y, Confer LA, Sun SH, et al. (2009) Stn1-Ten1 is an Rpa2-Rpa3-like complex at telomeres. Genes Dev 23: 2900-2914.

125. Mitton-Fry RM, Anderson EM, Hughes TR, Lundblad V, Wuttke DS (2002) Conserved structure for single-stranded telomeric DNA recognition. Science 296: 145-147.

126. Mitton-Fry RM, Anderson EM, Theobald DL, Glustrom LW, Wuttke DS (2004) Structural basis for telomeric single-stranded DNA recognition by yeast Cdc13. J Mol Biol 338: 241-255.

127. Puglisi A, Bianchi A, Lemmens L, Damay P, Shore D (2008) Distinct roles for yeast Stn1 in telomere capping and telomerase inhibition. EMBO J 27: 2328-2339.

128. Downs JA, Jackson SP (2004) A means to a DNA end: the many roles of Ku. Nat Rev Mol Cell Biol 5: 367-378.

129. Marcand S, Gilson E, Shore D (1997) A protein-counting mechanism for telomere length regulation in yeast. Science 275: 986-990.

130. Teixeira MT, Arneric M, Sperisen P, Lingner J (2004) Telomere length homeostasis is achieved via a switch between telomerase- extendible and -nonextendible states. Cell 117: 323-335.

131. Chang M, Arneric M, Lingner J (2007) Telomerase repeat addition processivity is increased at critically short telomeres in a Tel1-dependent manner in *Saccharomyces cerevisiae*. Genes & Development 21: 2485-2494.

132. Craven RJ, Petes TD (1999) Dependence of the regulation of telomere length on the type of subtelomeric repeat in the yeast *Saccharomyces cerevisiae*. Genetics 152: 1531-1541.

133. Mcgee JS, Phillips JA, Chan A, Sabourin M, Paeschke K, et al. (2010) Reduced Rif2 and lack of Mec1 target short telomeres for elongation rather than double-strand break repair. Nat Struct Mol Biol 17: 1438-1445.

134. Sabourin M, Tuzon CT, Zakian VA (2007) Telomerase and Tel1p preferentially associate with short telomeres in *S. cerevisiae*. Molecular Cell 27: 550-561.

135. Tseng S-F, Lin J-J, Teng S-C (2006) The telomerase-recruitment domain of the telomere binding protein Cdc13 is regulated by Mec1p/Tel1p-dependent phosphorylation. Nucleic Acids Res 34: 6327-6336.

136. Diede SJ, Gottschling DE (1999) Telomerase-mediated telomere addition *in vivo* requires DNA primase and DNA polymerases alpha and delta. Cell 99: 723-733.

137. Marcand S, Brevet V, Mann C, Gilson E (2000) Cell cycle restriction of telomere elongation. Curr Biol 10: 487-490.

138. Lin JJ, Zakian VA (1996) The *Saccharomyces* CDC13 protein is a single-strand TG1-3 telomeric DNA-binding protein *in vitro* that affects telomere behavior *in vivo*. Proc Natl Acad Sci USA 93: 13760-13765.

139. Hughes TR, Weilbaecher RG, Walterscheid M, Lundblad V (2000) Identification of the single-strand telomeric DNA binding domain of the *Saccharomyces cerevisiae* Cdc13 protein. Proc Natl Acad Sci USA 97: 6457-6462.

140. Mceachern MJ, Haber JE (2006) Telomerase-independent telomere maintenance in yeast. In: De Lange T, Lundblad V, Blackburn EH, editors. Telomeres. 2nd ed. Cold Spring Harbor, New York: Cold Spring Harbor Laboratory Press. pp. 199-224.

141. Goldstein G, Scheid M, Hammerling U, Schlesinger DH, Niall HD, et al. (1975) Isolation of a polypeptide that has lymphocyte-differentiating properties and is probably represented universally in living cells. Proc Natl Acad Sci U S A 72: 11-15.

142. Simpson MV (1953) The release of labeled amino acids from the proteins of rat liver slices. J Biol Chem 201: 143-154.

143. Ciechanover A, Hod Y, Hershko A (1978) A heat-stable polypeptide component of an ATP-dependent proteolytic system from reticulocytes. Biochem Biophys Res Commun 81: 1100-1105.

144. Hershko A, Ciechanover A, Rose IA (1979) Resolution of the ATP-dependent proteolytic system from reticulocytes: a component that interacts with ATP. Proc Natl Acad Sci U S A 76: 3107-3110.

145. Ciechanover A, Heller H, Elias S, Haas AL, Hershko A (1980) ATP-dependent conjugation of reticulocyte proteins with the polypeptide required for protein degradation. Proc Natl Acad Sci U S A 77: 1365-1368.

146. Wilkinson KD, Urban MK, Haas AL (1980) Ubiquitin is the ATP-dependent proteolysis factor I of rabbit reticulocytes. J Biol Chem 255: 7529-7532.

147. Hershko A, Ciechanover A, Heller H, Haas AL, Rose IA (1980) Proposed role of ATP in protein breakdown: conjugation of protein with multiple chains of the polypeptide of ATP-dependent proteolysis. Proc Natl Acad Sci U S A 77: 1783-1786.

148. Ciechanover A, Elias S, Heller H, Hershko A (1982) "Covalent affinity" purification of ubiquitin-activating enzyme. J Biol Chem 257: 2537-2542.

149. Hershko A (1983) Ubiquitin: roles in protein modification and breakdown. Cell 34: 11-12.

150. Pickart CM, Eddins MJ (2004) Ubiquitin: structures, functions, mechanisms. Biochim Biophys Acta 1695: 55-72.

151. Marques AJ, Palanimurugan R, Matias AC, Ramos PC, Dohmen RJ (2009) Catalytic mechanism and assembly of the proteasome. Chem Rev 109: 1509-1536.

152. Singh RK, Gonzalez M, Kabbaj MH, Gunjan A (2012) Novel E3 ubiquitin ligases that regulate histone protein levels in the budding yeast *Saccharomyces cerevisiae*. PLoS One 7: e36295.

153. Gmachl M, Gieffers C, Podtelejnikov AV, Mann M, Peters JM (2000) The RING-H2 finger protein APC11 and the E2 enzyme UBC4 are sufficient to ubiquitinate substrates of the anaphase-promoting complex. Proc Natl Acad Sci U S A 97: 8973-8978.

154. Leverson JD, Joazeiro CA, Page AM, Huang H, Hieter P, et al. (2000) The APC11 RING-H2 finger mediates E2-dependent ubiquitination. Mol Biol Cell 11: 2315-2325.

155. Tang Z, Li B, Bharadwaj R, Zhu H, Ozkan E, et al. (2001) APC2 Cullin protein and APC11 RING protein comprise the minimal ubiquitin ligase module of the anaphase-promoting complex. Mol Biol Cell 12: 3839-3851.

156. Thornton BR, Toczyski DP (2003) Securin and B-cyclin/CDK are the only essential targets of the APC. Nat Cell Biol 5: 1090-1094.

157. Thornton BR, Ng TM, Matyskiela ME, Carroll CW, Morgan DO, et al. (2006) An architectural map of the anaphase-promoting complex. Genes & Development 20: 449-460.

158. Zachariae W, Shevchenko A, Andrews PD, Ciosk R, Galova M, et al. (1998) Mass spectrometric analysis of the anaphase-promoting complex from yeast: identification of a subunit related to cullins. Science 279: 1216-1219.

159. Passmore LA, McCormack EA, Au SWN, Paul A, Willison KR, et al. (2003) Doc1 mediates the activity of the anaphase-promoting complex by contributing to substrate recognition. Embo J 22: 786-796.

160. Schwickart M, Havlis J, Habermann B, Bogdanova A, Camasses A, et al. (2004) Swm1/Apc13 is an evolutionarily conserved subunit of the anaphase-promoting complex stabilizing the association of Cdc16 and Cdc27. Mol Cell Biol 24: 3562-3576.

161. Hall MC, Torres MP, Schroeder GK, Borchers CH (2003) Mnd2 and Swm1 are core subunits of the *Saccharomyces cerevisiae* anaphase-promoting complex. J Biol Chem 278: 16698-16705.

162. Oelschlaegel T, Schwickart M, Matos J, Bogdanova A, Camasses A, et al. (2005) The yeast APC/C subunit Mnd2 prevents premature sister chromatid separation triggered by the meiosis-specific APC/C-Ama1. Cell 120: 773-788.

163. Penkner AM, Prinz S, Ferscha S, Klein F (2005) Mnd2, an essential antagonist of the anaphase-promoting complex during meiotic prophase. Cell 120: 789-801.

164. Au SW, Leng X, Harper JW, Barford D (2002) Implications for the ubiquitination reaction of the anaphase-promoting complex from the crystal structure of the Doc1/Apc10 subunit. J Mol Biol 316: 955-968.

165. Carroll CW, Enquist-Newman M, Morgan DO (2005) The APC subunit Doc1 promotes recognition of the substrate destruction box. Curr Biol 15: 11-18.

166. Zhang Z, Kulkarni K, Hanrahan SJ, Thompson AJ, Barford D (2010) The APC/C subunit Cdc16/Cut9 is a contiguous tetratricopeptide repeat superhelix with a homo-dimer interface similar to Cdc27. EMBO J 29: 3733-3744.

167. Zhang Z, Roe SM, Diogon M, Kong E, El Alaoui H, et al. (2010) Molecular structure of the N-terminal domain of the APC/C subunit Cdc27 reveals a homo-dimeric tetratricopeptide repeat architecture. J Mol Biol 397: 1316-1328.

168. Dube P, Herzog F, Gieffers C, Sander B, Riedel D, et al. (2005) Localization of the coactivator Cdh1 and the cullin subunit Apc2 in a cryo-electron microscopy model of vertebrate APC/C. Molecular Cell 20: 867-879.

169. Ohi MD, Feoktistova A, Ren L, Yip C, Cheng Y, et al. (2007) Structural organization of the anaphase-promoting complex bound to the mitotic activator Slp1. Mol Cell 28: 871-885.

170. Passmore LA, Booth CR, Venien-Bryan C, Ludtke SJ, Fioretto C, et al. (2005) Structural analysis of the anaphase-promoting complex reveals multiple active sites and insights into polyubiquitylation. Mol Cell 20: 855-866.

171. Buschhorn BA, Petzold G, Galova M, Dube P, Kraft C, et al. (2011) Substrate binding on the APC/C occurs between the coactivator Cdh1 and the processivity factor Doc1. Nat Struct Mol Biol 18: 6-13.

172. Herzog F, Primorac I, Dube P, Lenart P, Sander B, et al. (2009) Structure of the anaphase-promoting complex/cyclosome interacting with a mitotic checkpoint complex. Science 323: 1477-1481.

173. Passmore LA, Barford D (2005) Coactivator functions in a stoichiometric complex with anaphase-promoting complex/cyclosome to mediate substrate recognition. EMBO Rep 6: 873-878.

174. Glotzer M, Murray AW, Kirschner MW (1991) Cyclin is degraded by the ubiquitin pathway. Nature 349: 132-138.

175. King RW, Glotzer M, Kirschner MW (1996) Mutagenic analysis of the destruction signal of mitotic cyclins and structural characterization of ubiquitinated intermediates. Mol Biol Cell 7: 1343-1357.

176. Barford D (2011) Structure, function and mechanism of the anaphase promoting complex (APC/C). Q Rev Biophys 44: 153-190.

177. Pfleger CM, Kirschner MW (2000) The KEN box: an APC recognition signal distinct from the D box targeted by Cdh1. Genes Dev 14: 655-665.

178. Burton JL, Tsakraklides V, Solomon MJ (2005) Assembly of an APC-Cdh1-substrate complex is stimulated by engagement of a destruction box. Mol Cell 18: 533-542.

179. Burton JL, Solomon MJ (2001) D box and KEN box motifs in budding yeast Hsl1p are required for APC-mediated degradation and direct binding to Cdc20p and Cdh1p. Genes & Development 15: 2381-2395.

180. Pfleger CM, Lee E, Kirschner MW (2001) Substrate recognition by the Cdc20 and Cdh1 components of the anaphase-promoting complex. Genes & Development 15: 2396-2407.

181. Hilioti Z, Chung YS, Mochizuki Y, Hardy CF, Cohen-Fix O (2001) The anaphase inhibitor Pds1 binds to the APC/C-associated protein Cdc20 in a destruction box-dependent manner. Curr Biol 11: 1347-1352.

182. Schwab M, Neutzner M, Mocker D, Seufert W (2001) Yeast Hct1 recognizes the mitotic cyclin Clb2 and other substrates of the ubiquitin ligase APC. EMBO J 20: 5165-5175.

183. Matyskiela ME, Rodrigo-Brenni MC, Morgan DO (2009) Mechanisms of ubiquitin transfer by the anaphase-promoting complex. J Biol 8: 92.

184. Carroll CW, Morgan DO (2002) The Doc1 subunit is a processivity factor for the anaphase-promoting complex. Nat Cell Biol 4: 880-887.

185. da Fonseca PC, Kong EH, Zhang Z, Schreiber A, Williams MA, et al. (2011) Structures of APC/C(Cdh1) with substrates identify Cdh1 and Apc10 as the D-box co-receptor. Nature 470: 274-278.

186. Kraft C, Herzog F, Gieffers C, Mechtler K, Hagting A, et al. (2003) Mitotic regulation of the human anaphase-promoting complex by phosphorylation. EMBO J 22: 6598-6609.

187. Rudner AD, Murray AW (2000) Phosphorylation by Cdc28 activates the Cdc20-dependent activity of the anaphase-promoting complex. J Cell Biol 149: 1377-1390.

188. Steen JA, Steen H, Georgi A, Parker K, Springer M, et al. (2008) Different phosphorylation states of the anaphase promoting complex in response to

antimitotic drugs: a quantitative proteomic analysis. Proc Natl Acad Sci U S A 105: 6069-6074.

189. Stegmeier F, Amon A (2004) Closing mitosis: the functions of the Cdc14 phosphatase and its regulation. Annu Rev Genet 38: 203-232.

190. Mailand N, Diffley JF (2005) CDKs promote DNA replication origin licensing in human cells by protecting Cdc6 from APC/C-dependent proteolysis. Cell 122: 915-926.

191. Holt LJ, Krutchinsky AN, Morgan DO (2008) Positive feedback sharpens the anaphase switch. Nature 454: 353-357.

192. Kilian A, Bowtell DD, Abud HE, Hime GR, Venter DJ, et al. (1997) Isolation of a candidate human telomerase catalytic subunit gene, which reveals complex splicing patterns in different cell types. Hum Mol Genet 6: 2011-2019.

193. Bodnar AG, Ouellette M, Frolkis M, Holt SE, Chiu CP, et al. (1998) Extension of life-span by introduction of telomerase into normal human cells. Science 279: 349-352.

194. Vulliamy T, Marrone A, Szydlo R, Walne A, Mason PJ, et al. (2004) Disease anticipation is associated with progressive telomere shortening in families with dyskeratosis congenita due to mutations in TERC. Nat Genet 36: 447-449.

195. Osterhage JL, Friedman KL (2009) Chromosome end maintenance by telomerase. J Biol Chem 284: 16061-16065.

196. Ferguson JL, Chao WC, Lee E, Friedman KL (2013) The anaphase promoting complex contributes to the degradation of the *S. cerevisiae* telomerase recruitment subunit Est1p. PLoS One 8: e55055.

197. de Lange T, Blackburn EH, Lundblad V (2006) Telomeres; de Lange T, Blackburn EH, Lundblad V, editors. Cold Spring Harbor, NY: Cold Spring Harbor Laboratory Press.

198. Hughes TR, Evans SK, Weilbaecher RG, Lundblad V (2000) The Est3 protein is a subunit of yeast telomerase. Curr Biol 10: 809-812.

199. Lingner J, Cech TR, Hughes TR, Lundblad V (1997) Three Ever Shorter Telomere (EST) genes are dispensable for *in vitro* yeast telomerase activity. Proc Natl Acad Sci U S A 94: 11190-11195.

200. King RW, Deshaies RJ, Peters JM, Kirschner MW (1996) How proteolysis drives the cell cycle. Science 274: 1652-1659.

201. Peters JM, King RW, Hoog C, Kirschner MW (1996) Identification of BIME as a subunit of the anaphase-promoting complex. Science 274: 1199-1201.

202. Grossberger R, Gieffers C, Zachariae W, Podtelejnikov AV, Schleiffer A, et al. (1999) Characterization of the DOC1/APC10 subunit of the yeast and the human anaphase-promoting complex. J Biol Chem 274: 14500-14507.

203. Peters JM (2006) The anaphase promoting complex/cyclosome: a machine designed to destroy. Nat Rev Mol Cell Biol 7: 644-656.

204. Dawson IA, Roth S, Artavanis-Tsakonas S (1995) The *Drosophila* cell cycle gene fizzy is required for normal degradation of cyclins A and B during mitosis and has homology to the CDC20 gene of *Saccharomyces cerevisiae*. J Cell Biol 129: 725-737.

205. Schwab M, Lutum AS, Seufert W (1997) Yeast Hct1 is a regulator of Clb2 cyclin proteolysis. Cell 90: 683-693.

206. Visintin R, Prinz S, Amon A (1997) CDC20 and CDH1: a family of substrate-specific activators of APC-dependent proteolysis. Science 278: 460-463.

207. Yamano H, Tsurumi C, Gannon J, Hunt T (1998) The role of the destruction box and its neighbouring lysine residues in cyclin B for anaphase ubiquitin-dependent proteolysis in fission yeast: defining the D-box receptor. EMBO J 17: 5670-5678.

208. Jaspersen SL, Charles JF, Morgan DO (1999) Inhibitory phosphorylation of the APC regulator Hct1 is controlled by the kinase Cdc28 and the phosphatase Cdc14. Curr Biol 9: 227-236.

209. Visintin R, Craig K, Hwang ES, Prinz S, Tyers M, et al. (1998) The phosphatase Cdc14 triggers mitotic exit by reversal of Cdk-dependent phosphorylation. Mol Cell 2: 709-718.

210. Zachariae W, Schwab M, Nasmyth K, Seufert W (1998) Control of cyclin ubiquitination by CDK-regulated binding of Hct1 to the anaphase promoting complex. Science 282: 1721-1724.

211. Cohen-Fix O, Peters JM, Kirschner MW, Koshland D (1996) Anaphase initiation in *Saccharomyces cerevisiae* is controlled by the APC-dependent degradation of the anaphase inhibitor Pds1p. Genes Dev 10: 3081-3093.

212. Irniger S, Nasmyth K (1997) The anaphase-promoting complex is required in G1 arrested yeast cells to inhibit B-type cyclin accumulation and to prevent uncontrolled entry into S-phase. J Cell Sci 110 (Pt 13): 1523-1531.

213. Noton E, Diffley JF (2000) CDK inactivation is the only essential function of the APC/C and the mitotic exit network proteins for origin resetting during mitosis. Mol Cell 5: 85-95.

214. Spellman PT, Sherlock G, Zhang MQ, Iyer VR, Anders K, et al. (1998) Comprehensive identification of cell cycle-regulated genes of the yeast *Saccharomyces cerevisiae* by microarray hybridization. Mol Biol Cell 9: 3273-3297.

215. Larose S, Laterreur N, Ghazal G, Gagnon J, Wellinger RJ, et al. (2007) RNase III-dependent regulation of yeast telomerase. J Biol Chem 282: 4373-4381.

216. Irniger S, Piatti S, Michaelis C, Nasmyth K (1995) Genes involved in sister chromatid separation are needed for B-type cyclin proteolysis in budding yeast. Cell 81: 269-278.

217. Hildebrandt ER, Hoyt MA (2001) Cell cycle-dependent degradation of the *Saccharomyces cerevisiae* spindle motor Cin8p requires APC(Cdh1) and a bipartite destruction sequence. Mol Biol Cell 12: 3402-3416.

218. Page AM, Aneliunas V, Lamb JR, Hieter P (2005) *In vivo* characterization of the nonessential budding yeast anaphase-promoting complex/cyclosome components Swm1p, Mnd2p and Apc9p. Genetics 170: 1045-1062.

219. Amon A, Irniger S, Nasmyth K (1994) Closing the cell cycle circle in yeast: G2 cyclin proteolysis initiated at mitosis persists until the activation of G1 cyclins in the next cycle. Cell 77: 1037-1050.

220. Moll T, Tebb G, Surana U, Robitsch H, Nasmyth K (1991) The role of phosphorylation and the CDC28 protein kinase in cell cycle-regulated nuclear import of the *S. cerevisiae* transcription factor SWI5. Cell 66: 743-758.

221. Surana U, Amon A, Dowzer C, McGrew J, Byers B, et al. (1993) Destruction of the CDC28/CLB mitotic kinase is not required for the metaphase to anaphase transition in budding yeast. EMBO J 12: 1969-1978.

222. Baumer M, Braus GH, Irniger S (2000) Two different modes of cyclin clb2 proteolysis during mitosis in *Saccharomyces cerevisiae*. FEBS Lett 468: 142-148.

223. Surana U, Robitsch H, Price C, Schuster T, Fitch I, et al. (1991) The role of CDC28 and cyclins during mitosis in the budding yeast *S. cerevisiae*. Cell 65: 145-161.

224. Fitch I, Dahmann C, Surana U, Amon A, Nasmyth K, et al. (1992) Characterization of four B-type cyclin genes of the budding yeast *Saccharomyces cerevisiae*. Mol Biol Cell 3: 805-818.

225. Futcher B (1999) Cell cycle synchronization. Methods Cell Sci 21: 79-86.

226. Rodrigo-Brenni MC, Morgan DO (2007) Sequential E2s drive polyubiquitin chain assembly on APC targets. Cell 130: 127-139.

227. Kaiser P, Tagwerker C (2005) Is this protein ubiquitinated? Meth Enzymol 399: 243-248.

228. Tagwerker C, Flick K, Cui M, Guerrero C, Dou Y, et al. (2006) A tandem affinity tag for two-step purification under fully denaturing conditions: application in ubiquitin profiling and protein complex identification combined with *in vivo* cross-linking. Mol Cell Proteomics 5: 737-748.

229. Littlepage LE, Ruderman JV (2002) Identification of a new APC/C recognition domain, the A box, which is required for the Cdh1-dependent destruction of the kinase Aurora-A during mitotic exit. Genes Dev 16: 2274-2285.

230. Horn V, Thelu J, Garcia A, Albiges-Rizo C, Block MR, et al. (2007) Functional interaction of Aurora-A and PP2A during mitosis. Mol Biol Cell 18: 1233-1241.

231. Nasmyth K (2001) Disseminating the genome: joining, resolving, and separating sister chromatids during mitosis and meiosis. Annu Rev Genet 35: 673-745.

232. Martina M, Clerici M, Baldo V, Bonetti D, Lucchini G, et al. (2012) A balance between Tel1 and Rif2 activities regulates nucleolytic processing and elongation at telomeres. Mol Cell Biol 32: 1604-1617.

233. Gallant P, Nigg EA (1992) Cyclin B2 undergoes cell cycle-dependent nuclear translocation and, when expressed as a non-destructible mutant, causes mitotic arrest in HeLa cells. J Cell Biol 117: 213-224.

234. Wach A, Brachat A, Pohlmann R, Philippsen P (1994) New heterologous modules for classical or PCR-based gene disruptions in *Saccharomyces cerevisiae*. Yeast 10: 1793-1808.

235. Giaever G, Chu AM, Ni L, Connelly C, Riles L, et al. (2002) Functional profiling of the *Saccharomyces cerevisiae* genome. Nature 418: 387-391.

236. Goldstein AL, McCusker JH (1999) Three new dominant drug resistance cassettes for gene disruption in *Saccharomyces cerevisiae*. Yeast 15: 1541-1553.

237. Longtine MS, McKenzie A, 3rd, Demarini DJ, Shah NG, Wach A, et al. (1998) Additional modules for versatile and economical PCR-based gene deletion and modification in *Saccharomyces cerevisiae*. Yeast 14: 953-961.

238. Janke C, Magiera MM, Rathfelder N, Taxis C, Reber S, et al. (2004) A versatile toolbox for PCR-based tagging of yeast genes: new fluorescent proteins, more markers and promoter substitution cassettes. Yeast 21: 947-962.

239. Sikorski RS, Hieter P (1989) A system of shuttle vectors and yeast host strains designed for efficient manipulation of DNA in *Saccharomyces cerevisiae*. Genetics 122: 19-27.

240. Horton RM, Cai ZL, Ho SN, Pease LR (1990) Gene splicing by overlap extension: tailor-made genes using the polymerase chain reaction. Biotechniques 8: 528-535.

241. Lew DJ, Marini NJ, Reed SI (1992) Different G1 cyclins control the timing of cell cycle commitment in mother and daughter cells of the budding yeast *S. cerevisiae*. Cell 69: 317-327.

242. Belle A, Tanay A, Bitincka L, Shamir R, O'Shea EK (2006) Quantification of protein half-lives in the budding yeast proteome. Proc Natl Acad Sci U S A 103: 13004-13009.

243. Murray AW (1991) Cell cycle extracts. Methods Cell Biol 36: 581-605.

244. Passmore LA, Barford D, Harper JW (2005) Purification and assay of the budding yeast anaphase-promoting complex. Methods Enzymol 398: 195-219.

245. Rose MD, Winston F, Hieter P (1990) Methods in yeast genetics: a laboratory course manual. Cold Spring Harbor, NY: Cold Spring Harbor Laboratory Press.

246. Cox CJ, Dutta K, Petri ET, Hwang WC, Lin Y, et al. (2002) The regions of securin and cyclin B proteins recognized by the ubiquitination machinery are natively unfolded. FEBS Lett 527: 303-308.

247. Foe IT, Foster SA, Cheung SK, DeLuca SZ, Morgan DO, et al. (2011) Ubiquitination of Cdc20 by the APC occurs through an intramolecular mechanism. Curr Biol 21: 1870-1877.

248. Mateo F, Vidal-Laliena M, Canela N, Busino L, Martinez-Balbas MA, et al. (2009) Degradation of cyclin A is regulated by acetylation. Oncogene 28: 2654-2666.

249. Choi E, Choe H, Min J, Choi JY, Kim J, et al. (2009) BubR1 acetylation at prometaphase is required for modulating APC/C activity and timing of mitosis. EMBO J 28: 2077-2089.

250. Gurden MD, Holland AJ, van Zon W, Tighe A, Vergnolle MA, et al. (2010) Cdc20 is required for the post-anaphase, KEN-dependent degradation of centromere protein F. J Cell Sci 123: 321-330.

251. Jagus R, Beckler GS (2003) Overview of eukaryotic *in vitro* translation and expression systems. Curr Protoc Cell Biol Chapter 11: Unit 11 11.

252. Snow BE, Erdmann N, Cruickshank J, Goldman H, Gill RM, et al. (2003) Functional conservation of the telomerase protein Est1p in humans. Curr Biol 13: 698-704.

253. Sealey DCF, Kostic AD, Lebel C, Pryde F, Harrington L (2011) The TPR-containing domain within Est1 homologs exhibits species-specific roles in telomerase interaction and telomere length homeostasis. BMC Molecular Biology 12: 45.

254. Nougarede R, Della Seta F, Zarzov P, Schwob E (2000) Hierarchy of S-phase-promoting factors: yeast Dbf4-Cdc7 kinase requires prior S-phase cyclin-dependent kinase activation. Mol Cell Biol 20: 3795-3806.

255. Ghaemmaghami S, Huh W, Bower K, Howson R, Belle A, et al. (2003) Global analysis of protein expression in yeast. Nature 425: 737-741.

256. Rao H, Uhlmann F, Nasmyth K, Varshavsky A (2001) Degradation of a cohesin subunit by the N-end rule pathway is essential for chromosome stability. Nature 410: 955-959.

257. Michaelis C, Ciosk R, Nasmyth K (1997) Cohesins: chromosomal proteins that prevent premature separation of sister chromatids. Cell 91: 35-45.

258. Abdallah P, Luciano P, Runge K, Lisby M, Géli V, et al. (2009) A two-step model for senescence triggered by a single critically short telomere. Nat Cell Biol.

259. Teixeira MT, Forstemann K, Gasser SM, Lingner J (2002) Intracellular trafficking of yeast telomerase components. EMBO Reports 3: 652-659.

260. Wetzel R (1994) Mutations and off-pathway aggregation of proteins. Trends Biotechnol 12: 193-198.

261. Carrell RW, Lomas DA (1997) Conformational disease. Lancet 350: 134-138.

262. Epstein CB, Cross FR (1992) CLB5: a novel B cyclin from budding yeast with a role in S phase. Genes Dev 6: 1695-1706.